Erwin Hirschmann
no NASA CR #

(NASA-CR-156781) A COMPENDIUM OF MILLIMETER WAVE PROPAGATION STUDIES PERFORMED BY NASA Final Report, 29 Jul. - 31 Dec. 1977 (ORI, Inc.) 119 p HC A06/MF A01 CSCL 20N Unclas G3/32 28381 N78-29309

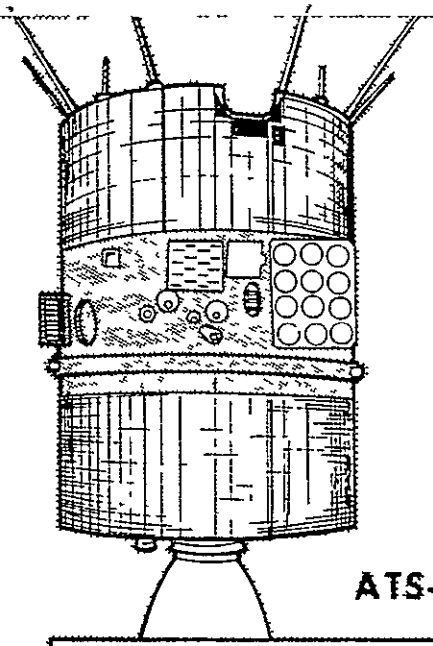

ATS-5

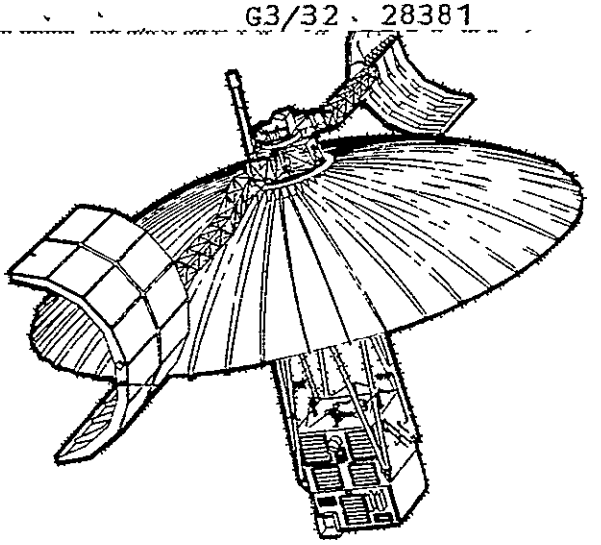

ATS-6

A COMPENDIUM OF MILLIMETER WAVE PROPAGATION STUDIES PERFORMED BY NASA

CTS

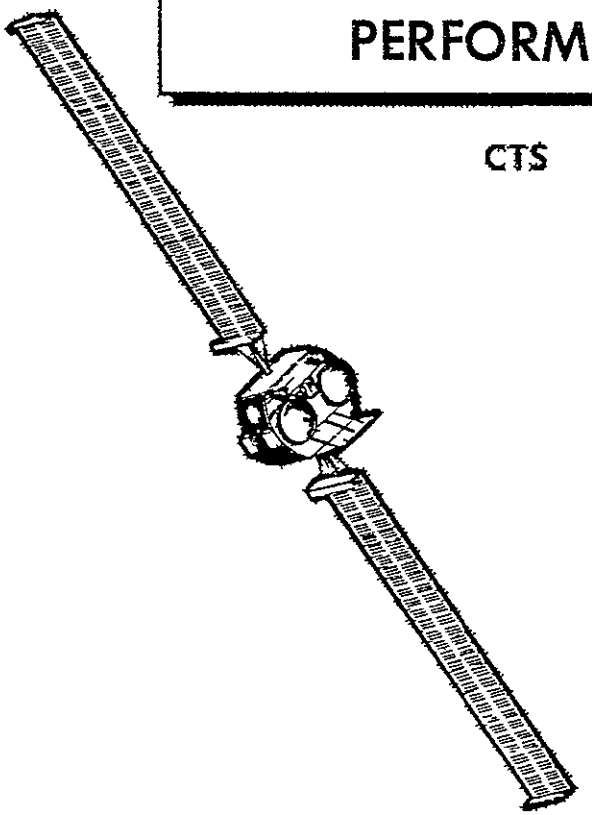

COMSTAR

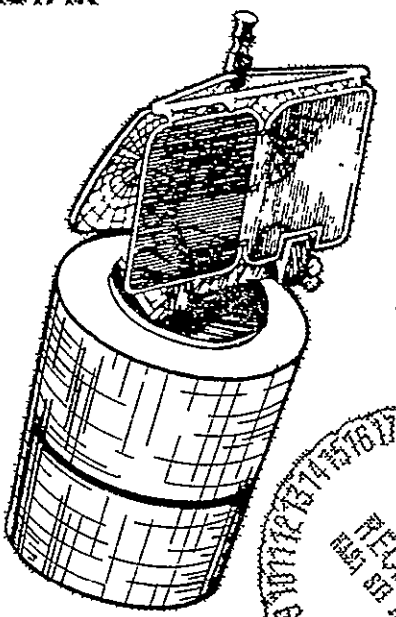

DECEMBER, 1977

1 Report No	2 Government Accession No	3 Recipient's Catalog No

4 Title and Subtitle	5 Report Date
A COMPENDIUM OF MILLIMETER WAVE PROPAGATION STUDIES PERFORMED BY NASA	November, 1977
	6 Performing Organization Code
7 Author(s) Drs. Roger Kaul, David Rogers, James Bremer	8 Performing Organization Report No
9 Performing Organization Name and Address ORI, Inc. 1400 Spring Street Silver Spring, Md. 20910	10 Work Unit No
	11 Contract or Grant No NAS5-24252
12 Sponsoring Agency Name and Address NASA Goddard Space Flight Center Greenbelt, Md. 20771 E. Hirschmann, Code 953, Technical Officer	13 Type of Report and Period Covered Final, July 29, 1977- December 31, 1977
	14 Sponsoring Agency Code

15 Supplementary Notes
Dr. D. Rogers is currently at COMSAT Research Laboratories, Clarksburg, Md.

16 Abstract
This compendium summarizes the key millimeter wave propagation experimental and analytical results obtained by NASA, universities and non-profit laboratories. The experiments were performed with the ATS-5, ATS-6, CTS and COMSTAR satellites, radars, radiometers and rain gauge networks. Analytic models have been developed for extrapolation of experimental results to new frequencies, locations, and communications systems. Extensive references are given to additional propagation literature.

17 Key Words (Selected by Author(s))	18 Distribution Statement
millimeter wave propagation, attenuation statistics, site diversity, low angle fading, depolarization, angle of arrival, bandwidth coherence.	Unlimited

19 Security Classif (of this report)	20 Security Classif (of this page)	21 No of Pages	22 Price
U	U	116	

TABLE OF CONTENTS *

*References listed after each section.

LIST OF FIGURES

LIST OF FIGURES (CONT.)

LIST OF FIGURES (CONT.)

LIST OF TABLES

I. INTRODUCTION

This compendium is a record of NASA's propagation research to the present, identifying specific objectives and accomplishments of the programs. The material is presented in a chronological format. Attention is restricted to frequencies above 4 GHz, hence the discussion primarily concerns wave propagation in the troposphere.

1.1 OVERVIEW OF PROGRAMS

For over a decade, the National Aeronautics and Space Administration (NASA) has performed, and also supported through contractual agreements, research in the field of radiowave propagation. The Goddard Space Flight Center has been responsible for the implementation of these programs. In view of NASA's statutory obligation to provide advisory services in the area of satellite communications (Ref. 1-1), the focus of NASA's propagation research has naturally been directed toward the optimization of satellite communications systems. These efforts, still ongoing, have included experiments ranging from radiometer and radar measurements to monitoring of satellite beacons and have been complemented with theoretical modeling. As has been noted elsewhere (Ref. 1-2, 1-3), the primary goal of the program is the development of experimentally verified methods for predicting important propagation phenomena.

Initially at the request of the Director of Telecommunications Policy a multi-agency committee was formed to prepare the United States position on interference between satellite Earth stations and microwave relay links for

the 1971 World Administrative Radio Conference (WARC). The committee included representatives from NASA, the Department of Commerce, the Federal Communications Commission and the Office of Telecommunications Policy. The committee's program objective was to acquire, analyze and disseminate space propagation data pertaining to frequencies below 10 GHz for a user community of space systems designers, operators, and regulatory agencies. To provide the space communications data, NASA implemented propagation and interference studies and experiments.

Anticipating that similar information would be required for frequencies above 10 GHz, NASA instituted communication link characterization studies addressing both propagation and interference effects. The technical approach was to obtain experimental data which complements analytical models. The ultimate goal in each technical area is the establishment of experimentally confirmed predictive procedures.

The current studies are being conducted as part of NASA's Technical Consultation Services (TCS) Program. This program was initiated by the Interagency Committee and has utilized the data base prepared for the 1971 WARC. Within the TCS program, the propagation studies are being termed the millimeter wave propagation and link characterization program.* The studies are being done by universities, non-profit laboratories and NASA personnel.

The present time is appropriate for a summary review of NASA's propagation research. First, recent results are brought together in a single document with extensive references to additional data. Second, new designs in satellite communications (broadcast satellites, public service communications system, time division multiple access systems, frequency reuse by means of orthogonal polarizations) should consider known propagation effects to assure reliable operation. Third, a compendium of NASA's research may be useful for assessing the scope and direction of future research, in light of the recent report by the National Academy of Sciences Space Applications Board Committee on Satellite Communications (Ref. 1-5). This committee recommended substantial

---

* Many measurements made to date have been in the 10 to 30 GHz frequency range which is usually termed the microwave regime. However, initially (Ref. 4) the program was to extend to 100 GHz which is well into the millimeter wave region. Thus, the name millimeter wave propagation program was assigned and has remained with the program.

increases in NASA's research and development in the space communications field. Finally, a summary of propagation study results can provide additional input into NASA's preparations for the General World Administrative Radio Conference in 1979.

1.2 SATELLITES USED FOR PROPAGATION RESEARCH

NASA's satellite millimeter wave propagation program began with the propagation experiment that was developed for NASA's fifth Applications Technology Satellite (ATS-5). Design studies for this space-borne experiment package were begun under NASA contract by Raytheon Corp. in 1964. These studies included detailed analyses (Refs. 1-4, 1-6) of potential experiment configurations and appropriate spacecraft orbits consistent with the goal of making measurements to assist in the characterization of Earth-space communications links at frequencies above 10 GHz. After further refinement, the ATS-5 propagation experiment was configured to include a 15.3-GHz downlink and a 31.65-GHz uplink on a geostationary spacecraft. The two prime areas of investigation were to be a comparison of signal effects versus meteorological data and a preliminary channel correlation analysis (Ref. 1-7). Concurrent with the development of the ATS-5 spacecraft, plans were made to institute 15.3-GHz receive capabilities at various ground facilities in the U.S. and Canada, and complementary ground measurements of meteorological conditions(e.g., with radiometers, radars, and rain gauges) were implemented at various sites.

The ATS-5 satellite was launched in August 1969 from Cape Canaveral, Florida, and was intended for geostationary 3-axis stabilized operation at 108 deg W longitude. Unfortunately, problems during the transfer orbit and synchronous injection phases caused the satellite to spin at about 76 rev/min at a final position of 105 deg W longitude. In spite of this spinning condition the propagation experiment aboard ATS-5 was still able to yield significant propagation information. The spin-modulated data format did of course eliminate the possibility of continuous recordings of signal amplitude and phase, and signal scintillations at frequencies above about 0.5 Hz could not be detected. Reviews of the ATS-5 propagation experiment configuration, hardware, and some results are available from Refs. 1-8 and 1-9. Further discussions of results are provided in Section 3 of this compendium.

Two space-borne propagation experiments were developed for the ATS-6 spacecraft which was successfully launched into a geostationary orbit at 94 deg W longitude in May 1974 (Ref. 1-10, 1-11). These experiments were designed by NASA and COMSAT Laboratories (Ref. 1-12). The NASA millimeter wave downlinks were at 20 and 30 GHz and via cross-strapping permitted engineering analyses at 4 GHz (downlink) and 6 GHz (uplink). The COMSAT experiment employed a space-borne transponder with 18- and 13-GHz uplinks downconverted to a 4-GHz downlink. This system design allowed multiple transmitters to be positioned at 15 sites east of the Mississippi River. All the propagation data on the 4-GHz downlink was received at a central receiving and data acquisition site and could be uniformly processed at one site having extensive computer capabilities. In later experiments, the 2-GHz transmitter installed on ATS-6 for the Tracking and Data Relay Experiment was also used in propagation studies (Ref. 1-13).

Using the ATS-6 propagation experiment links, studies were performed of rain attenuation, scintillations, depolarization, site diversity, coherence bandwidth, and analog and digital communications techniques. During the movements of ATS-6 from 94 deg W to 35 deg E longitude in June 1975, and back to 140 deg W in September of 1976, unique opportunities existed to study scintillations at low elevation angles (Refs. 1-13 to 1-15). These direct measurements of propagation parameters were augmented with ground measurements using radar, radiometers, and rain gauges, so that rain attenuation predicted by various experimenters will be presented in Section 3. It should be noted that ATS-6 is still operational; however, no experiments are now being performed.

NASA also supports propagation research using signals from the joint U.S.-Canadian Communications Technology Satellite (CTS), now called Hermes. This satellite was designed and built in Ottawa, Canada at the Communications Research Centre (CRC); NASA provided project management and a high-power 200-W traveling wave tube amplifier and power supply. The CTS which employs a 14-GHz uplink, a 12-GHz downlink and an 11.7-GHz beacon, was successfully launched into a geostationary orbit at 116 deg W longitude in January of 1976. Various NASA-supported researchers have monitored the 11.7-GHz beacon to investigate attenuation, angle-of-arrival, depolarization, and phase and amplitude scintillations (Ref. 1-16).

Additional GSFC support is being provided to researchers using the

recently launched COMSTAR satellite (Ref. 1-17). These satellites are part of the American Telephone and Telegraph Company's domestic satellite system, but include experimental beacons operating at 19.04 GHz and 28.56 GHz. The 19.04-GHz beacon transmits orthogonal linear polarizations, switched at a 1-KHz rate, while the higher frequency beacon transmits a single linear polarization. Three COMSTAR satellites are planned, to be placed in tightly maintained (0.1 deg) geosynchronous orbits spaced between 95 deg and 128 deg W longitude.

Two of the COMSTAR satellites, D1 and D2 were launched on May 13 and July 22, 1976, and have been positioned at 128^{o} and 95^{o} W longitude, respectively (Ref. 1-17). Both satellites contain beacons at 19.04 and 28.56 GHz. NASA funded research efforts include measurements of attenuation, comparison of radar predictions of rain attenuation with actually observed attenuation and depolarization measurements utilizing these beacons.

A summary of the millimeter wave satellite programs is shown versus time in Figure 1.2-1. The ATS-6 satellite remains operational but no propagation experiments are being conducted with the satellite at this time. Active propagation programs are underway with both the CTS and the two COMSTAR satellites, while these satellites provide services to other users. A decided advantage with these satellites, compared to the ATS series, is that the satellite beacons are always available since no time sharing with other experiments is required. Therefore, more accurate cumulative propagation statistics are expected to be developed with these satellites.

SATELLITE	FREQUENCY BANDS (GHz)	CALENDAR YEARS								
		69	70	71	72	73	74	75	76	77
ATS-5	15, 32	105°W								
ATS-6	13, 18, 20, 30						94°W			
ATS-6 RETURN	13, 18, 20, 30									140°W
CTS	12, 14								116°W	
COMSTARS	19, 18								128-95°W	

FIGURE 1.2-1. MILLIMETER WAVE SATELLITE PROGRAMS

REFERENCES

1-1. Public Law 87-624, the Communications Satellite Act of 1962.

1-2. Freibaum, J., "Effects of Propagation Phenomena and Frequency Allocation on the Growth of Satellite Communications," 1976 International Communications Conference, Philadelphia, Penna., pp. 12-19 to 12-24.

1-3. Eckerman, J., "A NASA Program to Characterize Propagation and Interference for Space Applications," AIAA Paper No. 72-577, AIAA 4th Communications Satellite Systems Conference, Washington, D.C., April 24-26, 1972.

1-4. "Final Report for Millimeter Communication Propagation Program," (three volumes), Raytheon Corp. Reports FR-65-334-1, -2, and -3, November 1965.

1-5. "Federal Research and Development for Satellite Communications," National Academy of Sciences, Washington, D.C., 1977.

1-6. "Final Report for Millimeter Communication Propagation Program Extension," (three volumes), Raytheon Reports U67-4201-1, -2, and -3, February 1967.

1-7. Binkley, W. O., L. Ippolito, J. L. King and R. B. Ratliff, "The ATS-E Millimeter Wave Propagation Experiment," NASA/GSFC Document X-733-68-196, Goddard Space Flight Center, April 1968.

1-8. Ippolito, L., "Millimeter Wave Propagation Measurements from the Applications Technology Satellite (ATS-V)," IEEE Trans. Antennas Propagation AP-18, 535-552, July 1970.

1-9. Ippolito, L., "Effects of Precipitation on 15.3 and 31.65 GHz Earth-Space Transmissions with the ATS-V Satellite," Proc. IEEE 59, 189-205, February 1971.

1-10. Ippolito, L. J., "ATS-6 Millimeter Wave Propagation and Communications Experiments at 10 and 30 GHz," IEEE Trans. Aerospace Electronic System AES-11, 1067-1082, November 1975.

1-11. Ippolito, L. J., "The ATS-6 Millimeter Wave Experiment," 20- and 30-GHz Millimeter Wave Experiments with the ATS-6 Satellite, NASA TN D-8197, p.1, National Aeronautics and Space Administration, Washington, D.C., April 1976.

1-12. "Data Analysis Report, Part I, ATS-F COMSAT Millimeter Wave Propagation Experiment," COMSAT Laboratories, September 1976.

1-13. Devasirvatham, D. M. J. and D. B. Hodge, "Amplitude Scintillations on Earth-Space Propagation Paths at 2 and 30 GHz," Ohio State University ElectroScience Laboratory Technical Report 4299-4, Columbus, Ohio, March 1977.

1-14. Vogel, W. J., A. W. Straiton and B. M. Fanin, "ATS-6 Ascending: Near Horizon Measurements over Water at 30 GHz," Electrical Engineering Research Laboratory Final Technical Report, University of Texas, Austin Texas, April 1977, also in Radio Science, Vol. 12, 757-765, Sept-Oct 1977.

1-15. "Measurements of SHF Tropospheric Fading at Low Elevation Angles Using the ATS-6 en Route West," Intelsat Memo BG/T-22-25E, 7 Nov. 1977.

1-16. Ippolito, L. J., "Characterization of the CTS 12-and 14-GHz Communications Links - Preliminary Measurements and Evaluation," ICC 76 Conference Record, 12-26 to 12-29, Philadelphia, Penna., June 1976.

1-17. Several papers describing the COMSTAR program and hardware are contained in the COMSAT Technical Review 7, No. 1, Spring 1977.

II. PROPAGATION DATA BASE

NASA has sponsored a program of experiments whose purpose is to characterize the propagation of centimeter and millimeter signals along transmission paths between satellites and ground stations. Supporting measurements have also been made to correlate meteorological parameters (primarily rain cell characteristics) with degradations in transmission. This research has been performed both by NASA facilities and by university-affiliated laboratories with long-term propagation programs. These university research groups include the Applied Physics Laboratory of Johns Hopkins University, the ElectroScience Laboratory of Ohio State University, the Electrical Engineering Research Laboratory of the University of Texas, the Electrical Engineering Department of Virginia Polytechnic Institute and State University (VPI & SU) and the MIT Lincoln Laboratory and Dept. of Meteorology. Additional work has been performed under contracts with companies such as Raytheon (Sudbury, Mass.), Westinghouse (Baltimore, Md.), Martin Marietta (Orlando, Fla.), COMSAT Laboratories (Clarksburg, Md.), and a government laboratory, NRL. Other organizations, such as Bell Laboratories (Holmdel, N.J.) and the Communications Research Centre (Ottawa, Canada), NELC, ESSA Wave Propagation Laboratory, AFCRL, USA SATCOM Agency, Rome Air Development Center, and Dept. of Transportation, have used NASA satellite signals in their own propagation programs. The results of these investigations are recorded in technical papers and reports under NASA sponsorship.

To assist the reader in identifying the institutions and the associated propagation research activities to date, a series of tables follow. These tables are arranged to provide

- propagation phenomena versus institution and satellite,
- propagation phenomena versus satellite system,
- propagation-related satellite characteristics versus satellite,
- propagation phenomena versus ground-based facilities.

These tables are intended to assist the reader in identifying the source of the particular information desired and for reference to the appropriate sections within this report, or the reference data base for more extensive information. An effort has been made throughout this compendium to reference both the original technical reports and open literature publications, where available.

An overall index of the propagation study areas cross referenced with institution and satellite is given in Table 2.1. These study areas, relating only to satellite-Earth links, are discussed in later sections of this compendium as indicated. A review of this table indicates: 1) a majority of the study areas have been performed by Ohio State, NASA (GSFC and Rosman), University of Texas, and Virginia Polytechnic Institute and State University (VPI & SU); 2) the study areas of attenuation and site diversity contain the largest data base.

Tables 2.2 through 2.4 delineate in more detail the propagation experiments related to the four satellites ATS-5, ATS-6, CTS and COMSTAR. At this time all of the ATS-6 studies have been completed. Experiments with ATS-6 are continuing at a reduced level since the launch of CTS and the first two of three COMSTAR satellites. The spinning of the ATS-5 satellite reduced the mission objective to studies of the average attenuation and scintillations (on a limited basis). In sharp contrast, the NASA and COMSAT-sponsored ATS-6 experiments were highly productive and have yielded extensive data bases. At this time work with the CTS is well underway and COMSTAR satellite measurements have been underway for one year. Active programs with these satellites are ongoing at three institutions.

TABLE 2.1

INDEX OF PROPAGATION STUDIES BY INSTITUTION AND SATELLITE

Investigator's Institution	Attenuation Scintillations (Sect 3 1)	Video Communication (Sect 3 1)	Site Diversity (Sect 3.2)	Low Angle Scintillations and Fade (Sect 3.3)	Depolarization (Sect 3.4)	Angle of Arrival (Sect 3.5)	Bandwidth Coherence (Sect 3.6)
University of Texas	ATS-5 ATS-6		ATS-6	ATS-6	CTS		
Martin-Marietta (Orlando)	ATS-5						
Ohio State University	ATS-5 CTS ATS-6		ATS-5 ATS-6	ATS-6		CTS	
CRC (Ottawa)	ATS-5						
COMSAT	ATS-5		ATS-6	ATS-6			
Battelle PNW	ATS-6						
VPI&SU	ATS-6 CTS COMSTAR			ATS-6	COMSTAR CTS ATS-6		
NASA Rosman, N C	ATS-5 ATS-6 CTS	ATS-6 CTS					ATS-6
NASA/GSFC	ATS-6 CTS	CTS	ATS-6				
APL	ATS-6 COMSTAR		ATS-6				
Westinghouse	ATS-6		ATS-6				ATS-6

TABLE 2.2

SUMMARY OF PROPAGATION EXPERIMENTS UTILIZING ATS-5

Link	Institution	Geometry of Link	Microwave Radiation Parameter(s)	Ground Station Antenna(s)	Experiment Data	Ancillary Meteorological Data	Reference(s)
ATS-5 to ground	U of Texas at Austin	54° elevation angle	15 3 GHz	Two 10 ft. paraboloids at Austin, one 16 ft paraboloid at Fort Davis	Attenuation	Sky temperature at 35 GHz, rain guages	2-1 2-3 2-4
ATS-5 to ground	Martin-Marietta (Orlando, FL)	48° elevation angle	15 3 GHz	10 ft parabola	Fades in signals	Tipping bucket rain gauges	2-2
ATS-5 to ground	Ohio State U (ESL)	37° elevation angle	15 3 GHz	30 ft fixed antenna, 15 ft mobile antenna	Diversity statistics, scintillations	15 5 GHz weather radar rain guages	2-3 2-4 2-17 2-18
ATS-5 to ground	Communications Research Center (Ottawa, Canada)	30° elevation angle	15 3 GHz	30 ft paraboloid	Attenuation	Sky temperature radiometry, 2 86 GHz radar backscatter	2-3 2-4
ATS-5 to ground	COMSAT (Clarksburg, Md)		15.3 GHz	16 ft dish	Attenuation	Sky temperature, solar radiation	2-3 2-4
Ground to ATS-5 and ATS-5 to ground	NASA/GSFC (at Rosman, N C)		31 65 GHz uplink, 15 3 GHz downlink	15 ft Cassegrain	Uplink and downlink attenuation	Radiometers at K_u and K_a bands Meteorological parameters	2-3 2-4

TABLE 2.3

SUMMARY OF PROPAGATION EXPERIMENTS UTILIZING ATS-6

Link	Institution	Geometry of Link	Microwave Radiation Parameter(s)	Ground Station Antenna(s)	Experiment Data	Ancillary Meteorological Data	References( )
ATS-6 to ground	COMSAT (Clarksburg, Md)	42° elevation angle	20 GHz and 30 GHz	3 m and 5 m dishes	Scintillation, fade measurements	Sky radiometry at 11 6, 20 and 30 GHz 6 rain gauges along path	2-6
ATS-6 to ground	Battelle PNL (Richland, Wash)	30° elevation angle	20 GHz	30 ft Cassegrain	Attenuation	Radiometry, 100 m from antenna	2-7
ATS-6 to ground	U of Texas at Austin	55° elevation angle, also 1 5 to 55°	30 GHz	Two 3 m paraboloids at Balcones, 1 5 m paraboloid at Austin	Site and frequency diversity, scintillation	Radiometry at 20 GHz	2-8 2-9
ATS-6 to ground	VPI & SU (Blacksburg, Va)	45° elevation angle also 10- 9°	20 GHz	4 ft diameter dual linear feed	Depolarization and attenuation	Rain and snow	2-10
ATS-6 to ground	GSFC, COMSAT, NRL, Westinghouse	42° elevation angle (40° at Westinghouse/ Baltimore)	20 GHz (CW) also 30 GHz at COMSAT and GSFC only	16 ft Cassegrain at GSFC 12 ft paraboloid at Westinghouse	Long baseline diversity, also scintillations and 20/30 GHz intensity ratios at GSFC, Differential fade across video band at Westinghouse	Rain rate, also 11 GHz sky temperature at COMSAT	2-11
ATS-6 to ground	GSFC at Rosman, North Carolina	47°	20 GHz and 30 GHz (CW and multitone)	4 7m dish at Rosman, N C	Attenuation, 20/30 GHz attenuation ratio, differential phase scintillation	Rain rate, radar rain gauge networks	2-11 2-25
ATS-6 to ground during repositioning of satellite	Ohio State U (ESL)	0 4° - 44° elevation angles	2 075 GHz and 30 GHz	4 6m Cassegrain antenna, 1 near polarization	Scintillations		2-12 2-13
ATS-6 to ground	Ohio State U (ESL)	42° elevation angle	20 GHz and 30 GHz	4 6m Cassegrain	Diversity and Scintillations	20 and 30 GHz radiometry	2-12 2-13
Ground to ATS-6 to ground	COMSAT	Uplinks from 39 ground terminals in the Eastern U S to ATS-6, downlink to Andover, Maine (elevation angle of 33 6°)	13 2 and 17 8 GHz uplinks 4 GHz downlink	4 GHz horn 32 5 dBI uplink antennas	Rainstorm attenuation correlation over a large geographic area site diversity	Rain gauge measurements at uplink stations	2-22
Ground to ATS-6 to ground	COMSAT (Clarksburg, Md and Friendship Airport (Westinghouse), Md)	3 6° - 14° elevation angles	13 2 GHz uplink 4 GHz downlink	4 GHz horn Uplink antennas greater than 33 dBI	Low elevation scintillation data on return of ATS-6 from Europe Two uplink stations for long baseline site diversity	Rain gauge measurements at uplink stations	2-23
Ground to ATS-6 to ground	APL (Wallops Island, Va)	42 3° elevation angle	13 2 and 17 8 GHz uplink 2 84 GHz radar	32 5 dBI antennas	Correlate S-band radar return with measured ground-satellite uplink attenuation	Rain gauges and disdrometer	2-24

TABLE 2.4

SUMMARY OF CURRENT PROPAGATION EXPERIMENTS UTILIZING CTS AND COMSTAR

Link	Institution	Geometry of Link	Microwave Radiation Parameter(s)	Ground Station Antenna(s)	Experiment Data	Ancillary Meteorological Data	Reference(s)
CTS to ground	U of Texas at Austin	49 4° elevation angle	11.7 GHz beacon, right-hand-circular polarization (RHCP)	3 m parabolic dish with turnstile feed	Attenuation, Cross-polarization	Rain rate	2-14
CTS to ground	VPI & SU	33° elevation angle	11.7 GHz beacon, (RHCP)	12 ft. parabola with dual polarized feed	Attenuation, Cross-polarization	Rain, wind, temperature	2-15
CTS to ground	Ohio State U. (ESL)	32 7° elevation angle	11.7 GHz beacon, (RHCP)	Self-phased array with four 0.6 m dishes in one meter square	Angle of arrival attenuation, scintillation	Rain rate 20 GHz radiometer	2-16
CTS to ground	NASA/Rosman, North Carolina	36° elevation angle	12 GHz video and tone downlinks, 11 7 GHz beacon	15 foot parabola	TV experiment, propagation, EMI experiments	Radars (3 and 8 GHz) and rain gauges	2-31
Ground to CTS to ground	NASA/GSFC	31° elevation angle	14 25 GHz uplink 12 GHz downlink 11 7 GHz beacon	10 ft. parabola uplink, 15 ft. parabola downlink	TV experiments, attenuation	Rain gauge	2-31
COMSTAR to ground	VPI & SU	44.2° elevation angle	19.04 GHz and 28.56 GHz linear polarization in two orthogonal directions	4 ft diameter prime focus disk with scaler feed horn and orthomode transducer	Cross-polarization, attenuation	Rain, wind speed	2-30
COMSTAR to ground	APL	41.6° elevation angle	28.56 GHz		Attenuation	Rain gauge and disdrometer, S-band radar	2-29

These tables reference only experimental data. Papers of purely theoretical nature, whether related to engineering or to socio-economic benefits of satellite communication systems, are not included.

Since the satellite parameters define to some extent the types of propagation experiments, Table 2.5 summarizes several of these key parameters. All of these geostationary satellites are positioned to view the continental U.S., however, ATS-6 provided a rare opportunity for studies of low angle fading when it was repositioned and then returned to 140^{o} W longitude. Additional details of the satellite hardware are available in the references, but in general the satellite beacon signals have been stable (except for the ATS-5 spin) and have provided signal plus noise-to-noise ratios in excess of 10dB except during high-fade periods at CONUS ground stations.

In addition to the Earth-space link measurements, additional experiments were performed employing terrestrial links and radar diagnostics of rain cells and rain gauge networks. These experiments, summarized in Table 2.6, were carried out early in the link characterization experimental program. The results of these studies are presented in Section 4 of this compendium. Analytical and modeling studies performed in this program are discussed in both Sections III and IV.

TABLE 2.5

SATELLITE PARAMETERS RELATED TO PROPAGATION STUDIES

Satellite	Launch Date	Satellite Position	Uplink Frequencies	Downlink Frequencies	Antennas	Reference(s)
ATS-5	8/12/69	Initially over Indian Ocean, drifted to 108° W longitude, remained spinning at 76 rpm	31 65 GHz with sidebands at ±1, ±10, and ±50 MHz from carrier	15 3 GHz with sidebands at ±0.1, ±1, ±50 MHz from carrier	Linearly polarized conical horns with 20° coverage and 19 1 dB boresight gain	2-3 2-4
ATS-6	5/30/74	94° W longitude for first year then move to 35° E long and returned to 140° W	COMSAT Exp 13 19 - 13 2 GHz 17 74 - 17 8 GHz	COMSAT Exp. 4 14 - 4 15 GHz 4 16 - 4.17 GHz NASA/GSFC Exp 20 and 30 GHz 8 sidetones Spaced ± 180 MHz	COMSAT EXP Dual-frequency linearly polarized dish NASA/GSFC Exp 20 GHz 6° x 9° horn 2° dish 30 GHz similar to above	2-5 2-11 2-22
CTS	1/17/76	116° W	14 0 - 14 5 GHz	11 7 GHz beacon 11 7 - 12 2 GHz	16° horn, RHCP for beacon	2-28
COMSTAR (satellites D1 and D2)	D1 5/13/76 D2 7/22/76	D1 128° W long D2 95° W long		Both satellites 19 04 and 28 56 GHz	Both satellites Linearly polarized offset parabolic dishes 19 04 GHz switched between vertical and horizontal polarization 28 56 GHz vertically polarized	2-29

TABLE 2.6

SUMMARY OF PROPAGATION EXPERIMENTS UTILIZING TERRESTRIAL LINKS AND RADAR DIAGNOSTICS

Link	Institution	Geometry of Link	Microwave Radiation Parameter(s)	Ground Station Antenna(s)	Experiment Data	Ancillary Meteorological Data	Reference(s)
Ground-to-ground	VPI	1 43 km line of sight	17 65 GHz, linear polarization, $\mp 45^{o}$ from vertical	4 ft diameter reflectors	Cross talk and direct attenuation	Rain rate	2-19
Atmosphere to ground	NRL (Waldorf, Md)	Elevation angles of 90, 60, 45, 30, 20, 10, 75, 3, 2, 1, 0.5, 0 2, and 0 0 degrees	15 3 GHz	60 ft Cassegrain	Atmospheric emissions as a function of elevation angle		2-20
Ground-to-ground	NASA/GSFC	4 6km path length	15 GHz, vertical polarization	1 2 paraboloid transmitter, 40 cm^2 horn receiver	Amplitude fluctuations and scintillations	Rain data (5 tipping buckets)	2-21
Rain radar	APL at Wallops Island	Within a 280 km diameter circle centered at Wallops Island 2^{o} elevation angle used to locate rain cells	60 ft antenna, raster scanned across rain cells	2.7 - 2.9 GHz 1, 2, or 5 μ sec pulses with frequency diversity	Statistics of rain cell sizes and spacings, Detailed structure of individual rain cells	Weather station data, tipping bucket measurements	2-26
Rain radar	MIT	Construction of 3-dimensional profiles of rain scattering intensities	3^{o} beamwidth @ 2 8 GHz 1^{o} beamwidth @ 9 4 GHz	2 8 GHz with 1 5 μ sec pulses 9 4 GHz with 2.0 or 0 5 user pulses	Rain cell distributions with high spatial and temporal resolution	Flow meter and tipping bucket rain data with 30 sec time resolution of rain fall, radiosondes from 3 nearest weather stations	2-27

REFERENCES

2-1. Millimeter Wave Group, ATS-5 Signal Characteristics at 15.3 GHz and Related Experiments at 15 and 35 GHz, Part I, Final Tech. Report, Contract No. NAS5-10387, Univ. of Texas at Austin.

2-2. Sukhia, Darius E., Martin Marietta Corporation, Satellite-to-Ground EHF Transmission, Task Auth. 3071C-0601-16600, December 1971.

2-3. Millimeter-Wave Propagation Experiments Utilizing the ATS-5 Satellite, NASA/GSFC X-751-70-428, November 1970.

2-4. Westinghouse Electric Corp., ATS-5 Millimeter Wave Propagation Experiment, Final Report, Contract NAS5-21598, January 1972.

2-5. Duffield, T. L., "Communications and Propagation Ground Receiving Station for the ATS-F Millimeter Wave Experiment," Trans. Int'l Telecom Conf., Minneapolis, Minn., June 1974, pp. 27F-1 to 27F-5.

2-6. Fang, D. J. and J. M. Harris, Precipitation-Attenuation Studies Based on Measurements of ATS-6 20/30-GHz Beacon Signals at Clarksburg, Maryland, Final Report, COMSAT Laboratories, Clarksburg, Md., August 1976.

2-7. Davis, K. C. and P. A. Ekstrom; ATS-6 MM-Wave Propagation Experiment, Batelle, Pacific Northwest Labs., Richland, WA, Final Report, Contract No. NAS5-20504, Sept 1976.

2-8. Vogel, W. J., A. W. Straiton, B. M. Fannin and N. K. Wagner, ATS-6 Attenuation Diversity Measurements at 20 and 30 GHz, Univ. of Texas at Austin, Contract No. NAS5-21982, Nov. 1975.

2-9. Vogel, W. J., A. W. Straiton and B. M. Fannin, "ATS-6 Ascending. Near Horizon Measurements Over Water at 30 GHz," Radio Science, 12, 757-765, Sept.-Oct. 1977.

2-10. Bostian, C. W., E. A. Manus, R. E. Marshall, H. N. Pendrak, W. L. Stutzman, P. H. Wiley and S. R. Kauffman; A 20-GHz Depolarization Experiment Using the ATS-6 Satellite; Virginia Poly. Tech. Inst. & State Univ., Final Report, Contract No. NAS5-21984, September 10, 1975.

2-11. Westinghouse Electric, ATS-6 Millimeter Wave Propagation Experiment Final Data Analysis Report, Contract No. NAS5-20904, September 1975.

2-12. Devasirvatham, D. M. J. and D. B. Hodge, Amplitude Scintillations on Earth-Space Propagation Paths at 20 and 30 GHz, Ohio State Univ., Electro-Science Lab., Tech. Report 4299-4, March 1977.

2-13. Hodge, D. B., D. M. Theobold and R. C. Taylor, ATS-6 Millimeter Wavelength Propagation Experiment, Ohio State Univ., ElectroScience Lab., Final Report 3863-6, January 1976.

2-14. Vogel, W. J. and A. W. Straiton, CTS Attenuation and Cross-Polarization Measurements at 11.7 GHz, Elect. Eng. Res. Lab., Univ. of Texas at Austin, Final Report, Contract NAS5-22576, April 1977.

2-15. Bostian, C. W., S. B. Holt, Jr., S. R. Kauffman, E. A. Manus, R. E. Marshall, W. L. Stutzman, and P. H. Wiley; A Depolarization and Attenuation Experiment Using the CTS Satellite, Volume 1. Experiment Description, Virg. Poly. Inst. and State University, Contract No. NAS5-22577, November 18, 1976.

2-16. Theobold, D. M. and D. B. Hodge; The OSU Self-Phased Array for Propagation Measurement Using the 11.7 GHz CTS Beacon, Ohio State Univ. ElectroScience Lab., Tech. Report No. 4299-1, November 1976.

2-17. Hodge, D, B., Space Diversity for Reception of Satellite Signals, Ohio State Univ., ElectroScience Lab., Tech. Report 2374-16, Grant No. NGR-36-008-080, October 1973.

2-18. Levis, C. A. and V. Ungvichian, Preliminary Analysis of 15 GHz Scintillations on an ATS-5 Satellite-to-Ground Path, Ohio State Univ., ElectroScience Lab., Final Report 3863-7, February 1976.

2-19. Bostian, C. W., W. L. Stutzman, P. H. Wiley and R. E. Marshall, The Influence of Polarization on Millimeter Wave Propagation Through Rain; Virg. Poly. Inst. & State Univ., Grant No. NGR-47-004-091, January 1, 1974.

2-20. LeFande, R. A., Atmospheric Absorption and Emission of Microwave Radiation· A Critical Study in Search of a Definitive Propagation Model of the Terrestrial Atmosphere, Naval Res. Lab., August 3, 1973.

2-21. Mondre, E., Correlation Analysis and Scintillation for 15 GHz Line-of-Sight Propagation Channels, NASA/GSFC TN D-5613, April 1970.

2-22. Hyde, G., Data Analysis Report on ATS-F COMSAT Millimeter Wave Propagation Experiment, Parts I and II, COMSAT Final Reports under Contract NAS5-21616, September 1976.

2-23. "Measurements of SHF Tropospheric Fading at Low Elevation Angles Using the ATS-6 en Route West," Intelsat Memo BG/T-22-25E, 7 Nov. 1977.

2-24. Goldhirsh, J., "Attenuation of Propagation Through Rain for an Earth-Satellite Path Correlated with Predicted Values Using Radar," IEEE Trans. Ant. Prop., AP-24, 800-806, Nov. 1976.

2-25. Ippolito, L. J., 20- and 30-GHz Millimeter Wave Experiments with the ATS-6 Satellite, NASA/GSFC TN D-8197, April 1976.

2-26. Katz, I., A. Arnold, J. Goldhirsh, T. G. Konrad, W. L. Vann, E. B. Dobson and J. R. Rowland, Radar-Derived Spatial Statistics of Summer Rain, Experiment Description, Appl. Phys. Lab., The Johns Hopkins Univ., NASA CR-2592, September 1975.

2-27. Austin, P. M., Some Statistics of the Small-Scale Distribution of Precipitation, reprint of Final Report of the Weather Radar Research Project, Mass. Inst. of Tech., NASA/GSFC X-751-72-149, July 1971.

2-28. Ippolito, L. J., "Characterization of the CTS-12 and 14-GHz Communications Links - Preliminary Measurements and Evaluation," ICC-76 Conf. Rec., Philadelphia, Penna., June 1976.

2-29. COMSAT Tech. Rev., Vol. 7, No. 1, Spring 1977 and Cox, D. C., "Design of the Bell Telephone Laboratories 19 and 28 GHz Satellite Beacon Propagation Experiment," ICC 1974 Conf. Record, June 17-19, 1974, pp. 27E-1 to 27E-5.

2-30. Katz, I., A. Arnold, J. Goldhirsh, T. G. Konrad, W. L. Vann, E. B. Dobson and J. R. Rowland, Radar-Derived Spatial Statistics of Summer Rain, Applied Physics Lab., The Johns Hopkins Univ., Laurel, Md., NASA CR-2592, September 1975.

2-31. Bostian, C. W., S. B. Holt, Jr., S. R. Kauffman, E. A. Manus, R. E. Marshall, W. P. Overstreet, R. R. Persinger, W. L. Stutzman and P. H. Wiley, A Depolarization and Attenuation Experiment Using the COMSTAR and CTS Satellites, Prog. Reports by Virg. Poly. Inst. and State Univ., Contract No. NAS5-22577, Dec. 22, 1976 and July 19, 1977.

2-32. Communications Link Characterization Experiment (CLCE), Technical Data Reports (3 volumes), Westinghouse Elect. Corp., Baltimore, Md., Jan., April, August 1977.

III. PROPAGATION RESEARCH USING SATELLITE LINKS

3.1 ATTENUATION

The quality of an Earth-space communication system can be degraded by the presence of attenuation in the troposphere. This attenuation is caused principally by rain and can be accepted in most communications systems because of the low percentages of time in which heavy rain occurs in the U.S. The long-term prediction of fade events can only be done statistically. Therefore, utilization of alternate links along lower attenuation paths must be preplanned (site diversity). Alternatively, the system design could choose to maintain the link margin by increased power levels, but this "brute force" solution is frequently costly and consumes large amounts of satellite platform resources.

These system design considerations have been one of the prime motivating factors for propagation investigators to spend a significant amount of time evaluating the magnitudes and frequency of tropospheric attenuation events on Earth-to-space paths. Models and diagnostic procedures (radiometers and radars) for the measurement of rain attenuation have been developed and will be discussed in Section IV of this compendium. In this section, the experimental attenuation measurements will be presented. The measurements will primarily deal with the ATS-5 and ATS-6 satellites, since they cover the 13.2 to 30 GHz frequency range and their data bases are sufficiently large to provide meaningful statistics. Measurements with the CTS and COMSTAR

satellites are now ongoing at several NASA installations and NASA-sponsored institutions. In future years these satellites will provide additional attenuation data bases.

3.1.1 Rain Attenuation

Attenuation for millimeter wave Earth-space communications links is caused by precipitation (hydrometeors). The magnitudes and durations of these effects depend on local storm properties. In principle, these can be characterized for large regions using long-term statistical samples. The demonstration of this direct approach is the basis for the experimental program.

Connection of the radio communication data to meteorological effects has been approached through several empirical relationships. The primary experimental measurements of rain attenuation A have been to:

a) evaluate the coefficients a and b in the empirical relationship (Ref. 3.1-1)

$$A\ (dB/km) = a\ R^{b}$$

where R is the rain rate, in mm/hr.

b) determine an effective rain path length L so that the product (AL) yields the total attenuation. The effective L considers the effects of uniform dispersed rain and rain cell structures.

c) determine the frequency scaling ratio for attenuation, i.e.,

$$\frac{A_{f_2}}{A_{f_1}} = c\ A_{f_1}^{\ d}$$

where c and d are frequency dependent constants and A_{f_1} and A_{f_2} are the attenuations per kilometer at frequencies f_1 and f_2.

d) determine the cumulative distributions of the rain attenuation events over a significant period of time for a variety of geographical sites, e g., worst month and annual statistics being the more useful time periods of presentation.

Early measurements of the attenuation versus rain gauge rates (Ref. 3.1-2) indicated a poor correlation to the relation $A = a R^b$. However, these rain measurements are the most readily available from the Weather Service and techniques for interpreting the time-retarded readings of several rain gauges along the satellite ground track have been developed (Ref. 3.1-3). Therefore, theoretical estimates and measurements of A and AL have been made at various institutions. Some typical results (A in dB/km, L in km, R in mm/hr) are given in Table 3 1-1 for the frequencies of ATS-5 and -6 and CTS. Theoretical calculations of the frequency parameters a and b are shown in Figures 3.1-1 and -2 (Ref. 3.1-4). Additional calculations of the a and b parameters are now being prepared for publication (Ref. 3.1-7).

One difficult parameter in measuring A is knowing the path length L through the precipitating media. Frequently, L has been estimated from rain gauge measurements (Ref. 3.1-4) and has been found to vary significantly with, among other parameters, the rain rate. The curves generated from ATS-5 (Ref. 3.1-2) are shown in Figure 3.1-3. Also shown in this figure are four storms (labelled 1 through 4) observed at Rosman, North Carolina in 1971. These are to be compared with the CY 1970 data which averages all the Rosman data (12,581 minutes) during 1970. The COMSAT plot was obtained from a combination of radiometer and direct measurements. In addition, the sun tracker data of Evans (Ref. 3.1-8) is shown. These curves do describe the generally accepted model of thunderstorms with intense rain cells of limited extent and lighter, more evenly distributed rain events.

It is useful to scale experimental results for rain attenuation available at one frequency to another frequency in order to estimate system performance through the same rainfall. This scaling is usually accomplished using the relations for frequencies f_1 and f_2

$$\frac{A_2 L}{A_1 L} = \frac{a_2}{a_1} R^{(b_2 - b_1)} \approx \frac{a_2}{a_1}$$

TABLE 3.1-1

THEORETICAL ESTIMATES AND MEASUREMENTS OF A AND AL

RESULT	FREQUENCY	MEASUREMENT LOCATION/PERIOD	REFERENCE
$A = 0.035\ R^{1.155}$	15.3 GHz	Predicted values for a and b	3.1-4
$A = 0.2\ R^{1.0}$	31.65 GHz	Predicted values for a and b	3.1-4
$AL = 2.365\ R^{0.3663}$	15.3 GHz	Rosman, N.C., 210 hr avg during 1970	3.1-5 & 6
$A = 0.0687\ R^{1.1}$	20 GHz	Predicted values for a and b	3.1-7
$A = 0.1649\ R^{1.035}$	30 GHz	Predicted values for a and b	3.1-7
$A = 0.0159\ R^{1\ 25}$	11 GHz	Predicted values for a and b	3.1-11
$AL = 0.1339\ R^{1.1006}$	11.7 GHz	Rosman, N.C., nearest bucket, data from one-year period	3.1-11
$AL = 0.1639\ R^{1.1081}$	11.7 GHz	Rosman, N.C., ground average rain rate, data from one year period	3.1-11
$AL = 0.5843\ R^{0.7863}$	11.7 GHz	Greenbelt, MD, data from one year period	3.1-11

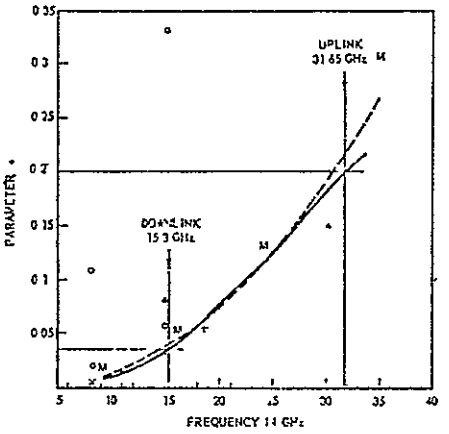

FIGURE 3.1-1. PARAMETER "a" AS A FUNCTION OF FREQUENCY (Ref. 3.1-4)

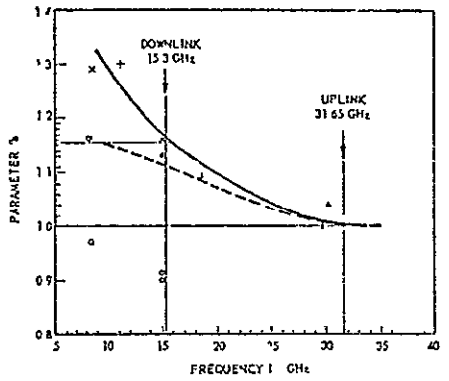

FIGURE 3.1-2. PARAMETER "b" AS A FUNCTION OF FREQUENCY (Ref. 3.1-4)

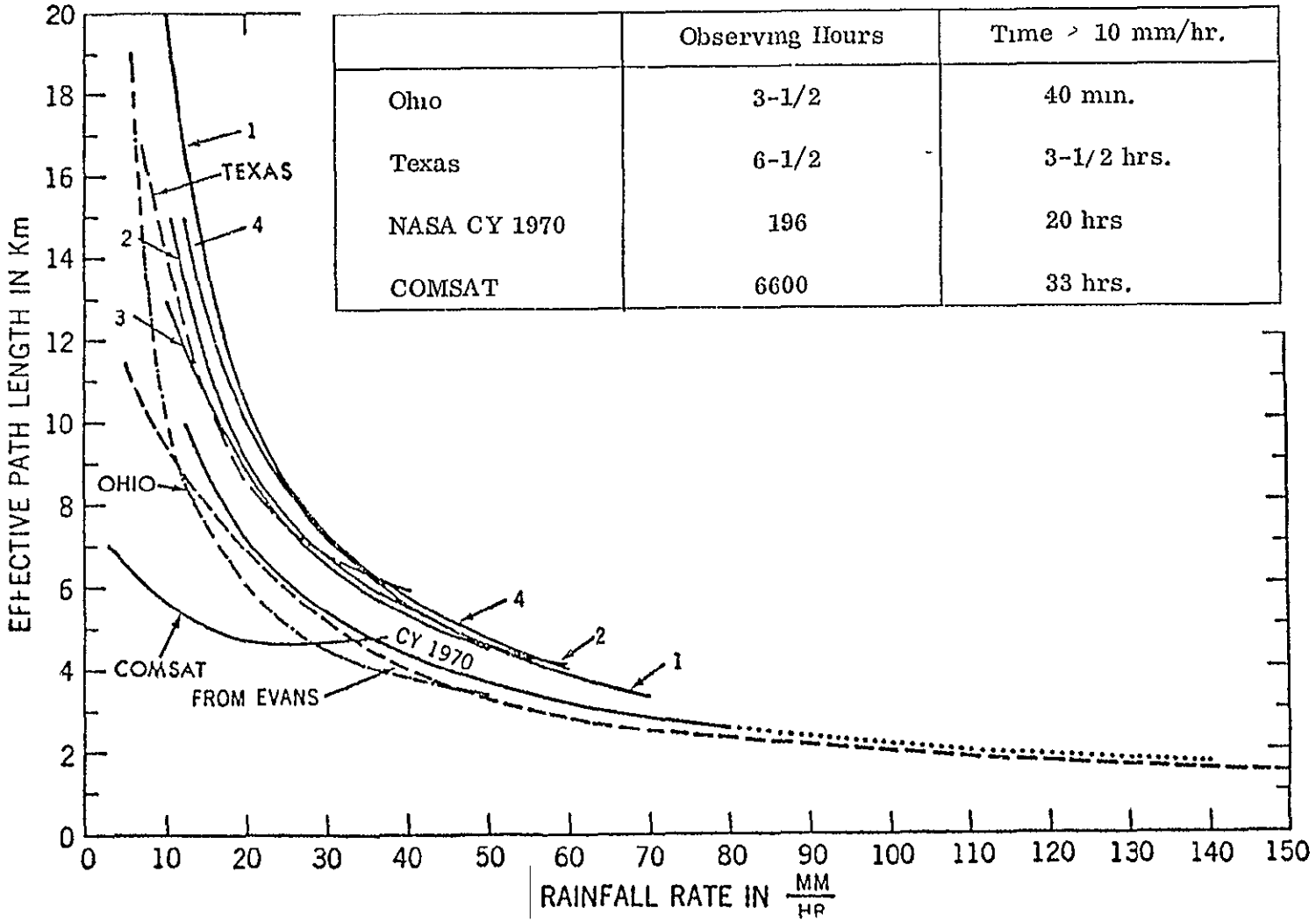

FIGURE 3.1-3. EFFECTIVE PATH LENGTH REQUIRED FOR A GIVEN RAINFALL RATE FROM 15.3 GHz MEASUREMENTS AT ROSMAN, NORTH CAROLINA

since $b_2 - b_1 \approx 0$. However, the assumption that the rain is homogeneous and the neglect of the rainfall rate factor, R^{b2-b1}, yields a poor approximation (Ref. 3.1-9). Assuming a Gaussian distribution to the spatial distribution of the rain, yields (Ref. 3.1-9)

$$\frac{A_2 L}{A_1 L} = \frac{a_2}{a_1} \left(\frac{A_1 L}{a_1} \sqrt{\frac{b_1}{\pi}} \right)^{\left(\frac{b_2}{b_1} - 1 \right) \sqrt{\frac{b_1}{b_2}}} .$$

Utilizing the numbers in Table 3.1-1, for $f_1 = 15.3$ GHz and $f_2 = 31.65$ GHz, yields $\frac{A_2 L}{A_1 L} = \frac{a_2}{a_1} = 5.7$ for the simplest approximation and

$$\frac{A_2 L}{A_1 L} = 5.7 \ (17.3 \ A_1 L)^{-0.134} = 4.2 \ (A_1 L)^{-0.134}$$

for the Gaussian spatial distribution.

Two examples of A_2/A_1 for the ATS-5 links are shown in Figures 3.1-4 and -5. In Figure 3.1-5 the measurements were made during nearly continuous rains, while high variations of rain rate were associated with Figure 3.1-4. It is assumed that the variations of drop size distribution accounts for the scatter in Figure 3.1-5. The ATS-6 results (Ref. 3.1-10) shown in Figure 3.1-6, including 287 minutes of rainfall, do not show a simple relationship between the attenuations at 20 and 30 GHz. Clearly, these results have not demonstrated the validity of the proposed models. However, when cumulative statistics (to be discussed in more detail below) are compared, the ratio appears to be much more uniform. A best fit curve for the 20 and 30 GHz measurements during July and August 1974, shown in Figures 3.1-7, yielded (Ref. 3.1-12)

$$\frac{A_{30} L}{A_{20} L} = 1.88 \ (A_{20} L)^{-0.0306}$$

The cumulative distribution of fades for ATS-5, ATS-6 and CTS have been measured by NASA at Rosman, North Carolina. In Figure 3.1-8 the ATS-5

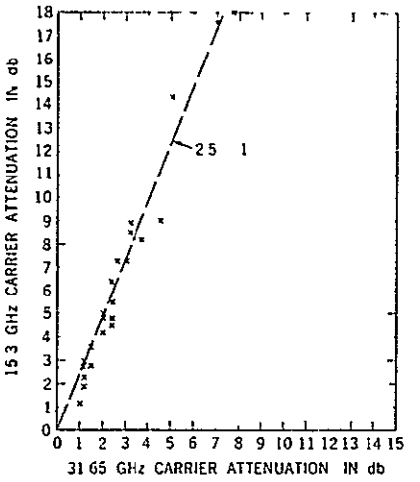

FIGURE 3.1-4. UPLINK-DOWNLINK ATTENUATION COMPARISON, DAY 167, 2000 to 2300 GMT, WC-7 (continuous rain) (June 16, 1970)

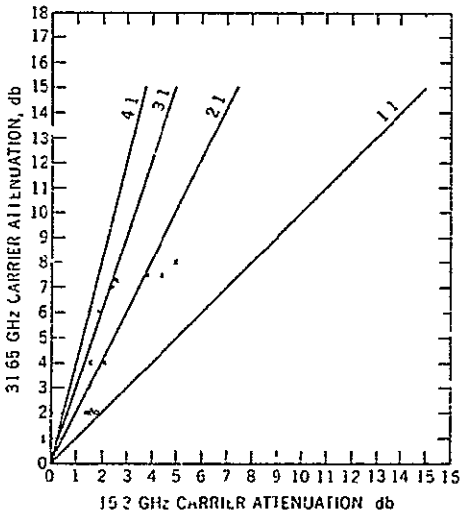

FIGURE 3.1-5. UPLINK-DOWNLINK CARRIER ATTENUATIONS, DAY 202, 1730 to 1800 GMT, WC-7 (continuous rain) (July 21, 1970)

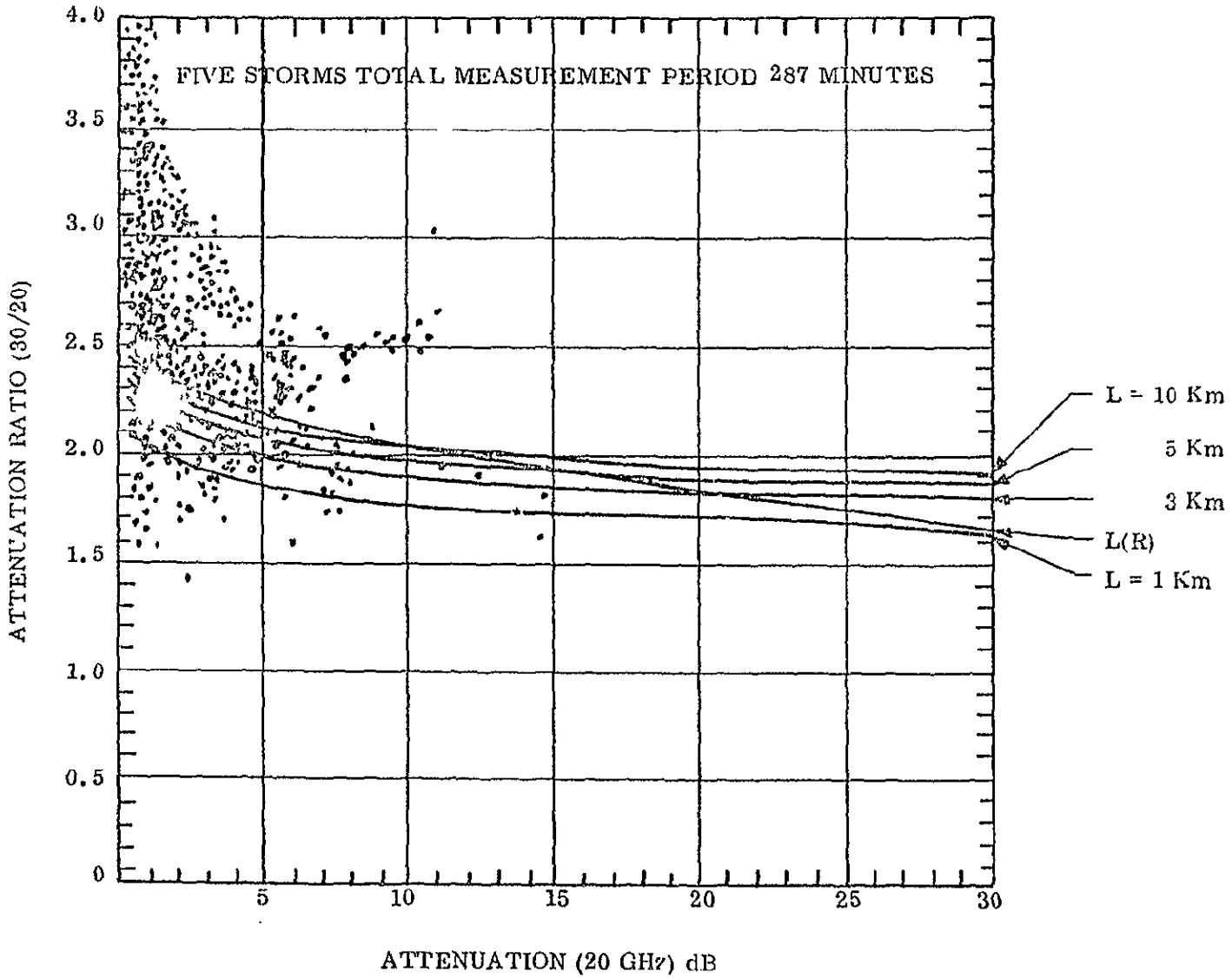

FIGURE 3.1-6. TOTAL ATTENUATION RATIO DATA

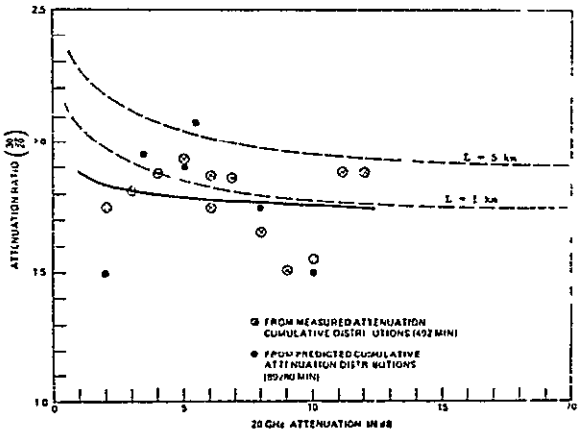

FIGURE 3.1-7. ATTENUATION RATIO FROM ATTENUATION STATISTICS, ROSMAN, N.C., JULY AND AUGUST 1974

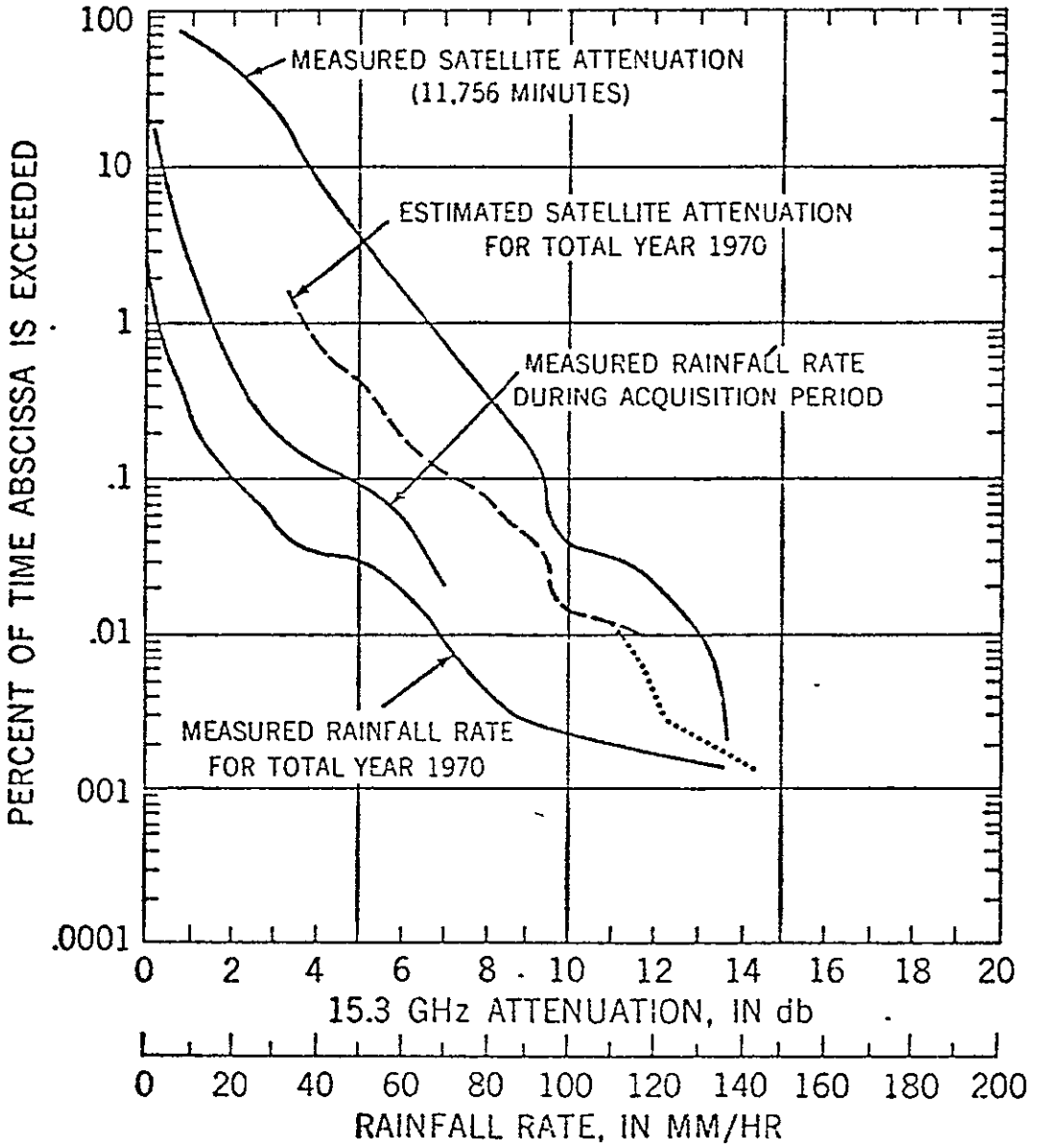

FIGURE 3.1-8. CUMULATIVE DISTRIBUTIONS FOR CALENDAR YEAR 1970, ROSMAN, N.C.

attenuation statistics from February 14 to December 31, 1970, including 11,756 minutes of attenuation measurements, are presented. Since the two rain rate distributions in Figure 3.1-8 are similar, the estimated satellite attenuation curve for CY 1970 was developed. The ATS-5 cumulative distributions for January 1 through August 3, 1971 are shown in Figure 3.1-9. A best fit equation for the CY 1970 Rosman data was developed and applied to other locations where instantaneous precipitation data was available. The resulting estimates are shown in Figure 3.1-10. These estimates demonstrate that variations of several orders of magnitude can be expected depending on location within the continental U.S.

The cumulative statistics for the ATS-6 satellite beacons for Rosman, North Carolina are given in Figure 3.1-11. From this long-term data taken from July 1974 to May 1975 (except for October, November, and December), the ratio $A_{30}L/A_{20}L \sim 2.1$. The rain rate exceeded 10 mm/hr (corresponding to approximately 5 dB attenuation) about 0.2 percent of the time. This reference point allows one to shift the curves in Figure 3.1-11 to cover the total time periods of July - October 1974 and January - May 1975 (Ref. 3.1-10).

The initial year's data from the 11.7 GHz CTS beacon has been analyzed for both the NASA Rosman and GSFC ground stations. The cumulative results for the period June 1976 to May 1977 are shown in Figures 3.1-12 and -13. The data in Figure 3.1-12 (GSFC) represents the total available CTS beacon time (318 days) while the Rosman data (Figure 3.1-13) represents a shorter period because measurements were only made 8 hours per day from June 1976 to March 1977. From March through June the data was recorded automatically 24 hours per day. The rain rate data was taken with a single tipping bucket at GSFC and with both a single bucket and a network of nine additional buckets under the beam (Ref. 3.1-11) at Rosman, NC. For comparison, the worst month data for this same year period is given in Figure 3.1-14. The Greenbelt (GSFC) data utilizes instantaneous measurements, compared to four second averages at Rosman. Consequently, the peak attenuation values below the 0.1% level are expected to be higher for Rosman. For percentage values near 0.01% and less, it has been observed that the data is dependent on the averaging time. Therefore the GSFC (Greenbelt) data is expected to be more representative of the worst month statistics.

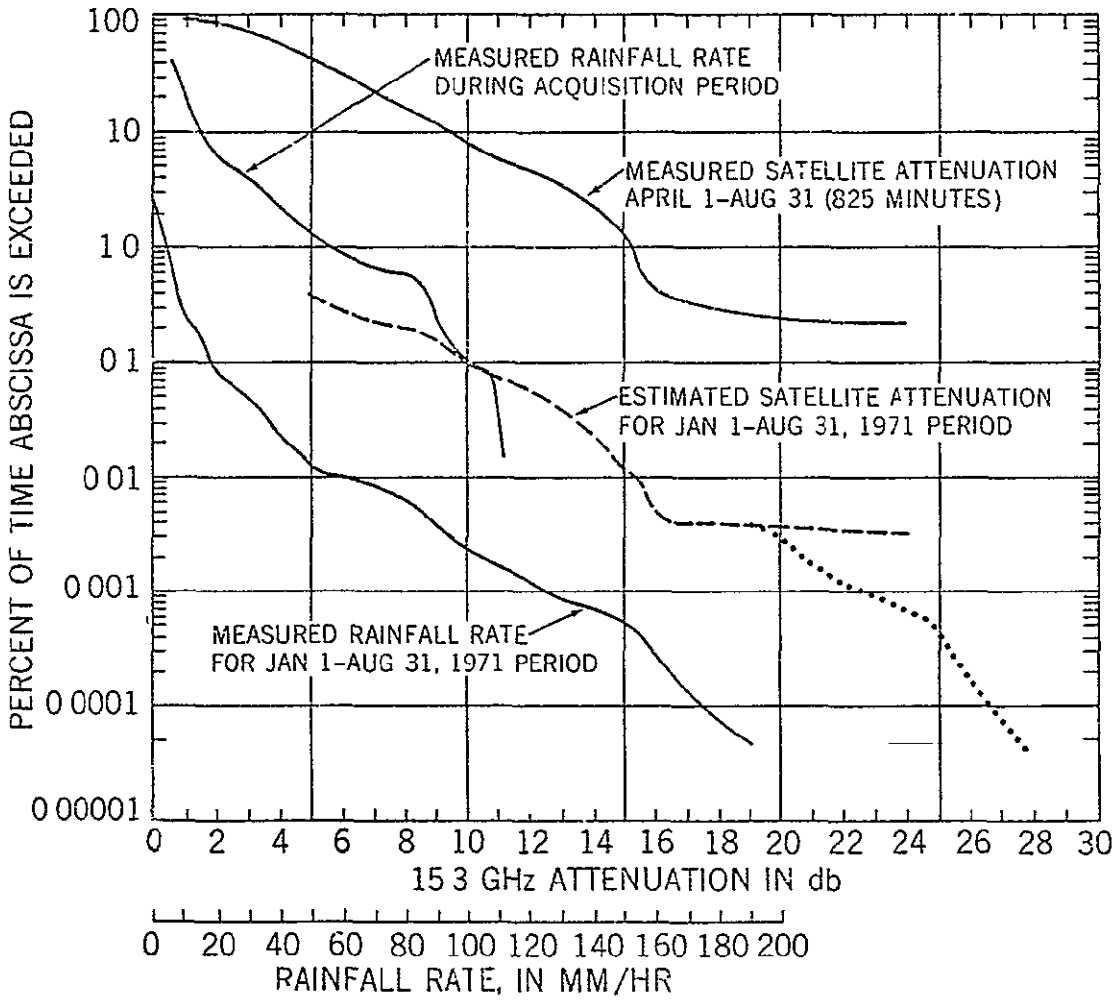

FIGURE 3.1-9. CUMULATIVE DISTRIBUTIONS FOR 1971, ROSMAN, N C.

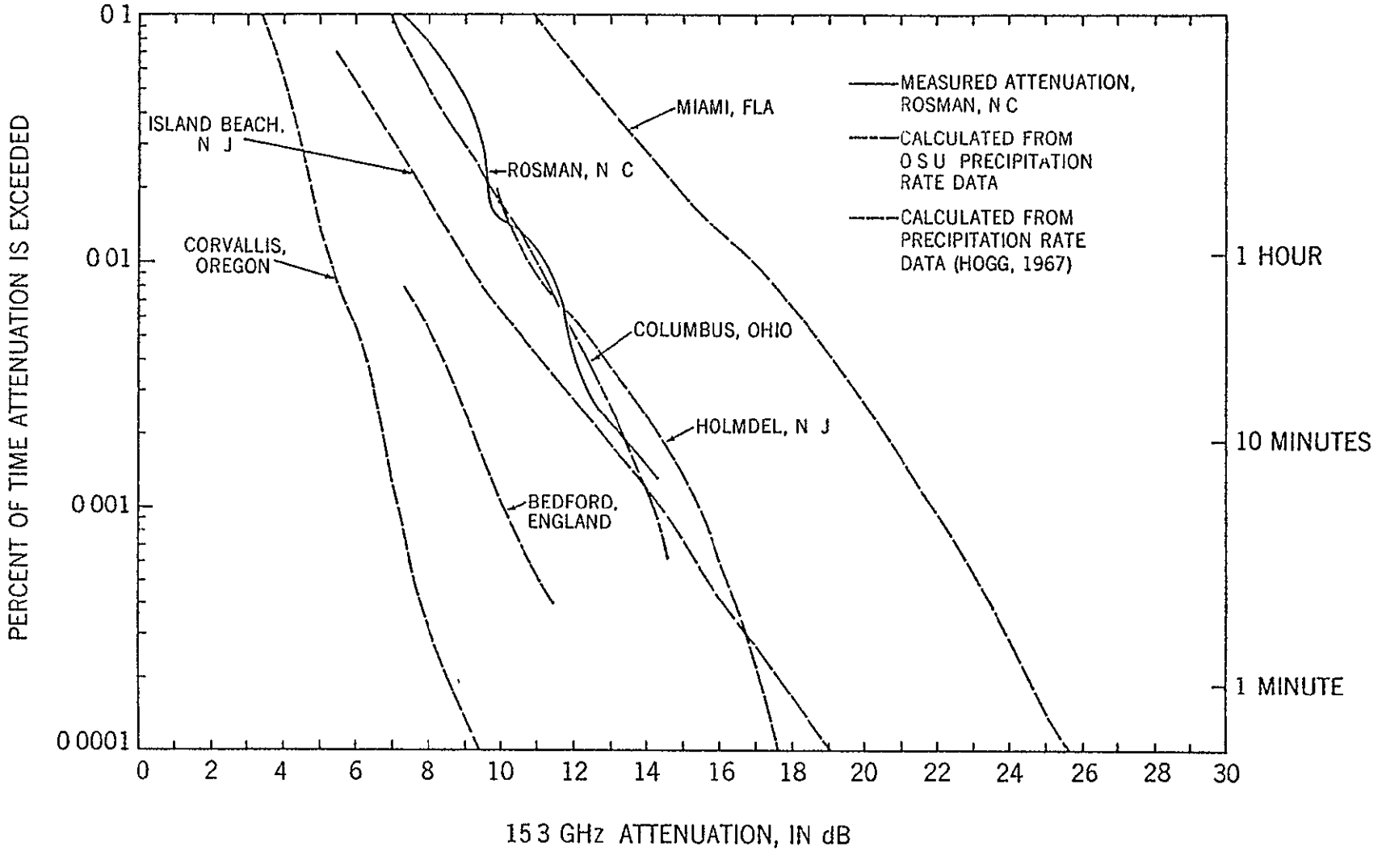

FIGURE 3.1-10. PREDICTED ATTENUATION DISTRIBUTIONS FROM PRECIPITATION RATE DATA FOR VARIOUS LOCATIONS

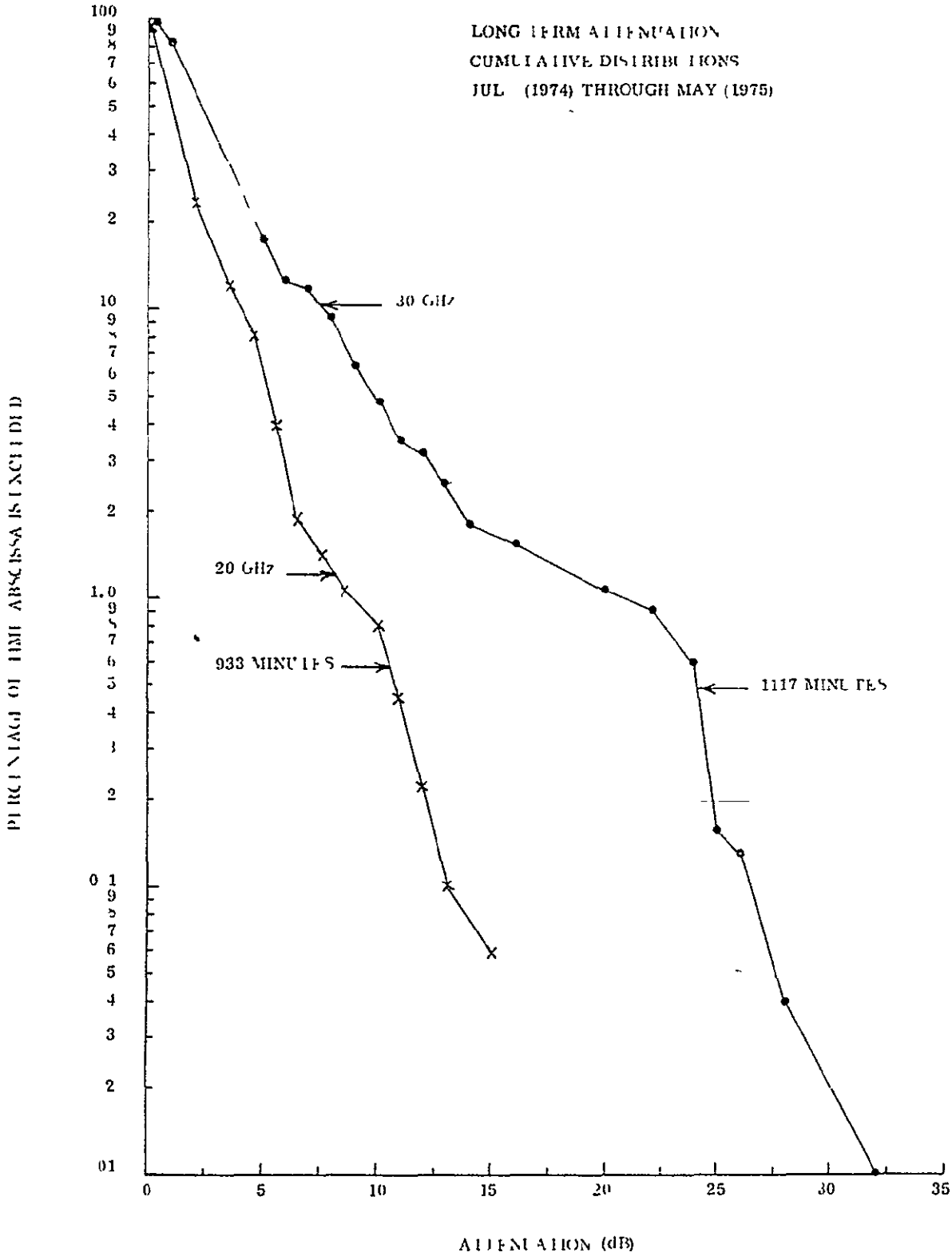

FIGURE 3.1-11. LONG-TERM ATTENUATION CUMULATIVE DISTRIBUTIONS

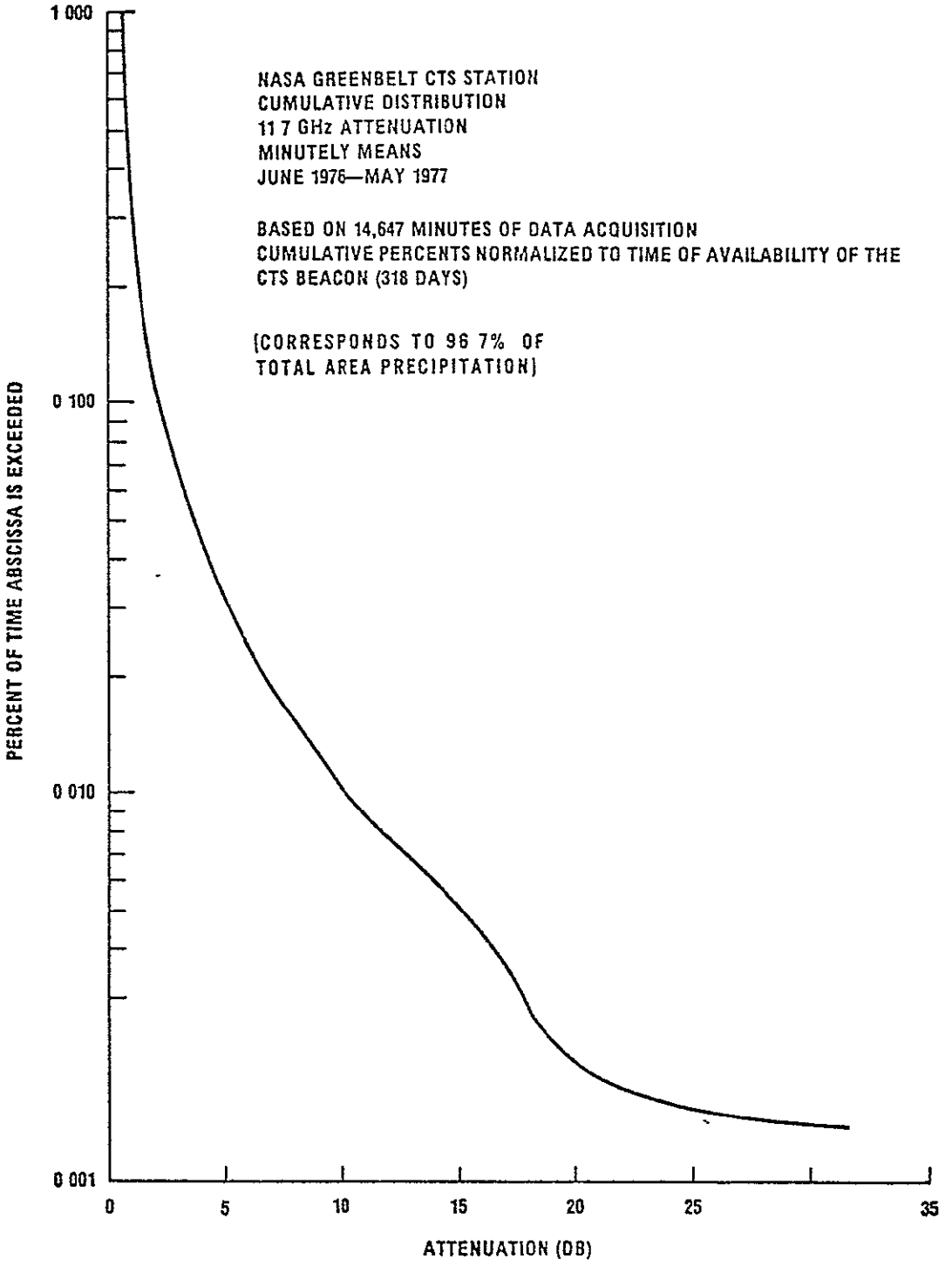

FIGURE 3.1-12. YEARLY CUMULATIVE DISTRIBUTION FOR 11.7 GHZ ATTENUATION MEASURED AT THE GREENBELT STATION (GSFC)

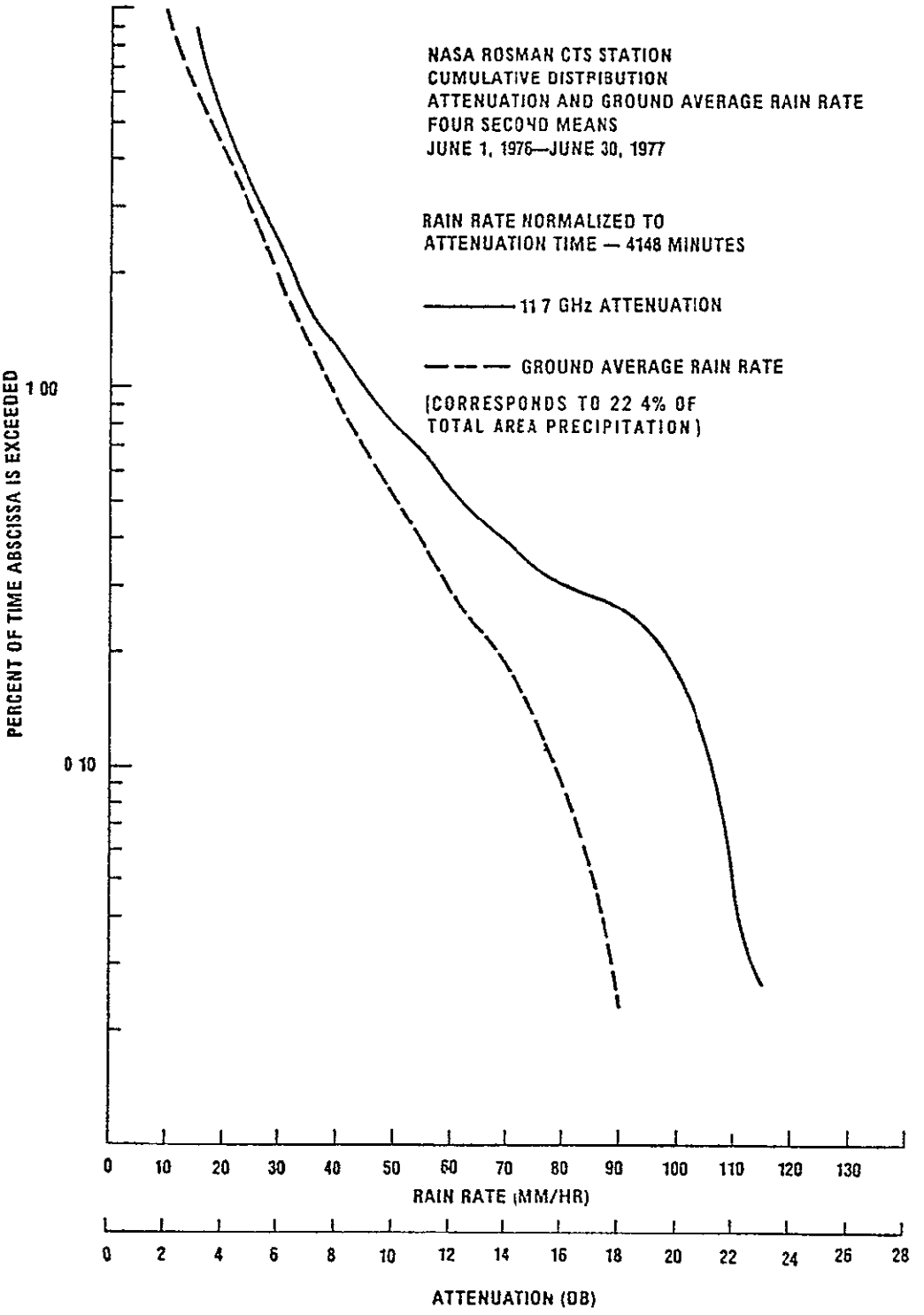

FIGURE 3.1-13. LONG-TERM GROUND-AVERAGED RAIN RATE AND ATTENUATION DISTRIBUTIONS AT THE ROSMAN, NORTH CAROLINA STATION

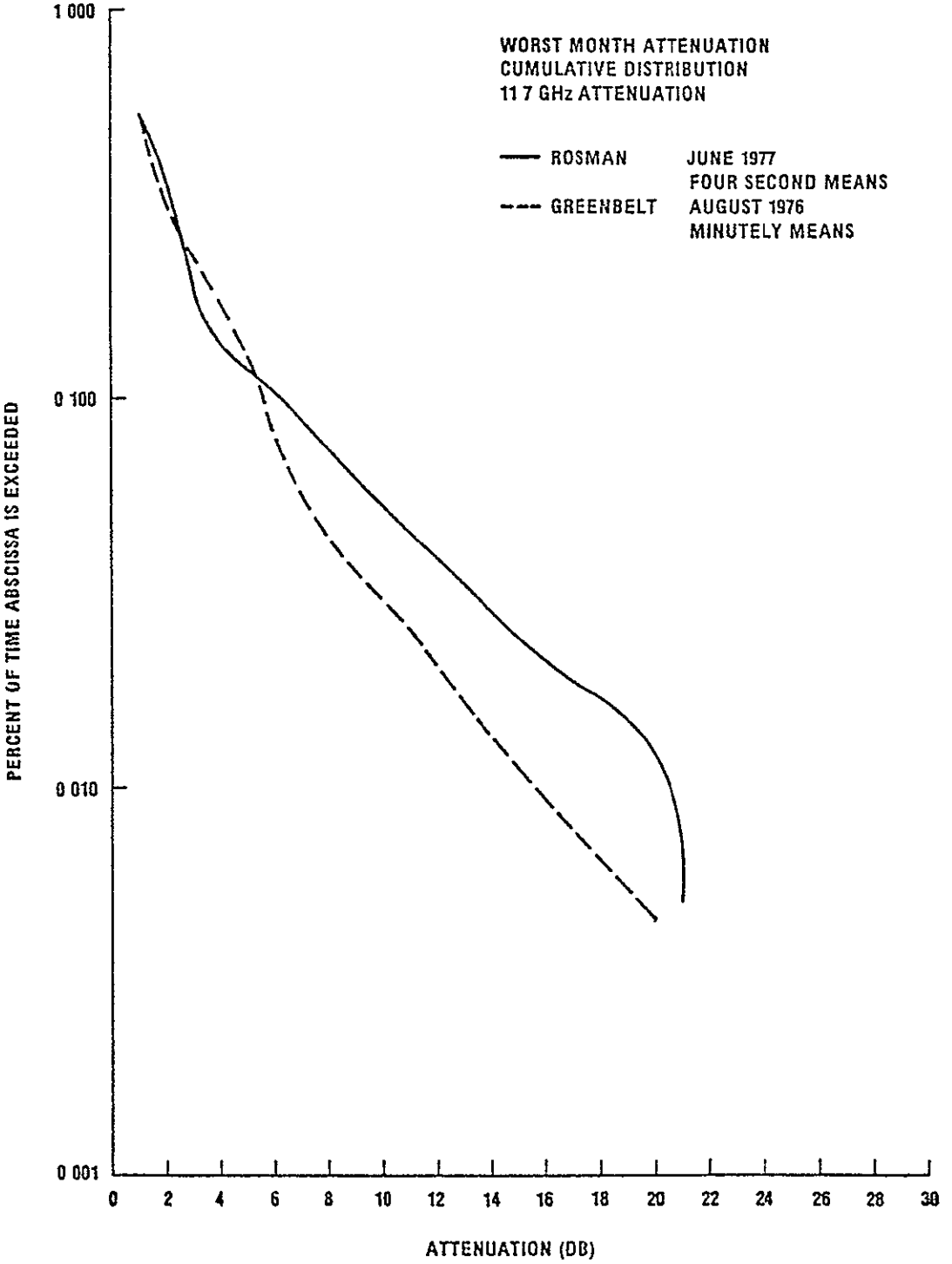

FIGURE 3.1-14. WORST MONTH ATTENUATION CUMULATIVE DISTRIBUTION 11.7 GHZ ATTENUATION

A summary of the first year's NASA attenuation measurements on the 11.7 GHz CTS beacon is presented in Table 3.1-2. In Greenbelt, May 1977 is also listed as a worst month but is probably not representative because of the violent storm on May 6. This single event dominated the month for over 0.01% (43 minutes) and is a very rare occurence.

3.1.2 Amplitude Scintillations

Amplitude scintillations on ATS-5 and ATS-6 have been measured during both clear and rainy weather. Because of the 76 revolutions/minute spin imparted to ATS-5, the scintillation measurements were limited to frequencies removed from the spin frequency. Analyses were performed at Ohio State and are reported in Ref. 3.1-13.

Scintillations of $\pm$ 1 dB have been recorded as a cloud passes through the ATS-6 20-GHz beam (Ref. 3.1-12). The fluctuation rate was fairly constant at about 16 cycles per minute. The scintillations lasted for about 200 seconds. In addition, short bursts of scintillations have been observed for 10 to 20 second intervals on clear days. Their amplitude reaches 3 dB pk-pk with a fluctuation rate of 20 Hz. The causes of the clear air bursts have not been determined and are presently under study.

3.1.3 Attenuation on Video Channels

NASA Goddard and Rosman are beginning to evaluate the effects of rain attenuation on television transmissions via the CTS satellite. To date, the scheduled video transmissions and rain events have not coincided (Refs. 3.1-11, 3.1-14 and 3.1-15).

Simulations of link carrier-to-noise (C/N) and test tone-to-noise (TT/N) ratios (in 4.2 MHz bandwidth) have been completed by varying the GSFC ground link transmitter power P_{tg} during clear weather. Reception was also done at GSFC. The results of these tests are given in Table 3.1-3. Note that 10 dB C/N is sufficient to yield a good picture.

TABLE 3.1-2. SUMMARY OF CTS 11.7 GHZ ATTENUATION STATISTICS

	PERCENTAGE VALUES		
	0.1%	0.01%	0.005%
Rosman (4 Sec. Mean) Yearly = 4148 Minutes (Less than 22.4% of Total Precipitation*)	2.2 dB	8 dB	11.2 dB
Worst Month June 1977 689 Minutes	6.4 dB	20.2 dB	21.2 dB
Greenbelt (Minutely Mean) Yearly = 14647 Minutes (Within 96.7% of Total Precipitation*)	2.1 dB	10 dB	15 dB
Worst Month August 1976 351 Minutes	5 dB	15.6 dB	19.4 dB
Worst Month May 1977 227 Minutes	6.5 dB	>30 dB	

*Corresponds To Total Area Precipitation.

TABLE 3.1-3

VIDEO SIGNAL QUALITY VERSUS LINK PARAMETERS

P_{ts}	P_{tg}	Link C/N	Link TT/N	Comments
96 watts	30 watts	12 dB	30.5 dB (est.)	Good clear picture
72 "	21 "	10.5 "	29.5 "	No noticeable noise
46 "	10 "	7.5 "	24 "	Noise becoming noticeable
36.5 "	8 "	6.2 "	21 "	Becoming objectionably noisy
29.5 "	5 "	5 "	15.5 "	Picture very noisy (objectionable)
23 "	4 "	3.9 "	6 "	Picture completely objectionable

REFERENCES

3.1-1 Gunn, L. S., and T. W. R East, "The Microwave Properties of Precipitation Particles," Jrnl. Royal Meteorological Soc., Vol. 80, 1954.

3.1-2 Robertson, E. A., and D. E. Sukhia, "Relationship Between the Atmos-Atmospheric Attenuation of Satellite Path Signals and Ground Rain Rate," in Papers from the 1972 Spring URSI Session on Experiments Utilizing the ATS-5 Satellite, compiled by L. J. Ippolito, NASA/GSFC Doc. X-751-72-208, May 1972.

3.1-3 Fang, D. J., and J. M. Harris, "A New Method of Estimating Microwave Attenuation Over a Slant Propagation Path Based on Rain Gauge Data," IEEE Trans. Ant. Prop., pp 381-4 (May 1976).

3.1-4 Ippolito, L. J.,"Millimeter Wave Propagation Measurements from the Applications Technology Satellite (ATS-V)," IEEE Trans. Ant. Prop., pp 535-552, July 1970.

3.1-5 Ippolito, L. J.,"Summary and Evaluation of Results from the ATS Millimeter Wave Experiment," in Papers from the 1972 Spring URSI Session on Experiments Utilizing the ATS-5 Satellite, compiled by L. J. Ippolito, NASA/GSFC Doc. X-751-72-208, May 1972

3.1-6 Harman, L. K.,"Rain Rate and Atmospheric Attenuation Statistics at Millimeter Wave Frequencies".

3.1-7 Rogers, D. R, Olson and D. B. Hodge, "The Basis of the aR^b Relation in the Calculation of Rain Attenuation," in preparation.

3.1-8 Evans, H. W.,"Attenuation on Earth-Space Paths at Frequencies Up to 30 GHz," Intl. Conf. Comm., Montreal, Canada, pp 27-1 to 27-5, June 1971.

3.1-9 Hodge, D. B.,"Frequency Scaling of Rain Attenuation," IEEE Trans. Aut. Prop., Vol. AP-25, pp 446-7, May 1977.

3.1-10 "ATS-6 Millimeter Wave Propagation Experiment Final Data Analysis Report," prepared by Westinghouse Elect. Corp., Baltimore, Md., Contract NA55-20904, September 1975.

3.1-11 "Communications Link Characterization Experiment (CLCE)," Vol. 3, Technical Data Report prepared by Westinghouse Elect. Co., Baltimore, Md., August 1977, Contract NA-55-20729.

3.1-12 Ippolito, L. J., "ATS-6 Millimeter Wave Propagation and Communications Experiments at 20 and 30 GHz," IEEE Trans. Aerospace and Electronics Syst., Vol. AES-11, pp 1067-1082, November 1975

3.1-13 Levis, C. A., and V. Ungvichian, "Preliminary Analysis of 15 GHz Scintillations on an ATS-5 Satellite-to-Ground Path," Final Report, Ohio State University ElectroScience Lab, February 1976.

3.1-14 "CTS Communications Link Characterization Experiment," Vol. 1, Tech. Data Report prepared by Westinghouse Elect. Corp., Baltimore, MD, Contract NAS5-20729, January 1977.

3.1-15 Harman, L., Private Communication, 1977.

3.2 SITE DIVERSITY

3.2.1 Overview

NASA has initiated, supported, directed and participated in the study and application of site diversity (sometimes referred to as path or space diversity) techniques to improve the reliability of Earth-satellite links. Above 10 GHz these links are primarily influenced by rain cells passing through the link path. By properly positioning two or more ground stations and utilizing the signals from the station having the strongest signal, a diversity gain results. This gain is shown schematically in Figure 3.2-1 for one station and is defined as the improvement in system margin at a given reliability level. Additional gain terms are defined when three or more stations are participating in site diversity.

The site diversity measurements have been made utilizing the beacons on both the ATS-5 and ATS-6 satellites at Ohio State University and utilizing the ATS-6 beacon at GSFC, COMSAT Laboratories, NRL, Westinghouse and the University of Texas. Therefore these results are applicable to the eastern and mid-USA. OSU has published an empirical fit to their ATS-5 diversity gain data (Ref. 3.2-1) which is

$$G = \left[A - 3.6\left(1 - e^{-0.24A}\right)\right] \quad \left[1 - e^{-0.46\, D\left(1 - e^{-0.26A}\right)}\right]$$

where G is the diversity gain in dB

A is the fade attenuation in dB

D is the separation between stations in km.

This relation fit the OSU and Bell Telephone Laboratories data (Ref. 3.2-1) to $\pm$ 0.75 dB in the 15 to 16 GHz frequency range. The following data also demonstrates that the diversity gain is relatively independent of frequency in the 13 to 30 GHz region and is only slightly dependent on the rain cell direction of motion with respect to the link path for moderate elevation angles ($30\text{-}50^{\circ}$).

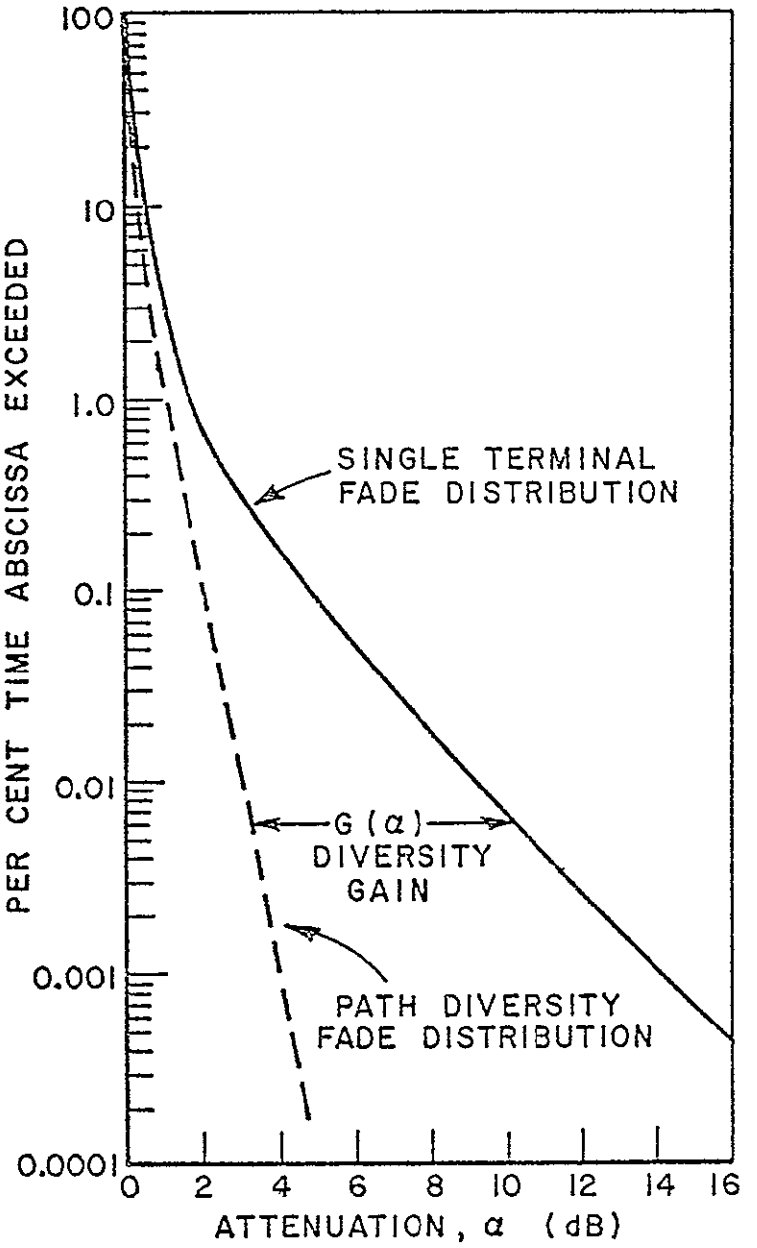

FIGURE 3.2-1. TYPICAL FADE DISTRIBUTION

3.2.2 Site Diversity Experiments with ATS-5

Ohio State University (OSU) and Bell Telephone Laboratories (BTL) have made measurements of the diversity gain versus site separation distance. OSU used the ATS-5 beacon at 15.3 GHz and BTL used radiometer temperature data (related to rain attenuation) to measure fade depths at seven different terminal spacings ranging from 3.2 to 31.4 km (Refs. 3.2-1, -2). These results are summarized in Figure 3.2-2 which demonstrates that the diversity gain is relatively independent of separation distances greater than 8 km, and for fade depths greater than 3 dB the diversity gain is 2 to 3 dB below the ideal diversity gain for two stations. These results have generally been accepted as being representative of the realizable diversity gain and the separation distance dependence of the diversity gain.

3.2.3 Site Diversity Experiments with ATS-6

Based on the ATS-5 results more advanced diversity experiments were conducted utilizing the 20 and 30 GHz beacons on ATS-6. A long-baseline site diversity experiment (Ref. 3.2-3) including the four sites at NASA/GSFC, NRL, COMSAT and the Westinghouse Defense and Electronics Systems Center near Baltimore, MD was established with site separation distances ranging from 27.9 km to 75.8 km. For these site separations it appeared that the probability for separate rain cells affecting more than one site at the same time was higher than for 8 km (nominal) separations. Also the weather patterns (i.e., the percentage of time a fade exceeded a specified value) were significantly different at the various sites. The resulting diversity gain was therefore small compared to that shown in Figure 3.2-2.

Both OSU and COMSAT continued to investigate the separation distance dependence of the diversity gain and the optimum orientation of the sites with respect to the rain cell motion and the satellite link. At the OSU site both OSU and COMSAT conducted experiments. The OSU stations (Ref 3.2-4) were located in a triangular configuration, while COMSAT's terminals were arranged in an E-W orientation as shown in Figure 3 2-3. The OSU data shown in Figure 3.2-4 clearly indicates that the NW-SE orientation of the sites yielded the highest diversity gain and that the diversity gain decreases slightly for 30 GHz compared to 20 GHz. Other OSU data indicated that for a

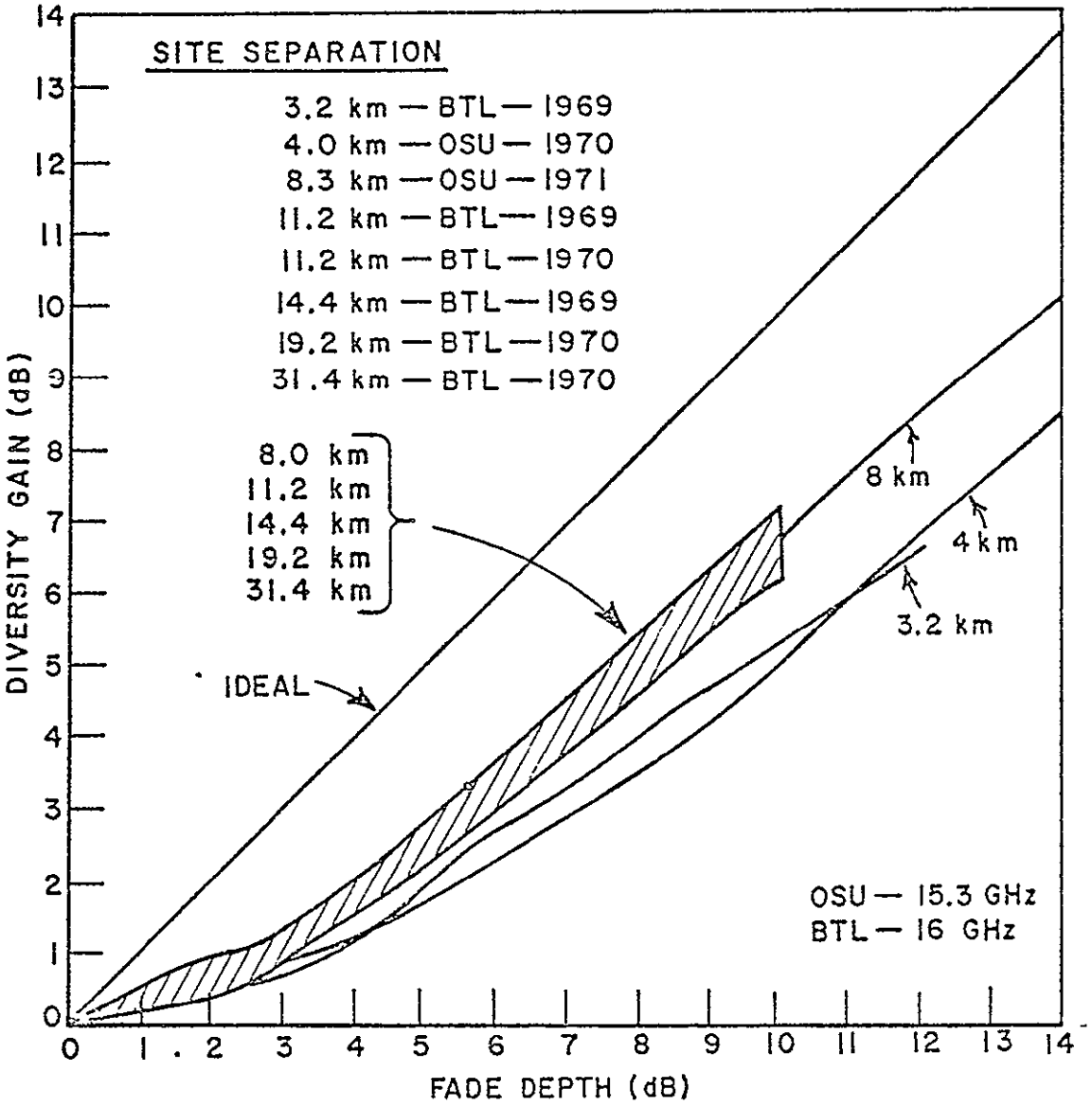

FIGURE 3.2-2. DIVERSITY GAIN VS. FADE DEPTHS

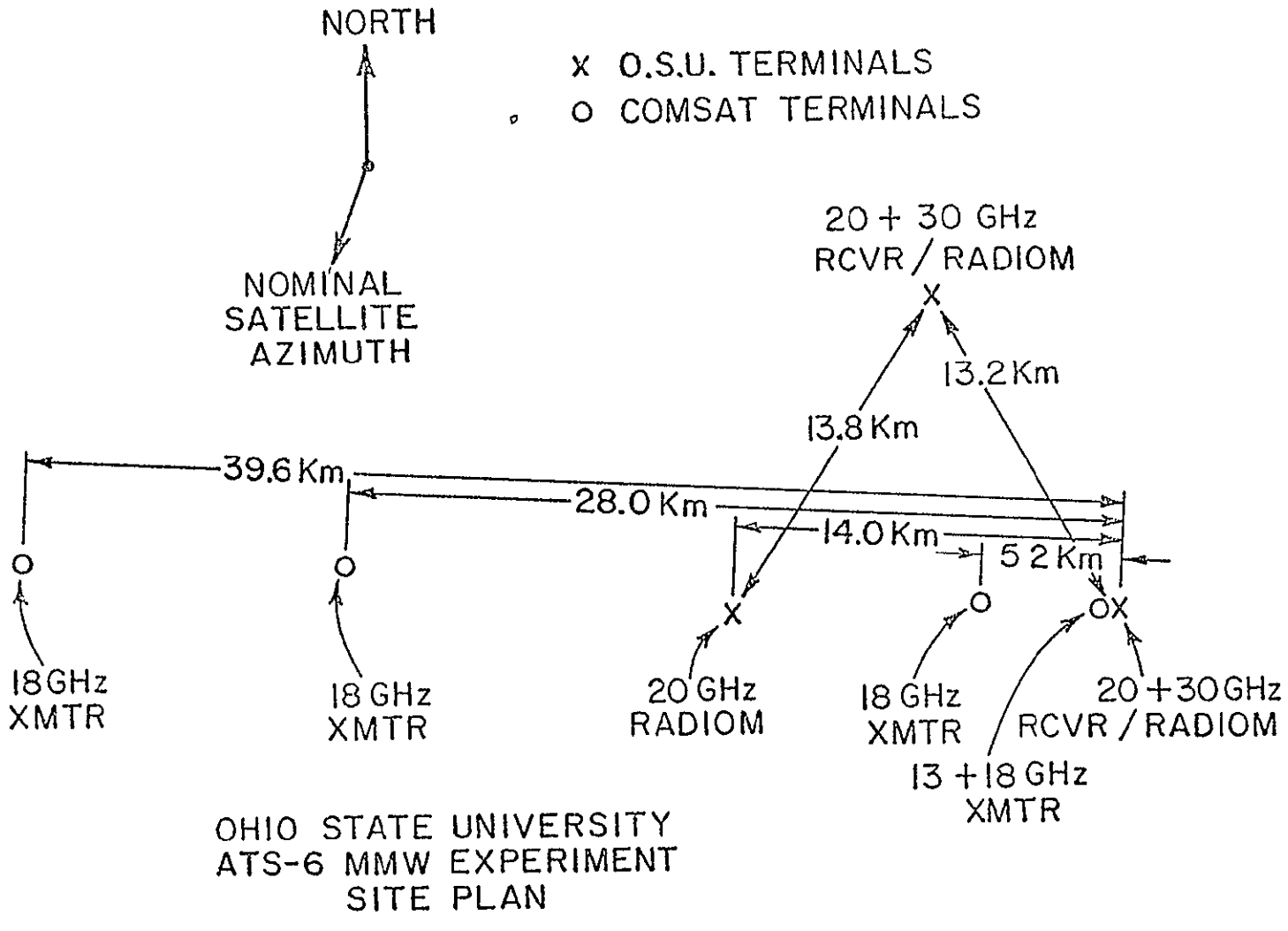

FIGURE 3.2-3. OSU ATS-6 MMW EXPERIMENT SITE PLAN

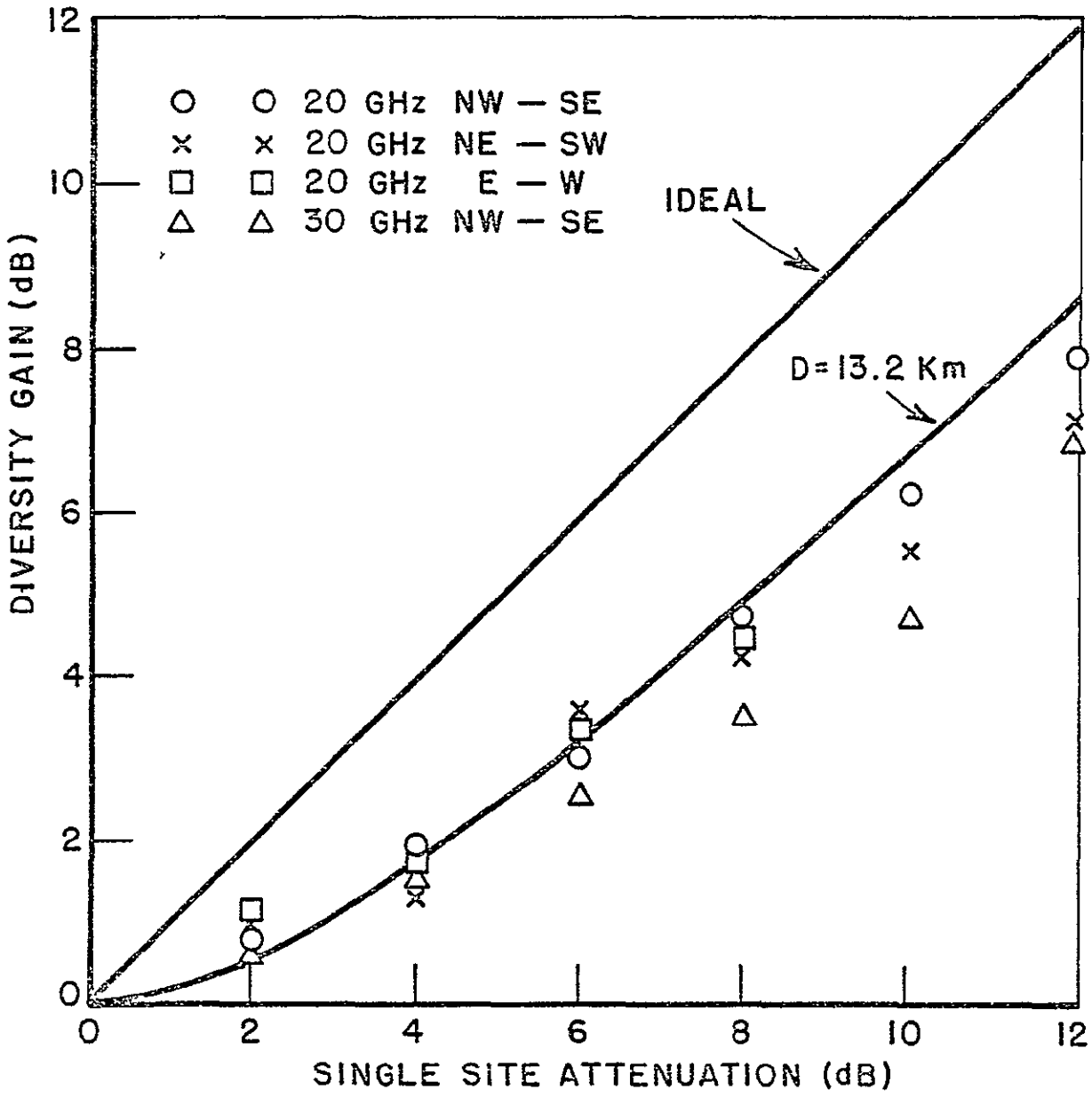

FIGURE 3.2-4. DIVERSITY GAIN VS. SINGLE SITE ATTENUATION

separation distance of 13.2 km the diversity gain at 30 GHz exceeded that at 20 GHz (see Figure 3.2-5). The solid curves in Figures 3.2-4 and 5 are plots of the empirical relation presented in Section 3.2.1.

At the University of Texas a two-site diversity experiment was conducted at 30 GHz over a separation distance of 11 km in a N-S orientation (Ref 3.2-5). The diversity gain measured over a 93 day period is shown in Figure 3.2-6. This data agrees closely with the OSU/BTL results given in Figure 3.2-5 and extends the OSU data to fade depths of the order of 25 dB.

Three groups of ground stations participated in the COMSAT 18 GHz site diversity experiment (Ref 3.2-6). Each site employed four stations spaced in an E-W orientation at 4, 12 and 8 miles. This COMSAT data appears similar to OSU, BTL, and U of T data up to fade depths of the order of 10 dB. At higher fade depths the COMSAT diversity gain remained constant or decreased. Similar results were observed at the other two COMSAT diversity sites.

As an example of the effectiveness of utilizing site diversity, the University of Texas group estimated that their two-station system was equivalent to raising the fade margin at one site by 20 dB. In particular, assuming a 10 dB link margin at 30 GHz, the reliability of one station was 99.83% and increased to 99.997% with two stations.

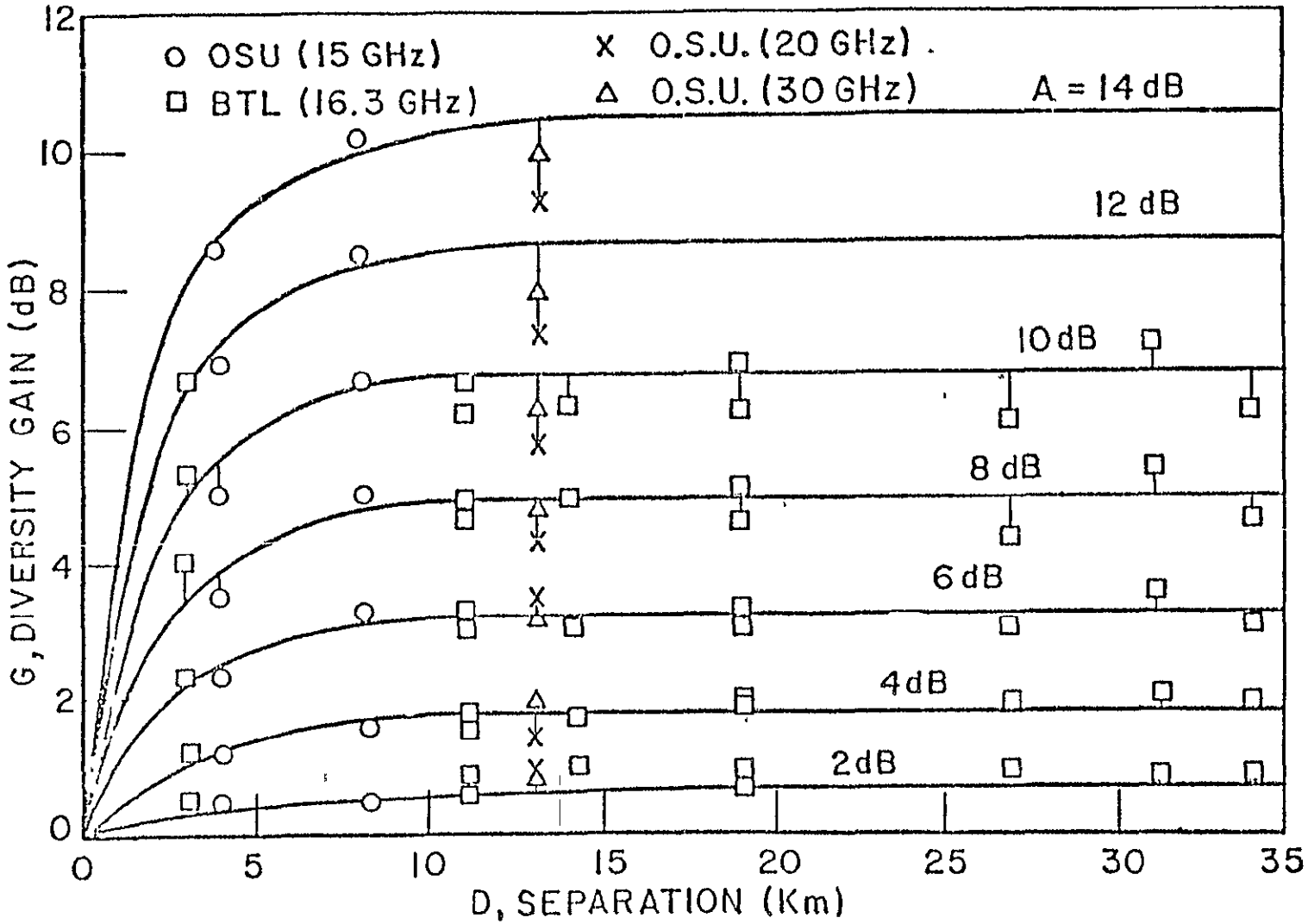

FIGURE 3.2-5. DIVERSITY GAIN VS. SEPARATION DISTANCE

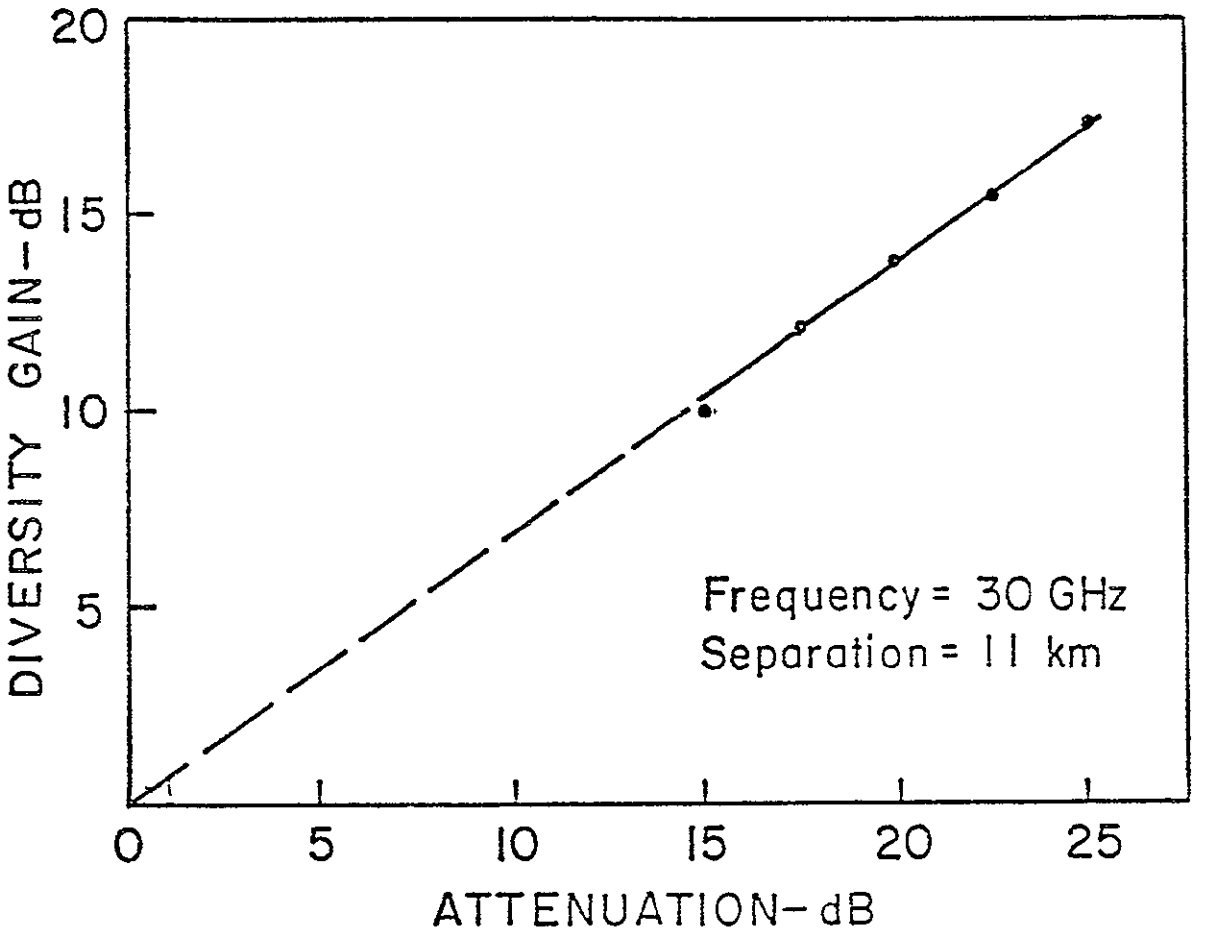

FIGURE 3.2-6. DIVERSITY GAIN AS A FUNCTION OF SINGLE SITE ATTENUATION

REFERENCES

3.2-1 Hodge, D.B., "An Empirical Relationship for Path Diversity Gain," I.E.E.E Trans. Ant. & Prop. AP-24, 250 (March, 1976); and D.B Hodge, "Space Diversity for Reception of Satellite Signals," Dept. of Elec. Eng., Ohio State University, Columbus, Ohio, Tech. Report 2374-16, October, 1973.

3.2-2 Wilson, R. W., "A Three-Radiometer Path-Diversity Experiment," Bell System Tech. Jrnl. 49, (1970); and R.W. Wilson and W.L. Mannel, "Results from a Three Radiometer Path Diversity Experiment," Proc. Conf on Propagation of Radio Waves at Freq. above 10 GHz, London, April, 1973.

3.2-3 "ATS-6 Millimeter Wave Propagation Experiment," Westinghouse Electric Corp., Baltimore, MD report for NASA/GSFC, Contract NAS5-20904, September, 1975.

3.2-4 Hodge, D.B., D.M. Theobold and R.C. Taylor, "ATS-6 Millimeter Wavelength Propagation Experiment," Final Report 3863-6, Ohio State University ElectroScience Lab., January, 1976.

3.2-5 Vogel, W.J., A.W. Straiton, B.M. Fannin and N.K. Wagner, "ATS-6 Attenuation Diversity Measurements at 20 and 30 GHz, Final Report of Elect. Eng. Res. Lab., University of Texas at Austin, November, 1975.

3.2-6 Hyde, G., "Data Analysis Report on ATS-F COMSAT Millimeter Wave Propagation Experiments," Parts I and II. COMSAT Final Reports, September, 1975.

3.3 LOW ANGLE SCINTILLATIONS/FADING

Measurement of low elevation angle scintillations or fading have been made while ATS-6 was descending and ascending for US observers. In addition, measurements of non-synchronous satellites have been made as their path sweeps through the atmosphere (Ref 3.3-1). These latter measurements are not reported here

As ATS-6 was being moved to 35° E longitude, experimenters at the Virginia Polytechnic Institute and State University measured the 20 GHz carrier amplitude during clear and rainy tropospheric conditions from 9° elevation angle down (Ref 3.3-2). During clear weather the average signal decreased due to clear air attenuation, but 2-3 dB scintillations with a period of 4 minutes were observed at 9° elevation angle. As the weather became hazier, the amplitude of the scintillations remained near 2 dB but the period decreased to 6 seconds. As the elevation angle decreased to 4 degrees, signal fluctuations averaged 7 dB. During rainy conditions, fades of 15 to 20 dB were observed for 10 mm/hr. rain rates. These high values are assumed due to the long path length at low elevation angles.

Ohio State University also observed the descent of ATS-6 (Ref 3.3-3) from 42 to 2° elevation angle. The variances of the scintillations as a function of elevation angle are given in Figure 3.3-1. Because the distribution suggested a cosecant behavior, a minimum mean-square-error curve was fit to the data as noted in Figure 3.3-1.

During the return of ATS-6 to 140° W longitude (ascending for U.S. observers) Ohio State and COMSAT conducted elevation-angle measurements over land, while the University of Texas observed over water. The ascending OSU data (Ref 3.3-4) was taken at 2.075 and 30 GHz from -0.7 to 43.9° elevation angles (not corrected for refraction) with no discernable precipitation along the path. The resulting variance is similar to Figure 3.3-1 except that the 2 GHz variance is about 10 dB below the 30 GHz data. OSU also observed that the received power level was significantly below that predicted by simple atmospheric path loss calculations. The power spectra of the scintillations, other than the general reduction of amplitude of all components, was similar for all elevation angles and for the presence or lack of cumulus clouds.

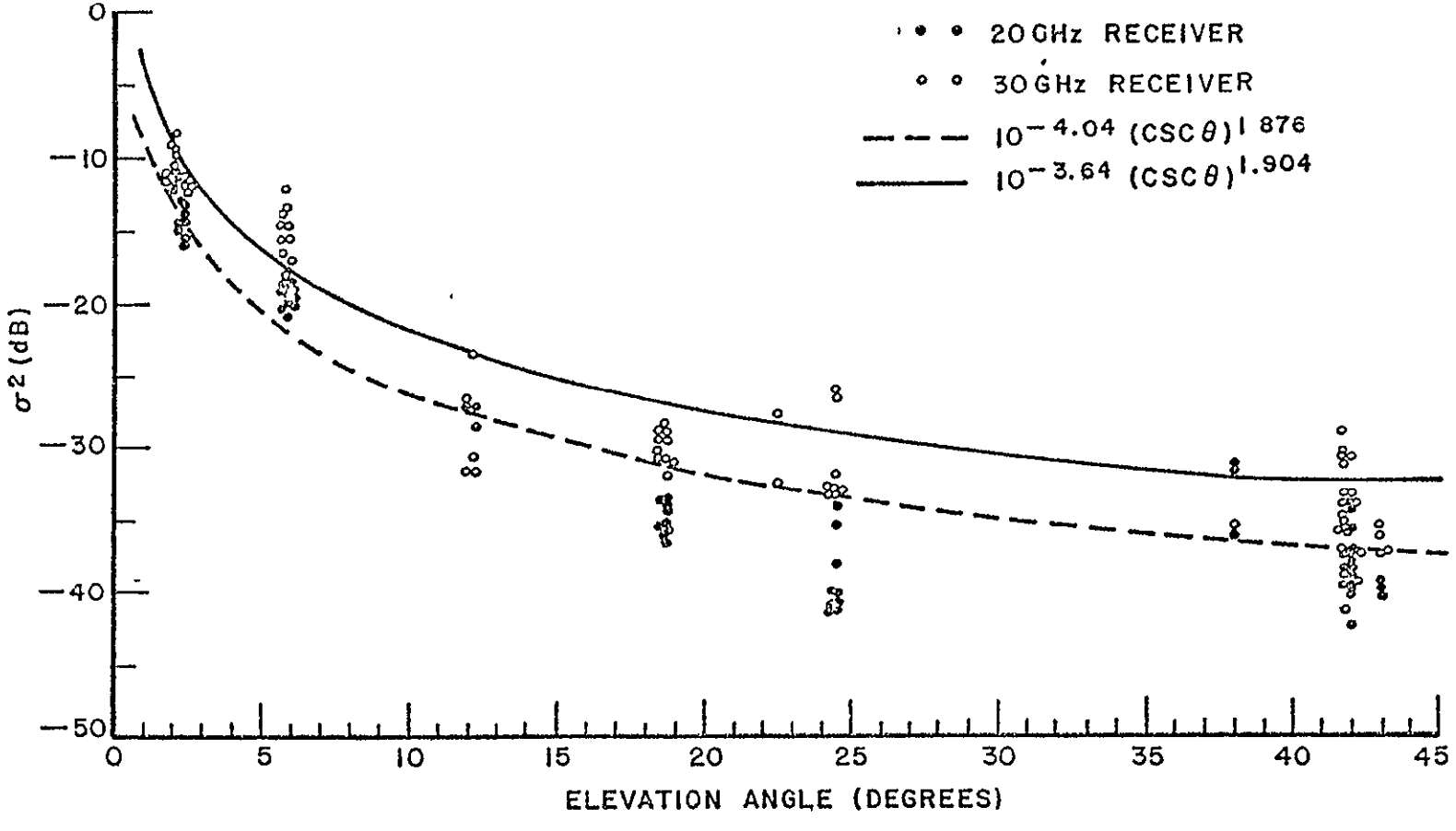

FIGURE 3.3-1. VARIANCE VS. ELEVATION ANGLE

COMSAT Laboratories (Ref 3.3-5) conducted 13.2 GHz measurements at COMSAT and Westinghouse's Facility at Friendship Airport near Baltimore (Ref 3.3-5) as the elevation angle increased from 3.6 to 14 degrees. The results from the Clarksburg site are given in Figure 3 3-2. The crosses denote the median signal levels and the minimum and maximum signal levels recorded during each 45-minute period are indicated by the vertical solid lines. The median signal strength was on the order of 3 dB lower than the predicted clear sky signal strengths. Typical fluctuation periods were 2 seconds with up to 15 dB amplitude fluctuations.

The University of Texas (Ref 3.3-6) installed a 30 GHz receiver at Port Aransas, Texas, to obtain a propagation path entirely over water. The beacon was monitored for at least one hour each day for 16 days in September 1976 while the elevation angle varied from 1.5 to 17.3^{o}. The results presented here are based on 3.36 hours of data (15% of the data base). The cumulative distributions of the log attenuation relative to the day's mean attenuation for an arbitrarily chosen record per elevation angle are shown in Figure 3.3-3. Negative values of the ordinate represent signal levels above the mean. A rain event was observed while the satellite was near 8.5^{o} elevation angle. Because the rain was over water, no rate was measured. However, the mean attenuation increased by 16 dB and the standard deviation increased to 2.7 dB during the rain.

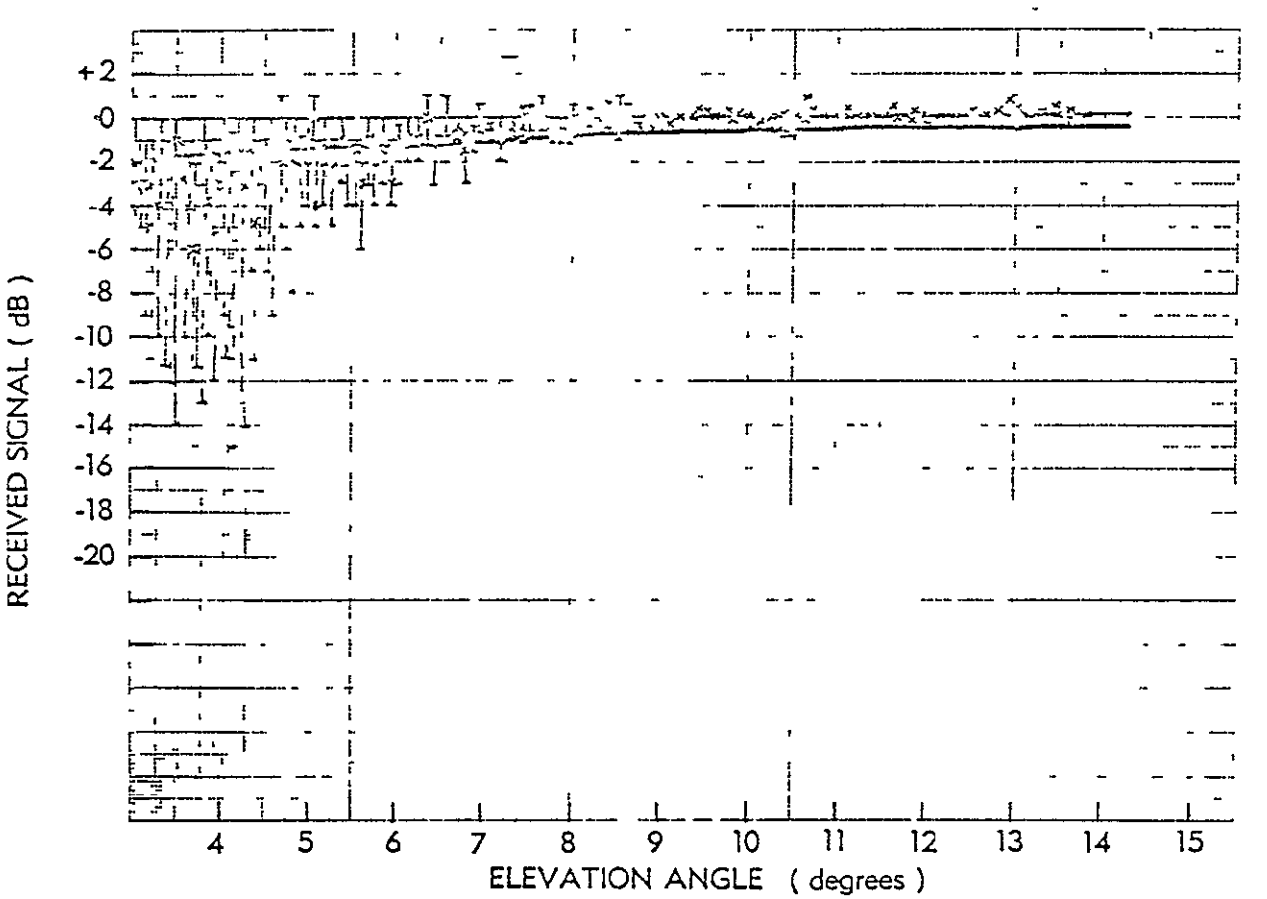

FIGURE 3.3-2. CLARKSBURG CARRIER MEDIAN SIGNAL LEVEL (X) AND FLUCTUATION (I) OF THE RECEIVED SIGNAL AS A FUNCTION OF THE ELEVATION ANGLE

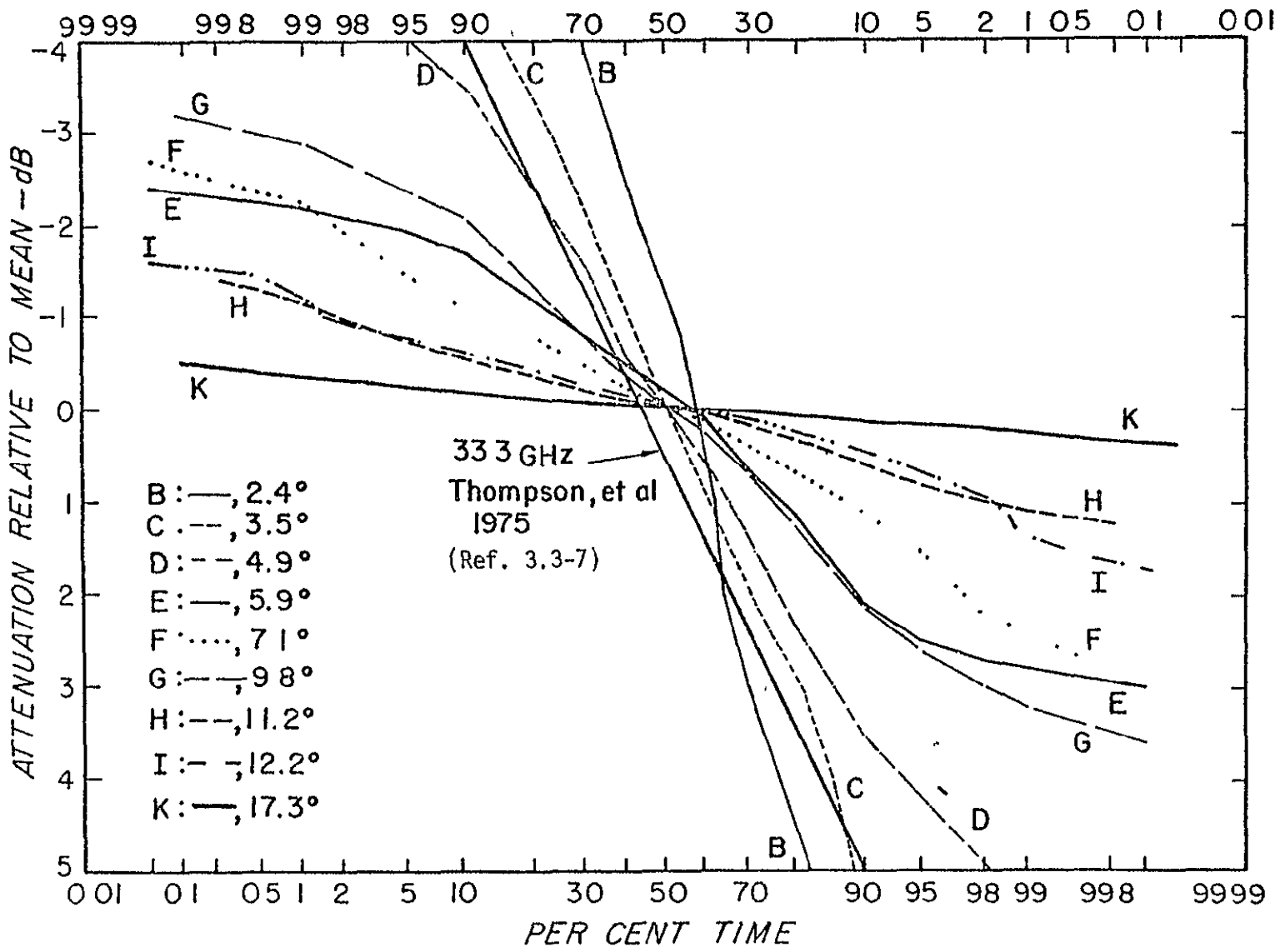

FIGURE 3.3-3. CUMULATIVE DISTRIBUTION OF SIGNAL ATTENUATION

REFERENCES

3.3-1 Crane, R.K., "Tropospheric Scintillation at Microwave Frequencies on an Earth-Space Path," Proc. URSI Meeting, La Baule, France, pgs 415-9 (28 April - 6 May 1977).

3.3-2 Stutzman, W.L., C. W. Bostian, E.A. Manus, R.E. Marshall and P.H. Wiley, "ATS-6 Satellite 20 GHz Propagation Measurement at Low Elevation Angles," Electronics Letters Vol 11, Nos. 25/26, pp 635-6 (11 December 1975).

3.3-3 Hodge, D.B, and D.M. Theobold, "Scintillations Observed on the ATS-6 20 and 30 GHz Downlinks," URSI/USNC Meeting, Boulder, CO, October, 1975 and D.B. Hodge, D.M. Theobold and R.C. Taylor, "ATS-6 Millimeter Wavelength Propagation Experiment," Ohio State University Electro-Science Report 3863-6, January 1976.

3.3-4 Hodge, D.B., D.M. Theobold and D.M.J. Devasirvatham, "Amplitude Scintillation at 20 and 30 GHz on Earth-Space Paths," Proc. URSI Meeting, La Baule, France, pgs. 421-5 (28 April - 6 May 1977).

3.3-5 "Measurements of SHF Tropospheric Fading at Low Elevation Angles Using the ATS-6 in Route West," INTELSAT Memo BG/T-22-25E, 7 November 1977.

3.3-6 Vogel, W.J., A.W. Straiton, and B.M. Fannin, "ATS-6 Ascending. Near Horizon Measurements Over Water at 30 GHz," Radio Science, Vol. 12, pp 757-765, September-October 1977.

3.3-7 Thompson, M.C., Jr., L.E. Woods, H.B. Janes and D. Smith, "Phase and Amplitude Scintillations in the 10 to 40 GHz Band," IEEE Trans. Cent. Prop., Vol AP-23, pp 792-797, 1975.

3.4 DEPOLARIZATION

Frequency reuse, achieved by utilizing orthogonally polarized signals over the same path and at the same frequency, has stimulated investigators to research the depolarization effects for signals above 10 GHz. Rain, snow and ice crystals will cause depolarization resulting in a reduction in dual channel isolation. The measurement of depolarization involves the complex effects of the atmosphere, the polarization utilized and the off-boresight polarization characteristics of the antenna. At this time, measurement statistics for the overall effect are being acquired, but separating the various contributions to depolarization is just beginning.

In 1974 Virginia Polytechnic Institute and State University (VPI & SU) began observing the north-south linear polarization of the ATS-6 20-GHZ beacon which at the spacecraft is maintained to $\pm 0.1^{0}$. They found that mechanical and satellite misalignments were not sufficient to explain the variations they observed during clear weather, nor were Faraday rotation and dielectric stratification a satisfactory explanation (Ref 3.4-1). Measurements at 20 GHz on ATS-6 during snow squalls indicated one depolarization event during the heaviest snow squall of the 1974-75 winter when the cross polarization ratio (CPR) rose from -33 dB to -21 dB. The CPR is defined as

$$10 \log_{10} \left[\frac{\text{power output from cross-polarized port}}{\text{power output from co-polarized port}} \right]$$

$$= \left[I(dB) \right]^{-1} = \left[\text{Isolation} \right]^{-1}$$

During rain events, there appeared to be little correlation between the mean attenuation, the CPR and the rain gauge rates. No explanation is offered for these results. At low elevation angles additional depolarization anomalies were observed, however, several of these were associated with multipath signals entering the antenna sidelobes. These early results, completed in August 1975, stimulated considerable interest in additional studies with the CTS and COMSTAR satellites.

VPI & SU has continued their depolarization studies with both the CTS 11.7 GHz right-hand circularly polarized downlink and the COMSTAR D2 19.04 GHz switched linear and 28.56 GHz linearly polarized beacons. To date only a limited number of storms have been reported in the literature (Ref 3.4-2 and -3), their data base is continuing. The results of one storm in June 1977 are shown in Figure 3.4-1. Herein the rain occurred for 160 minutes and peaked at 29 mm/hr. The isolation versus time plots show that the 11.7 GHz isolation rose about 3.8 dB average due to a phase shift of the signal resulting in a better match to the antenna. Simultaneously the 19.04 GHz vertical isolation decreased 4.5 dB to a minimum of 22 dB and the horizontal isolation was about 2 dB lower than the vertical isolation. The 28.56 GHz clear-weather isolation was low at 22 dB, but the isolation dropped to 19 dB during the peak rain events.

The signal phases experienced maximum excursions of approximately 100^{o}. The 11 GHz signal showed a more frequent phase variation than the 19 and 28 GHz signals. These results, for the same June storm, are shown in Figure 3.4-2. Other storms have been observed, but none have had the intensity of this June 22-23, 1977, storm. VPI & SU is now continuing to develop its statistical data base on isolation and phase angle variations.

At the University of Texas at Austin studies of the CTS 11.7 GHz beacon attenuation and cross-polarization isolation are ongoing. During the period from 12 June 1976 to 30 August 1976 (80 days) there were eleven days with more than 2.5 mm total precipitation (Ref 3.4-4). Data for the heaviest rain event is shown in Figure 3.4-3. The rain rate was measured with a single tipping bucket rain gauge located near the antenna. An accumulation of 1 minute samples for this 80-day period is presented in Figure 3.4-4. A least squares fit for all data with attenuations greater than 2 dB yields a cross-polarization isolation (CPI):

$$CPI = 38.9 - 17.4 \log A$$

where CPI and attenuation A are in dB. For comparison the theoretical curves (Ref 3.4-5) have been included. The logarithmic fit of the points deteriorates below 3 dB attenuation. A contributing factor to this is the

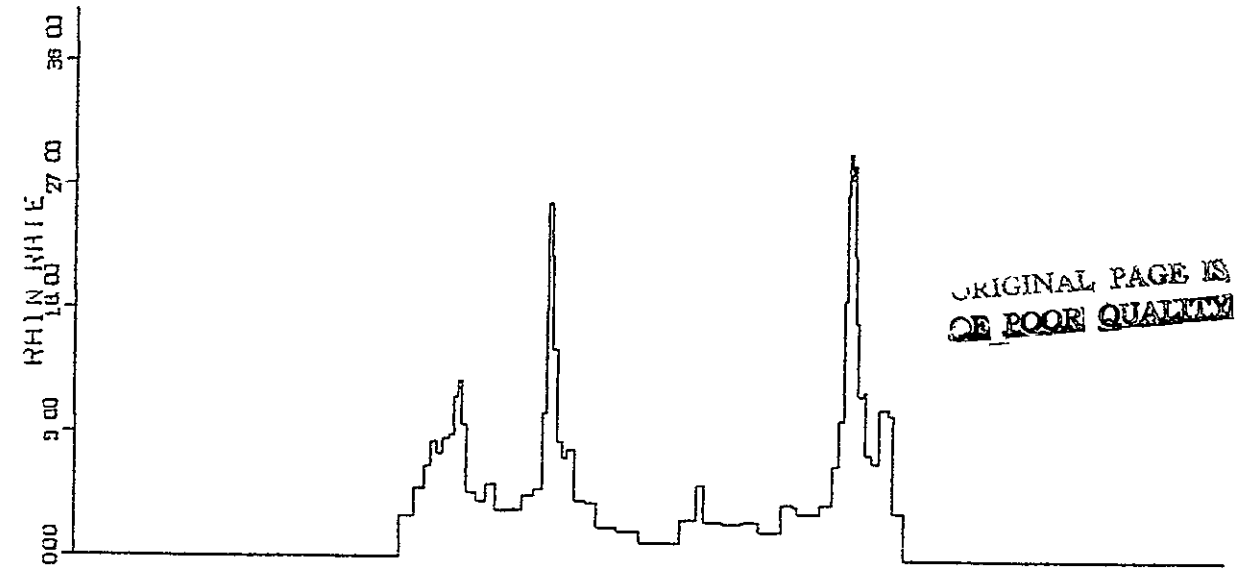

Fig 3.4-1A Rain rate (mm/hr) versus time (minutes), June 22-23, 1977

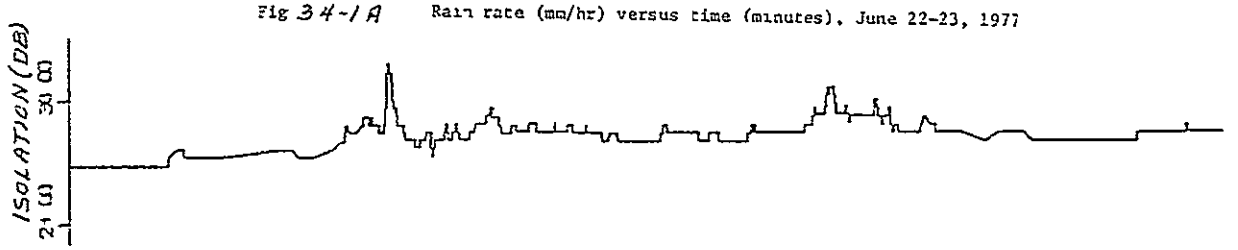

Fig 3.4-1B 11 GHz isolation (dB) versus time (minutes), June 22-23, 1977

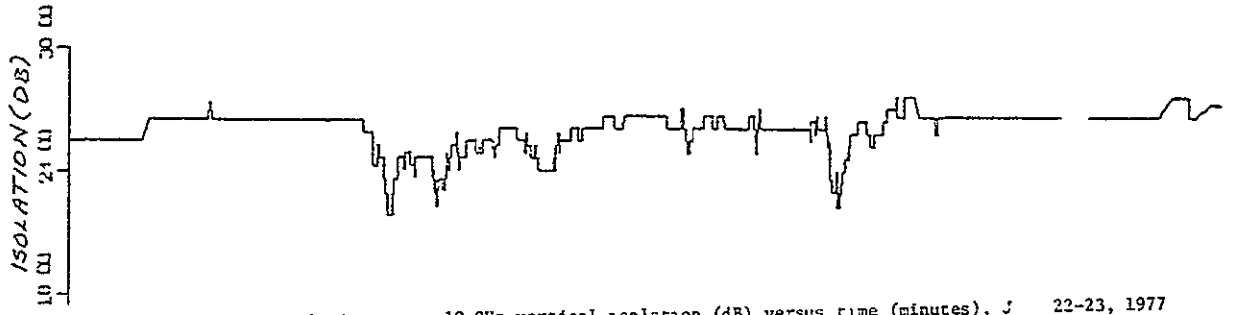

Fig 3.4-1C 19 GHz vertical isolation (dB) versus time (minutes), June 22-23, 1977

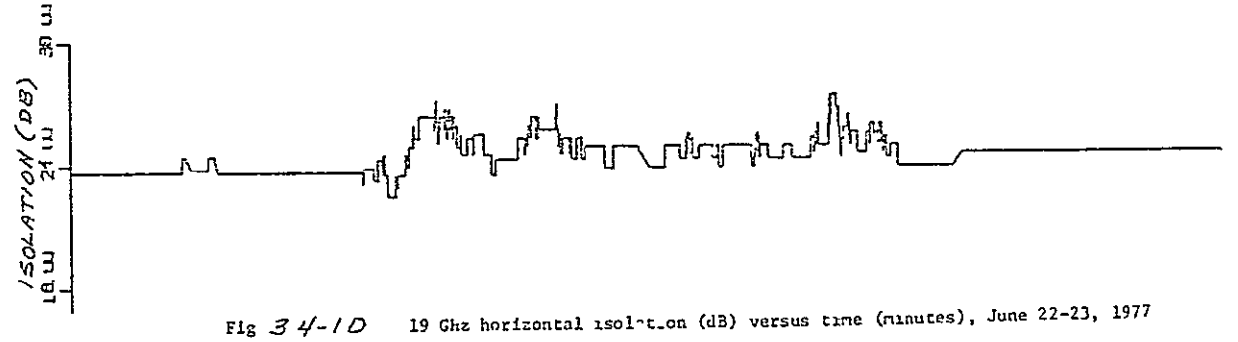

Fig 3.4-1D 19 GHz horizontal isolation (dB) versus time (minutes), June 22-23, 1977

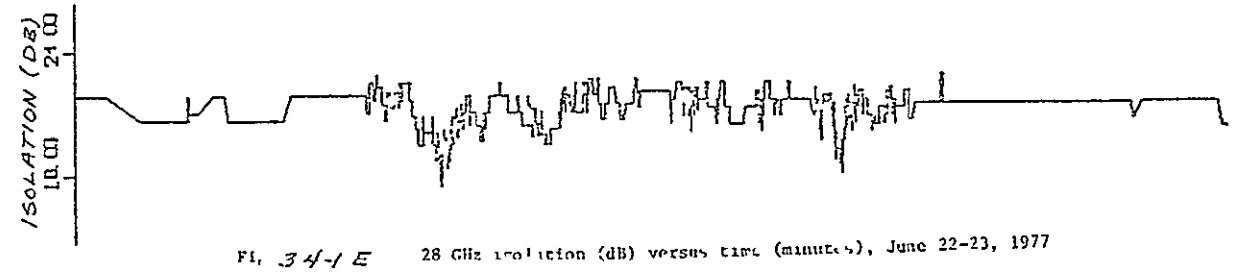

Fig 3.4-1E 28 GHz isolation (dB) versus time (minutes), June 22-23, 1977

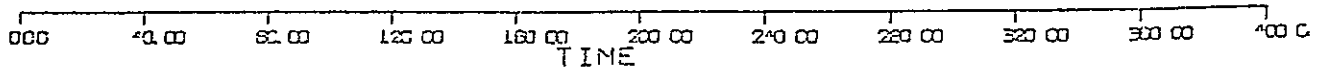

FIGURE 3.4-1. CROSS-POLARIZATION, ISOLATION AND RAIN RATE VERSUS TIME

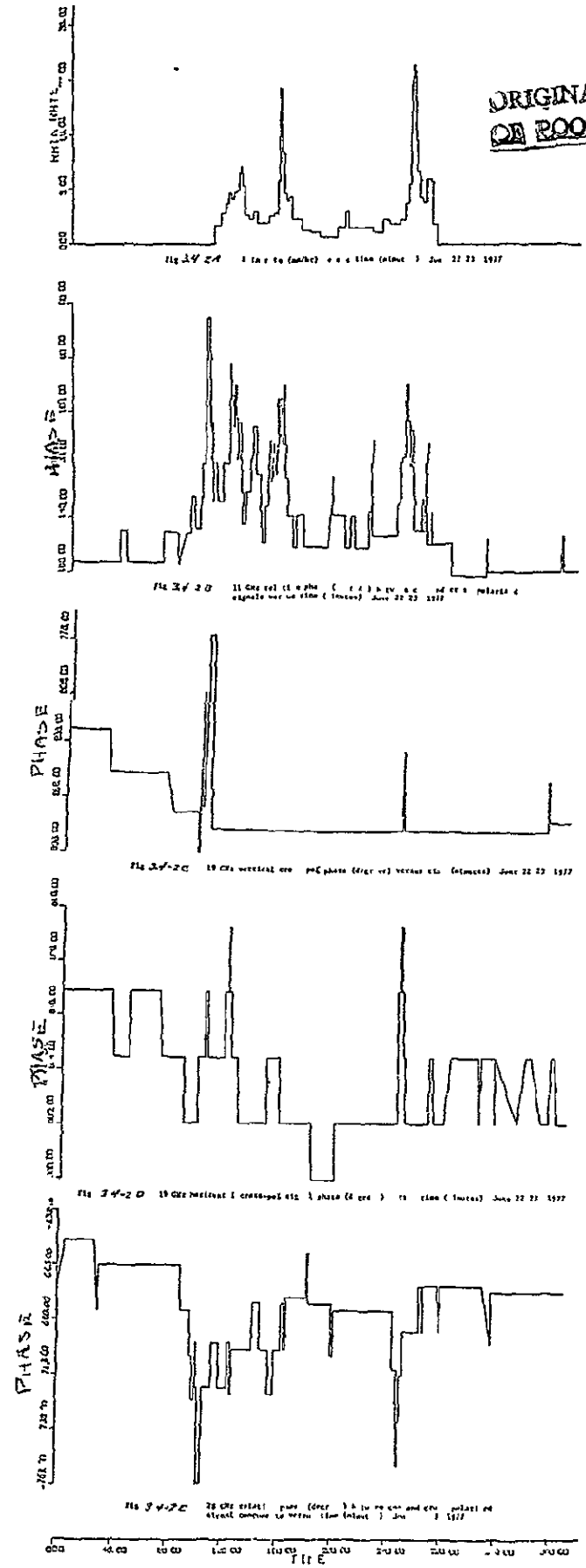

FIGURE 3.4-2. RELATIVE PHASE AND RAIN RATE VERSUS TIME

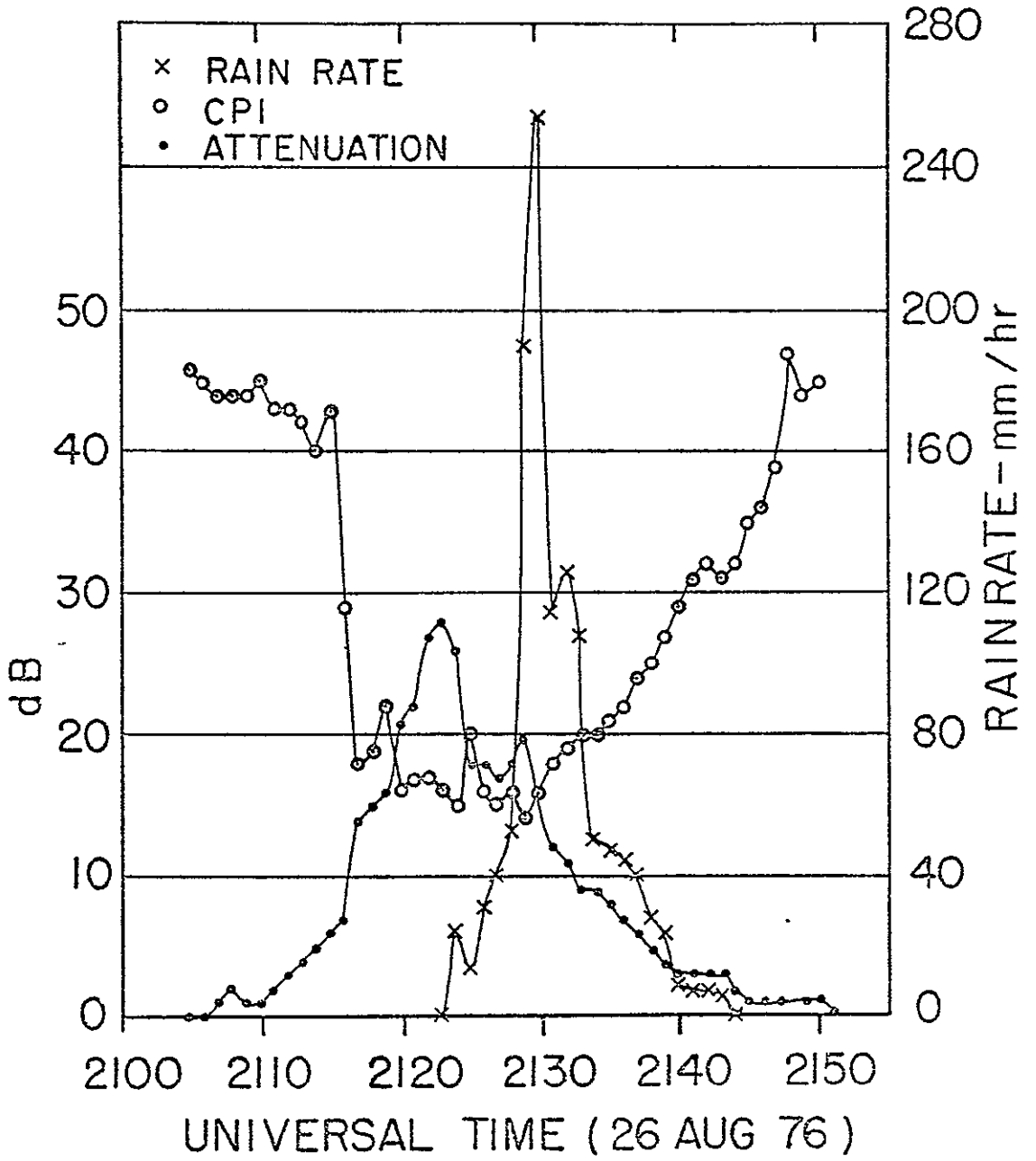

FIGURE 3.4-3. DATA FOR THUNDERSTORM OF 26 AUGUST 1976

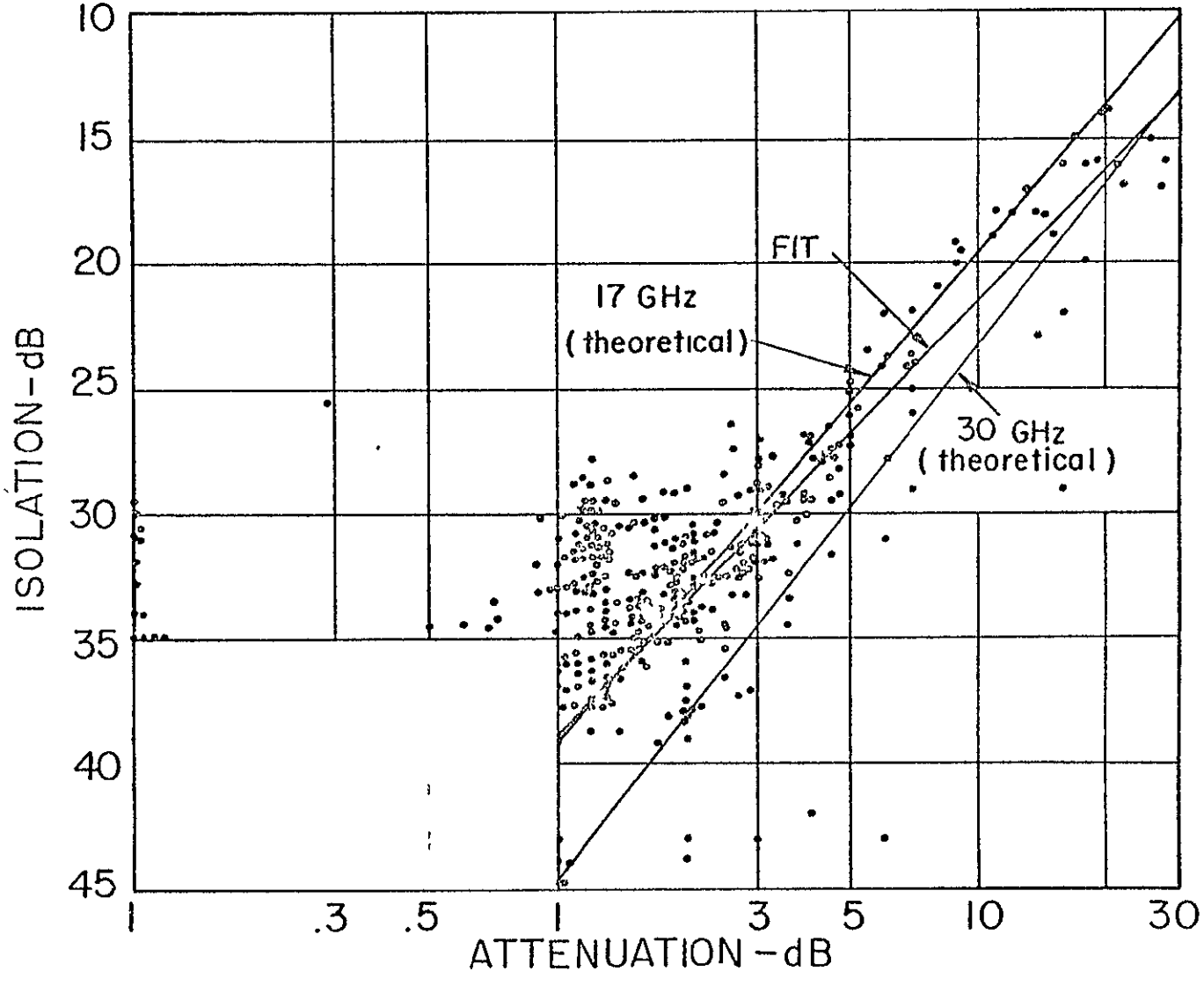

FIGURE 3.4-4. ISOLATION VS. ATTENUATION, 12 JUNE 1976-30 AUGUST 1976

anisotropic phase shift introduced by frozen particles (ice). These particles have very low attenuation. An example of the ice-induced depolarization is shown in Figure 3.4-5. Clearly the rapid cross-polarization changes are not correlated to the signal attenuation. These results indicate that in some cases Earth-space links will be limited by attenuation, while in others depolarization will be the dominant factor.

The depolarization resulting from ice (sometimes referred to as anomalous depolarization) is now being actively studied by European investigators. These investigators became aware of this effect because the local elevation angles to the US and Canadian synchronous satellites are lower in Europe, and therefore their propagation paths extend through much more ice resulting in significant depolarization. Their results are reviewed in the Proc. URSI Meeting, La Baule, France, 28 April-6 May, 1977.

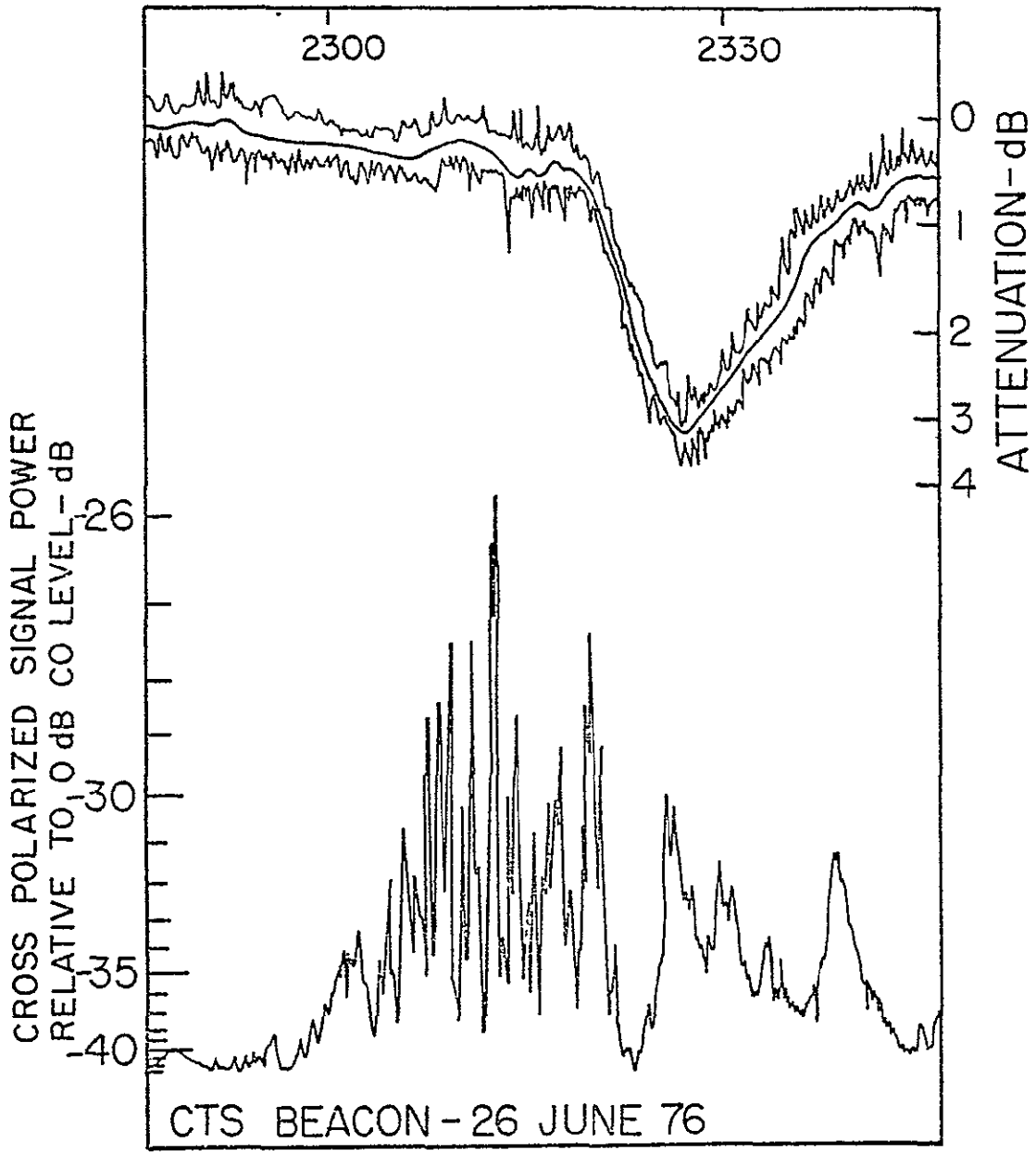

FIGURE 3.4-5. CHART RECORD FOR ICE DEPOLARIZATION

REFERENCES

3.4-1 Bostian, C.W., E.A. Manus, R.E. Marshall, H.N. Pendrak, W.L. Stutzman, P.H. Wiley, S.R. Kauffman, "A 20 GHz Depolarization Experiment Using the ATS-6 Satellite," Virginia Polytechnic Institute and State University Final Report, Contract NAS5-21984, September 10, 1975.

3.4-2 Bostian, C.W., S.B. Holt, Jr., S.R. Kauffman, E.A. Manus, R.E. Marshall, W.L. Stutzman and P.H. Wiley, "Rain Depolarization and Attenuation Measurements at 11.7, 19.04, and 28.56 GHz A Description of the Experiment and Some Preliminary Results," Proc. URSI Meeting, La Baule, France, pp 403-8 (28 April-6 May, 1977).

3.4-3 Bostian, C.W., S.B. Holt, Jr., S.R. Kauffman, E.A. Manus, R.E. Marshall, W.P. Overstreet, R.R. Persinger, W.L. Stutzman and P.H. Wiley, "A Depolarization and Attenuation Experiment Using the COMSTAR and CTS Satellites," Virginia Polytechnic Institute and State University. Quart. Tech. Prog. Report III, Contract NAS5-22577, July 19, 1977.

3.4-4 Vogel, W.J, and A.W. Straiton, "CTS Attenuation and Cross-Polarization Measurements at 11.7 GHz," Final Report by Elect. Eng. Res. Lab., University of Texas at Austin, Contract NAS5-22576, April 1977.

3.4-5 Vogel, W.J., B.M. Fannin and A.W. Straiton, "Polarization Effects for Millimeter Wave Propagation in Rain," Tech. Report No. 73-1, Elect. Eng. Res. Lab., University of Texas at Austin, December 1973.

3.5 ANGLE OF ARRIVAL

Communication links operating above 10 GHz frequently utilize antennas whose beamwidths are of the order of tenths of a degree. For these narrow beamwidths, variations in the angle of arrival of a microwave signal can result in significant AM modulation of the signal. Therefore studies are now ongoing to characterize the fluctuations in the angle of arrival for the CTS 11.7-GHz beacon at Ohio State University (OSU). As part of these studies OSU is attempting to resolve whether the apparent fluctuations are due to variations in the direction of the propagation vector $\vec{k}$ of a plane wave or if the wave front is being distorted resulting in a spatial dependence to the $\vec{k}$ vector If the latter is the case, large aperture antennas will average over the wavefront resulting in a reduced AM effect on the received signals at a ground station.

The measurements are being made with a 2 x 2 matrix of 0.6m diameter parabolic antennas arranged on a 1m square matrix (see Fig 3.5-1 and Ref 3.5-1). The detection circuitry shown in Figure 3.5-2 indicates the amplitude and phase information available to the investigators. The angle of arrival resolution in one plane is $\pm$ 0.05 deg for the system. Data in a 80 Hz bandwidth is recorded at a 1/3 sample per second rate with an option of 10 samples per second.

Initial OSU data (Ref 3.5-1) has demonstrated that for a 2dB fade during a rain, 0.06 deg pk-pk angle of arrival fluctuations were observed. For a 12dB fade the fluctuation amplitude increased to 0.16 deg pk-pk. Additional data (Ref 3.5-2) taken with the system in Figures 3.5-1 and -2 indicate that antenna gain degradation due to angle of arrival scintillations accounts for the reduced signal levels compared to predicted levels at low elevation angles. Design curves for gain degradation as a function of antenna aperture size, frequency and elevation angle are being developed. The angle fluctuation versus amplitude measurements are continuing with the objective of determining if $\vec{k}$ is space dependent over the array aperture.

FIGURE 3.5-1. THE OSU SQUARE ARRAY OPERATING AT 11.7 GHZ (CTS BEACON)

ORIGINAL PAGE IS
OF POOR QUALITY

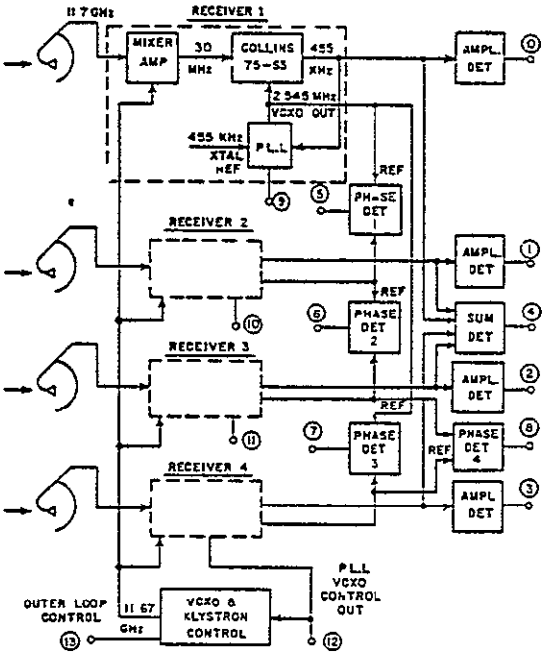

FIGURE 3.5-2 THE OSU RECEIVER SYSTEM FOR AMPLITUDE AND PHASE MEASUREMENTS

REFERENCES

3.5-1 Theobold, D.M., and D.B. Hodge, "The OSU Self-Phased Array for Propagation Measurements Using the 11.7 GHz CTS Beacon," Technical Rpt ESL 4299-1 for NASA/GSFC Contract NAS5-22575, November 1976.

3.5-2 Theobold, D.M., and D.B. Hodge, "An Empirical Model for Antenna Gain Degradation Due to Angle of Arrival Fluctuation in the Troposphere," Electro. Sci. Lab., Ohio State Univ., abstract submitted to National Radio Science Meeting, Boulder, CO, January 9 - 13, 1978.

3.6 BANDWIDTH COHERENCE

The ATS-6 beacons at 20 and 30 GHz were both capable of being modulated with ±180, ±360, ±540 and ±720 MHz signals. These signals allowed measurements of coherence over a 1.44 GHz range centered on 20 and 30 GHz The required receiving and recording equipment was available at NASA's Rosman ground station to utilize these signals (Ref 3 6-1). Measurements of both the attenuation (selective fading) and the phase between signals were possible for averaging intervals of one second, four seconds and one minute.

In general, only minor phase variations across the 1.44-GHz range were noted for signal levels when the receiver remained locked on the signals. Also, the phase and amplitude variations were most evident for the shorter (one- and four-second) averaging periods compared to the one-minute period.

Typical selective fading events across the 1.44 GHz bands are shown Figures 3.6-1 and 3.6-2 for 20- and 30-GHz carriers, respectively These are four-second averages taken on day 270 of 1974 just before the onset of a fade event (232000Z), at the beginning of the fade event (232352Z), and before receiver lock was lost during the fade event (232428Z). Except for fade depths in excess of 20 dB, the accuracy of the attenuation measurements is ±1 dB. These results, while representative of those taken at Rosman, do not appear to be sufficiently accurate for deep fades because the signal levels approach the noise floor of the receiver. For one-minute averages, no measurable selective fading was observed (Ref 3.6-2).

Measurement of the phase between the 0.72-GHz sidebands and the 20- and 30-GHz sidebands showed no variation for fades less than 12 dB at 30 GHz for one-second averaging. On another occasion, a variation of 20^{o} between the 20.72 and 20.0 GHz signals was noted, but this occurred for a fade of the order of 20 dB at 20 GHz. These results are in agreement with analytic results by Meneghini (Ref 3.6-3).

The ATS-6 satellite links at 4-, 20- and 30-GHz have also been employed to demonstrate high data rate digital transmissions (Ref 3.6-4). Data rates of 100 kbps to 15 Mbps using bi- and quadriphase signal structures were downlinked to Rosman, N.C. The test results indicated that the links

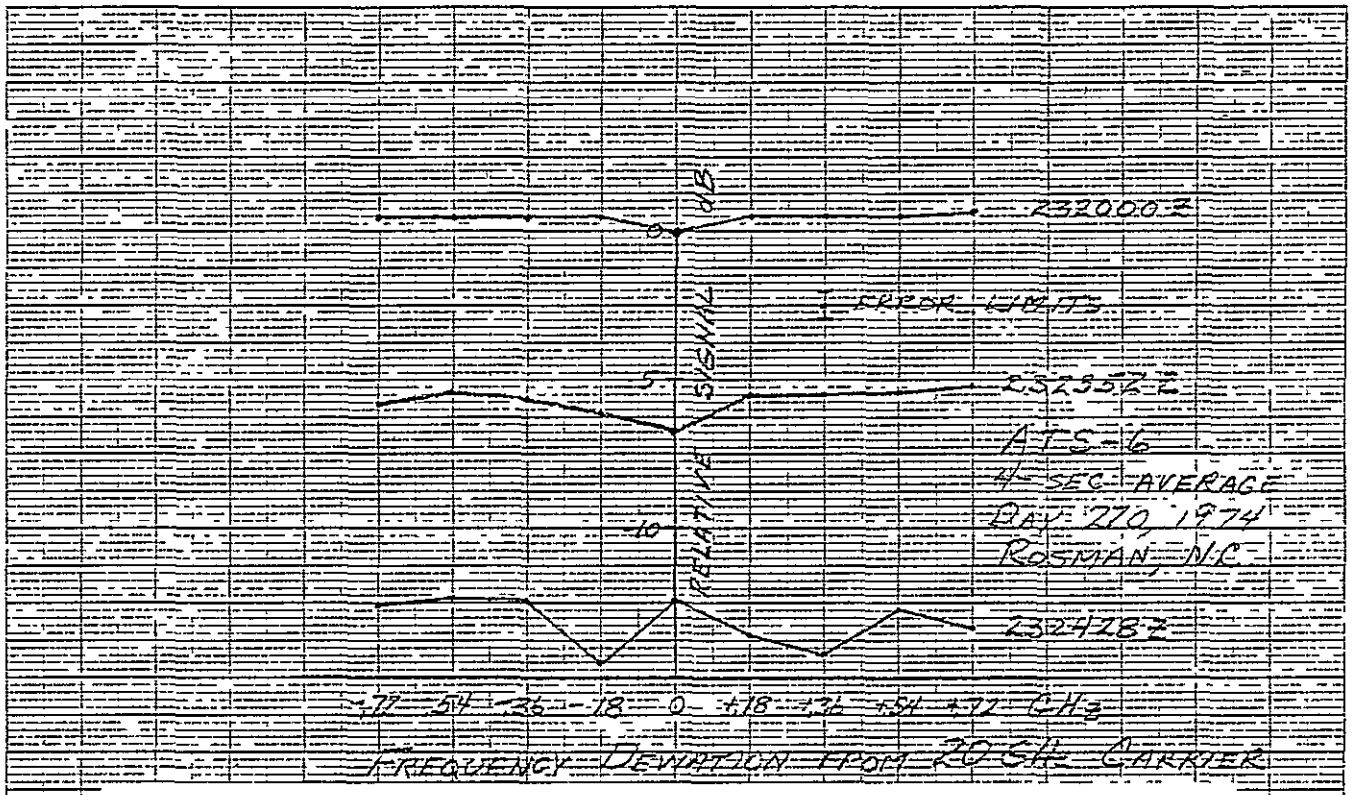

FIGURE 3.6-1. SELECTIVE FADING NEAR 20 GHZ

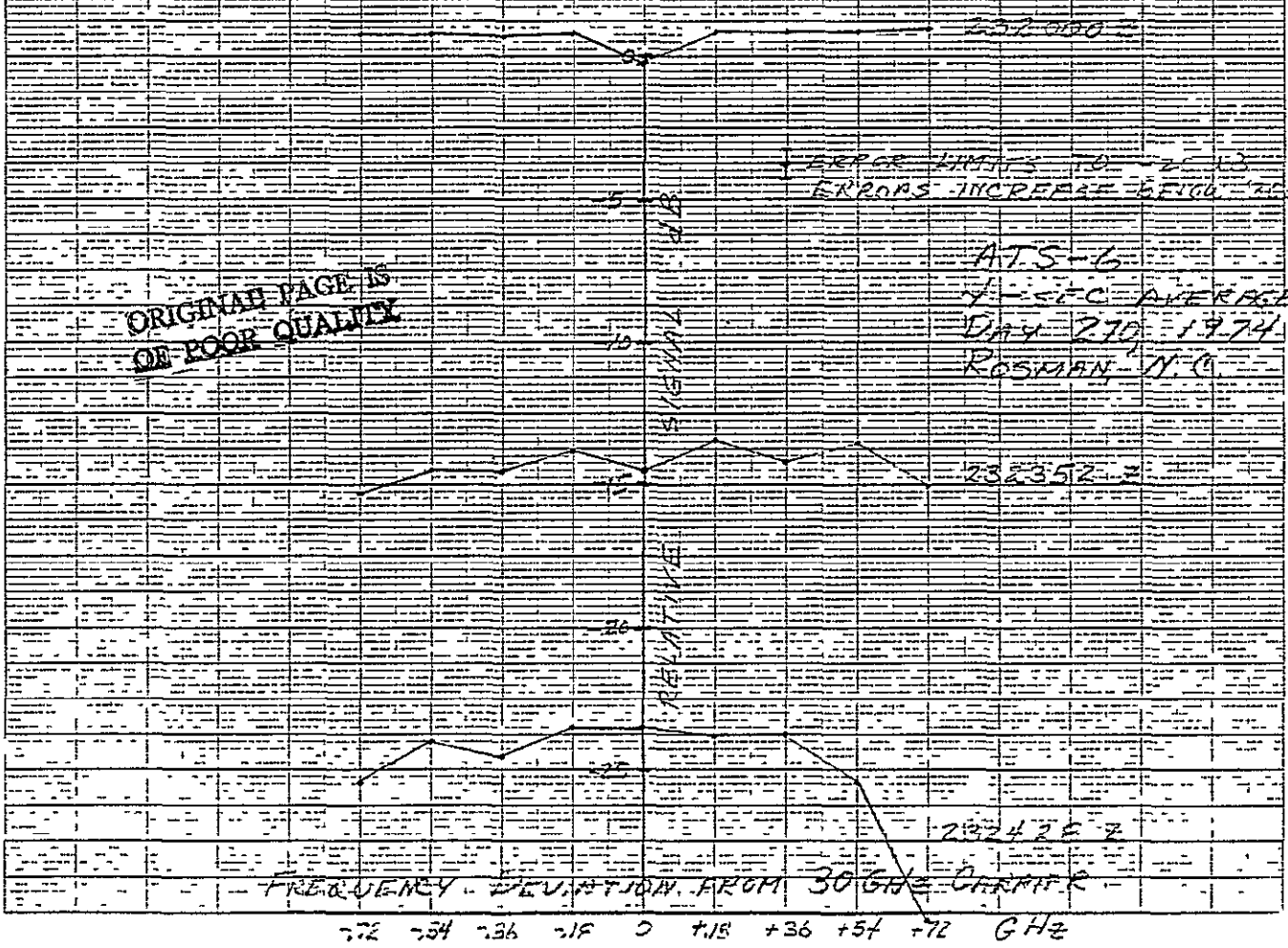

FIGURE 3.6-2. SELECTIVE FADING NEAR 30 GHZ

(20- & 30 -GHz) could support telemetry rates in excess of 15 Mbps for bi-phase modulation (30 Mbps for quadriphase) with minimal signal degradation from dispersive effects. The results were obtained in clear weather.

Theoretical calculations have been carried out for pulse transmissions through rain (Ref 3.6-5). These calculations indicate that above 10 GHz the rain attenuates, but pulse distortion does not become significant until the rain-induced attenuation exceeds 100 dB. For carrier frequencies below 10 GHz, in temperate climates, pulse width increases of 2 and 60% were calculated for 3.6 GHz bandwidth pulses (pulse length = 0.3 nanosecond) at 49 mm/hr and 196 mm/hr, respectively. At 3 GHz bandwidth the pulse length increases only 30% at 196 mm/hr and continues to decrease rapidly with decreasing bandwidth. Therefore, based on the ATS-6 coherent sideband and digital results, the ongoing CTS video measurements (Ref 3.6-6) and the theoretical calculations, bandwidth coherence is not a significant contributor to Earth-space link degradations.

REFERENCES

3.6-1 ATS-6 Millimeter Wave Propagation Experiment, Final Data Analysis Report, prepared for NASA/GSFC by Westinghouse Electric Corporation, Baltimore, MD., September, 1975.

3.6-2 Ibid., page 3-7.

3.6-3 Meneghini, R., "Review of Data Analysis Procedures for the ATS-6 Millimeter Wave Experiment," NASA/GSFC Document X-951-75-235, August 1975.

3.6-4 Tu, K., D.R. Kahle and B.H. Batson, "ATS-6 Quadriphase Transmission Tests, Inst. Soc. of Amer. Reprint 75-564, 1975.

3.6-5 Crane, R.K., "Coherent Pulse Transmission Through Rain," IEEE Trans Ant. Prop. AP-15, 252 (March, 1967).

3.6-6 Ippolito, L.J., "Characterization of the CTS 12 and 14 GHz Communications Links - Preliminary Measurements and Evaluations," 1976 Int'l Comm. Conf. Record, Phila., PA., page 12-26 (June, 1976).

IV. ADDITIONAL PROPAGATION RESEARCH EFFORTS

NASA has coordinated the experimental measurements of satellite beacons with the development of theoretical models and ground-based diagnostic experiments. The theoretical models have emphasized rain attenuation and depolarization on satellite links. The diagnostic experiments have involved use of radiometers, radars and rain gauges for correlation with the signal effects discussed in Section III.

4.1 THEORETICAL MODELING

One of NASA's initial theoretical propagation modeling activities was to predict the magnitude of rain-scattered interference for terrestrial-space paths. The interference resulted in a modification to the coordination distance (Ref 4.1-1) and an increased probability of interference between stations. The results of these studies provided an input for the 1971 World Administrative Radio Conference for Space Telecommunications.

A review of the scattering and absorption by hydrometeors (raindrops, hail, snow and sleet) yielded a qualitative value for the attenuation. In addition, for non-spherical raindrops it was observed that there was a 20 percent difference between horizontal and vertical attenuation (Ref 4.1-2).

Studies of the evolution of clouds indicated that a significant amount of water and ice can contribute to the attenuation by clouds before any rain reaches the ground. Also due to updrafts within clouds, the amount of rain

measured at the ground may only be a fraction of the rain contributing to the attenuation.

To circumvent some of the deficiencies of rain gauges, the use of radiometers was proposed to estimate path attenuation from the apparent sky brightness temperature T_s. However, because T_s is proportional to (1-exp(A/constant)), attenuations A greater than 10 to 15 dB are not distinguishable. Use of the sun as a source of microwaves, which does not saturate, have been utilized by several observers for attenuations up to 30 dB, but the variable sun tracking angles and lack of data at night tend to limit the statistical value of these results.

Also radars have been studied as a means to diagnose the spatial distribution of the attenuating media. Unfortunately, the calibration of the radar becomes critical since the backscatter and return beam's attenuation are both frequency dependent and the radar attenuation may be quite large.

Based on these general results it appears that, depending on the type of meteorological correlation to link measurements being performed, one or a combination of these diagnostic techniques is most applicable. Ongoing studies, reported below, have shown this to be the case and current experimenters with the CTS and COMSTAR satellites are employing all three techniques.

To support the experimental measurements, Westinghouse Corp. has prepared for NASA/GSFC a computer program which calculates:

- attenuation
- 16 and 35 GHz sky temperatures
- integrated radar reflectivity

for comparison with observed parameters (Ref 4.1-3). As inputs the program requires ground temperature and rain rate. The comparisons of the model results with the measured data yielded the following:

- the model consistently underestimates the sky temperatures and the carrier attenuation, probably due to the inaccurate rain measurements
- the Ku-band (15 GHz) integrated radar return does not appear to correlate with the model or the carrier attenuation. Apparently, because of attenuation the radar only "sees" backscatter from the leading edge of the rain and therefore is not indicative of the entire rain volume.

Ohio State University (Ref 4.1-4) also developed a model for the structure of rain cells and the attenuation associated with them. The model for a cylindrical storm cell as shown in Figure 4.1-1 represents the region of intense rain usually associated with the convective cells which produce severe fading. The model is statistical and utilizes readily available information, e.g., hourly rain rates rather than instantaneous rates. The system and climate parameters utilized in the model include frequency, path elevation angle, rain rate distribution and rain cell dimensions. The model yields the fade distribution for a single site and the joint fade distribution for site diversity terminal pairs. Figure 4.1-2 is an example of the comparison of the model with the Rosman 1970 cumulative distribution. Comparisons with other single and multiple site OSU data also confirmed the usefulness of the model.

Based on their experimental findings for terrestrial links, the Virginia Polytechnic Institute and State University has developed a model to predict the depolarization of millimeter waves due to rain (Ref. 4.1-5). Since raindrops tend to be elongated, an electric field vector oriented along the narrow demension of the drop is attenuated less than when oriented along the wide dimension and the phase is affected differently for different orientations of the electric field with respect to the drop. These effects change the state of the polarization and give rise to a component which is cross-polarized with respect to the input polarization state. The model assumes that all drops are the same size, identically oriented with a mixture of shapes and that the forward scattering properties of a simple raindrop are known. The model yields the total field amplitude, path attenuation and cross-polarization for various drop canting angles, rain rates and path lengths. As shown in Figures 4.1-3 and 4 the results of the model are in good agreement with all data taken during the last five months of 1972 and averaged together for each one mm/hr of rain rate.

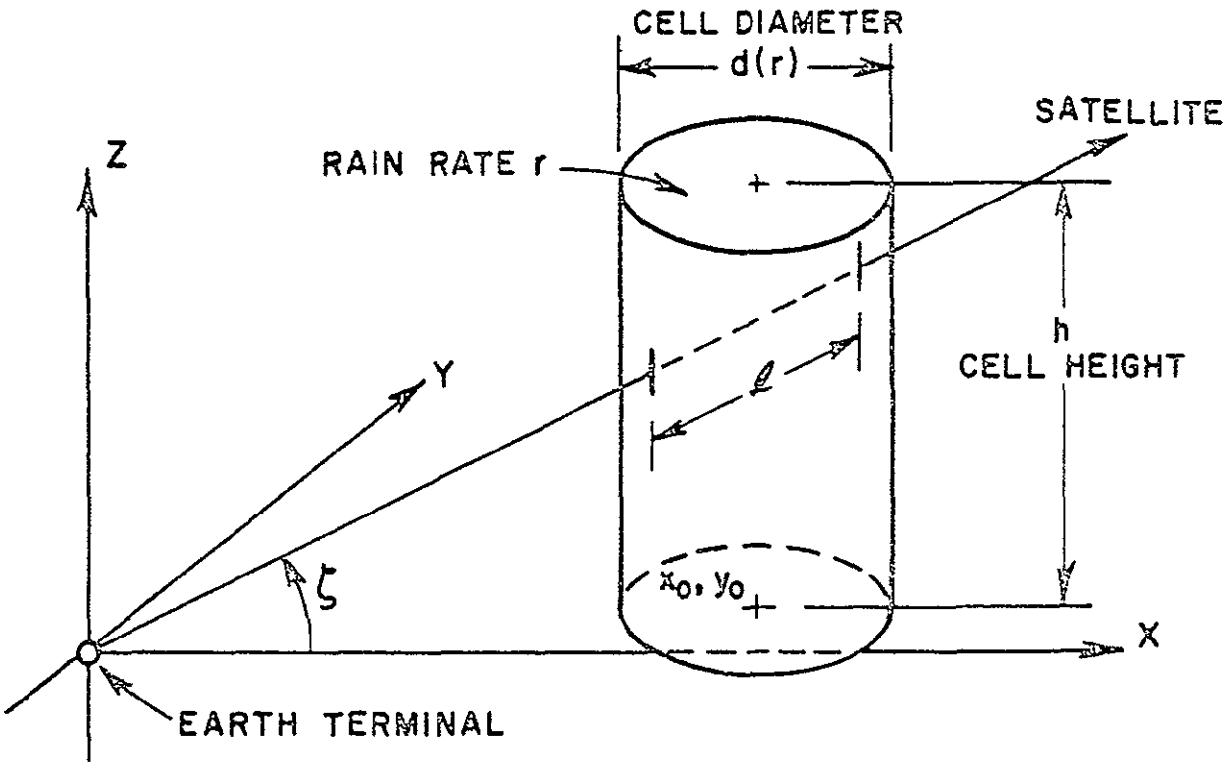

FIGURE 4.1-1. MODEL STORM CELL AND COORDINATE AXES.

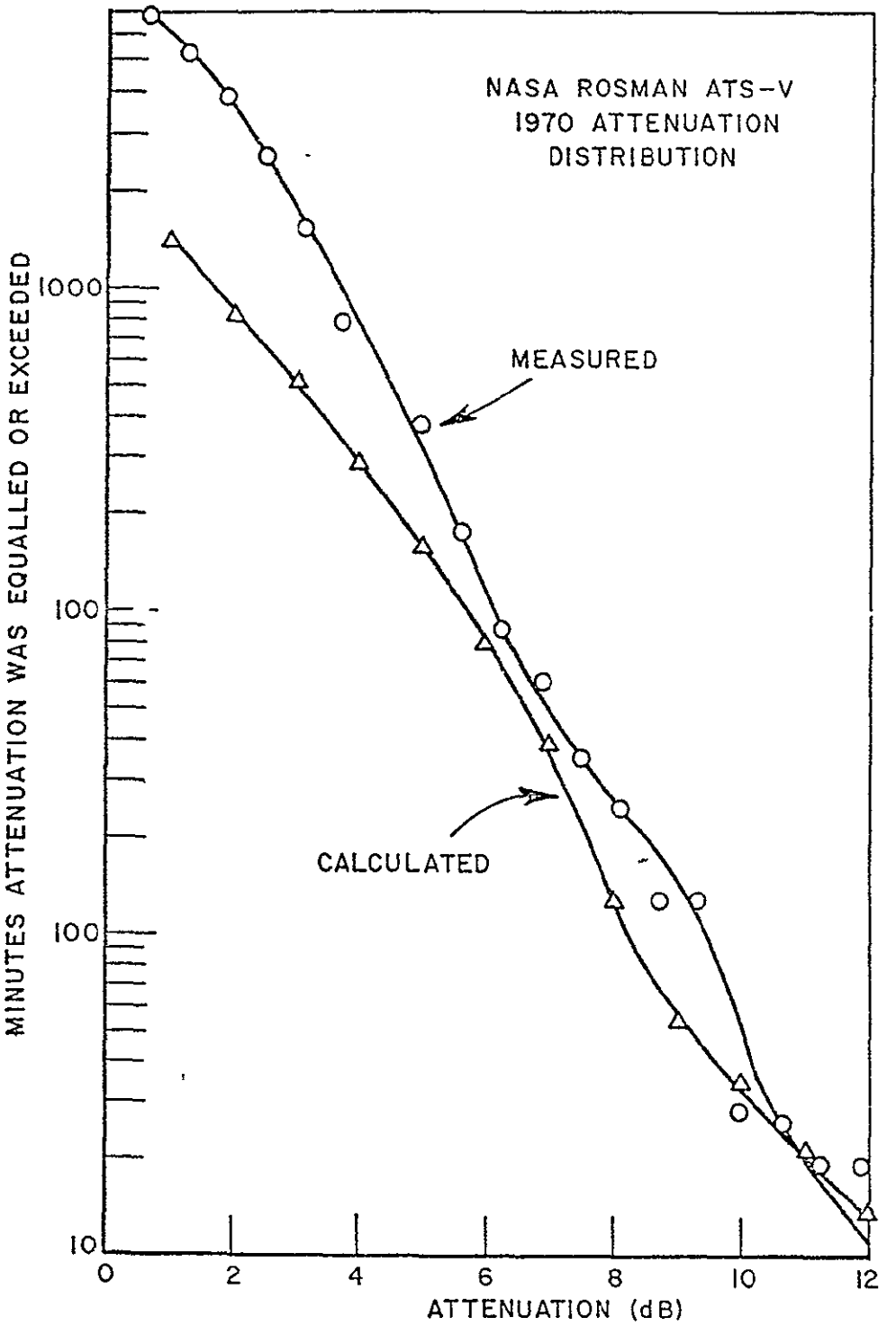

FIGURE 4.1-2. CALCULATED AND MEASURED FADE DISTRIBUTIONS

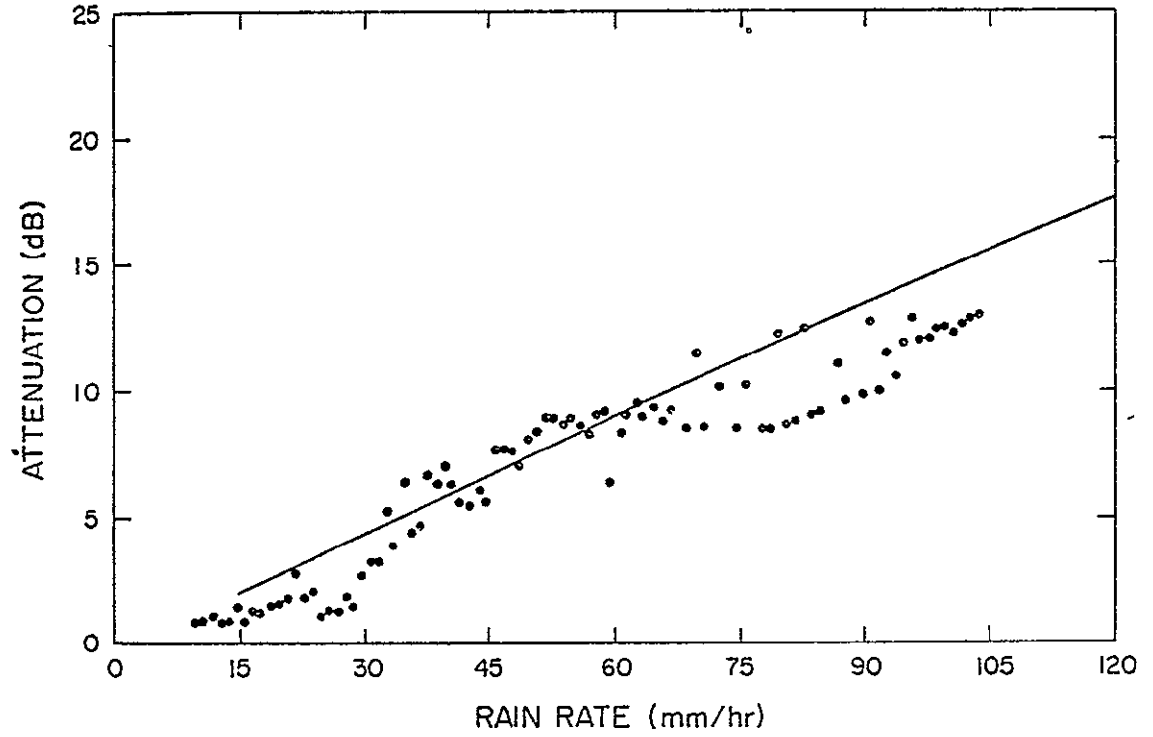

FIGURE 4.1-3. PLOT OF ATTENUATION VERSUS RAIN RATE OF ALL DATA TAKEN DURING THE LAST FIVE MONTHS OF 1972 AND AVERAGED TOGETHER FOR EACH ONE MM/HR OF RAIN RATE.

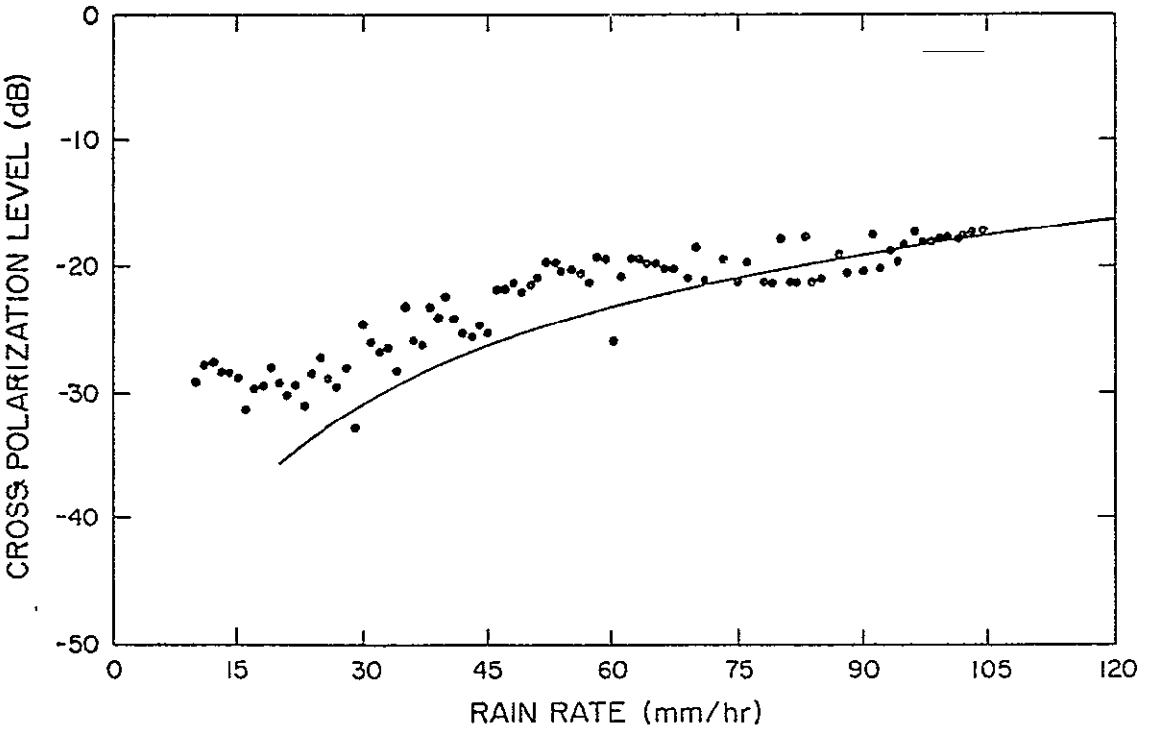

FIGURE 4.1-4. PLOT OF CROSS POLARIZATION LEVEL VERSUS RAIN RATE OF ALL DATA TAKEN DURING THE LAST FIVE MONTHS OF 1972 AND AVERAGED TOGETHER FOR EACH ONE MM/HR OF RAIN RATE.

REFERENCES

4.1-1 "Interference Due to Rain," NASA/GSFC Doc. X-750-71-211, May 1971.

4.1-2 "ATS-5 Signal Characteristics at 15.3 GHz and Related Experiments at 15 and 35 GHz," Elec. Eng. Res. Lab. Final Report, Univ. of Texas at Austin, NAS5-10387, June 1972

4.1-3 "ATS-5 Millimeter Wave Propagation Experiment," Section 5, Westinghouse Elect. Corp.' Final Report under Contract NAS5-21598, January 1972.

4.1-4 L.R. Zintsmaster, "The Estimation of Attenuation Statistics for Earth-Space Millimeter Wavelength Propagation," in ElectroScience Lab., Ohio State University Semi-Annual Status Report 2374-9, May 1972, and in "Earth-Satellite Propagation Above 10 GHz," pg. 7-1, compiled by L.J. Ippolito, NASA GSFC Doc. X-751-72-208, May 1972.

4 1-5 P.H. Wiley, W.L. Stutzman and C.W. Bostian, "A New Model for Rain Depolarization," Jrnl. Rech. Atmos., pp147-153 (1974), and C.W. Bostian, W.L. Stutzman, P.H. Wiley and R.E. Marshall, "The Influence of Polarization on Millimeter Wave Propagation through Rain," Final Report, Virginia Polytechnic Institute and State University, NASA Grant NGR-47-004-091, January 1, 1974.

4.2 RADIOMETRIC MEASUREMENT TECHNIQUES

A sky-viewing radiometer measures the following three radiative thermal emission terms

a) the transmission term (e.g. emission from the sun)
b) the scattering term
c) the absorption term (the reradiation from the atmospheric medium)

These terms are frequency dependent and both the transmission and absorption terms contain the radiative attenuation, A, which is the quantity experimenters desire to determine. An emperical equation has been derived (Ref. 4.2-1) which relates the attenuation with the sky temperature T_s, but the scaling of this relation with frequency is unclear. The relation is

$$A(dB) = -10 \log_{10}\left(\frac{T_m - T_s}{T_m}\right)$$

where T_m is the mean absorption temperature in ^oK of the attenuating medium 1.12 (ground temperature in ^oK) -50^oK (Ref. 4.2-2).

In general the dynamic range of radiometers is limited to 10 or 15 dB of attenuation, but they have two significant attributes·

1) they are sensitive to small values of attenuation such as those associated with snow and ice, and
2) they do not require a satellite beacon for their operation. Therefore they have frequently been used in studies at sites and frequencies where direct satellite transmissions are not available for development of cumulative fade statistics (Ref 4.1-1 and -2).

These attributes have been exploited for both the ATS-5 and ATS-6 millimeter wave characterization programs.

With ATS-5 Ohio State University directly correlated the sky temperature T_s versus the signal level at the receiver output as shown in Figure 4.2-1. For this 15 minute period the correlation between the attenuation A and T_s was found to be 0.9. This value is probably pessimistic since small antenna pointing errors significantly influence the attenuation measurements while having little effect on T_s. OSU, COMSAT Laboratories and the Bell Telephone Laboratories also utilized radiometers to obtain more data regarding site diversity gain versus attenuation

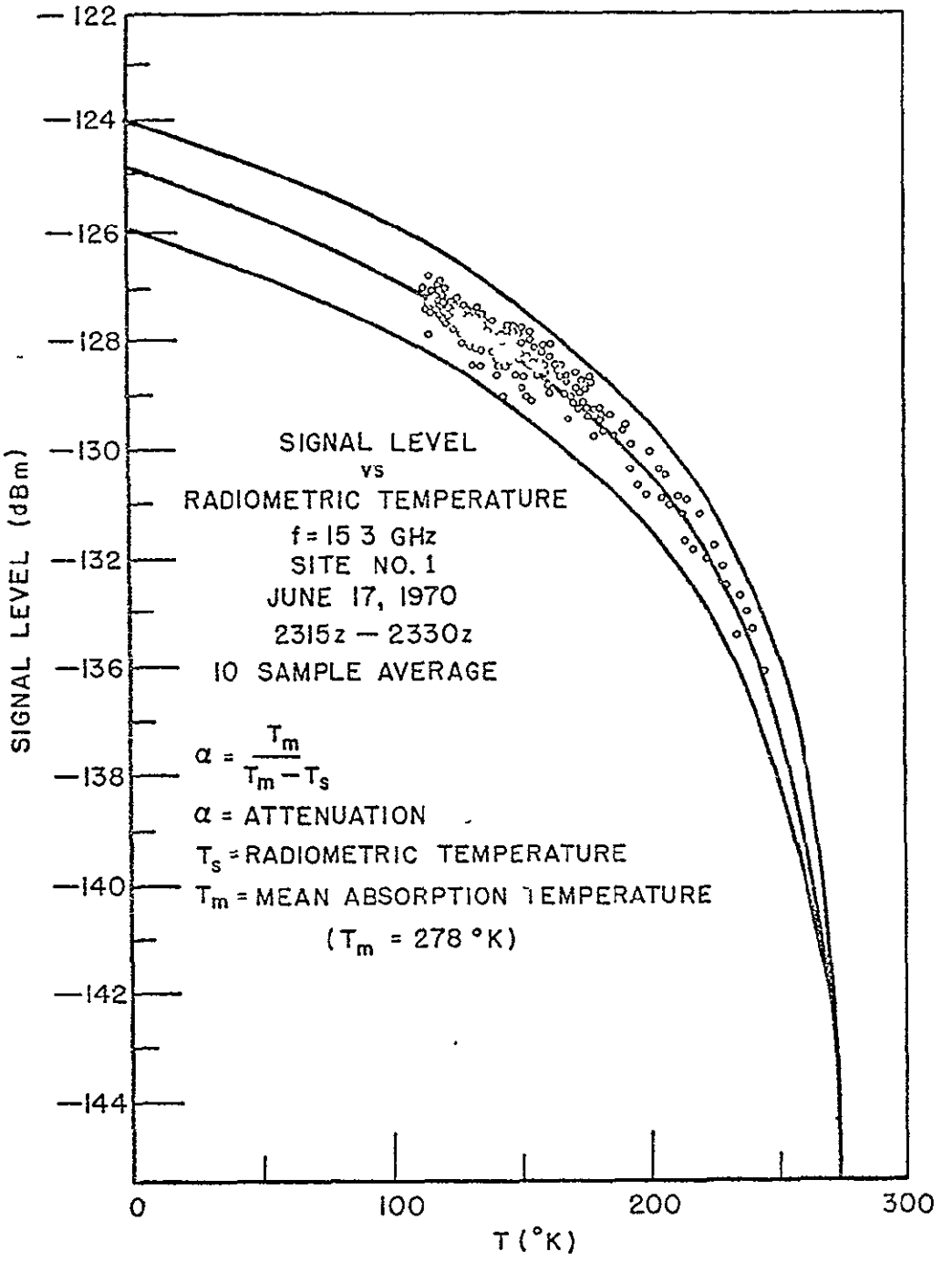

FIGURE 4.2-1. RECEIVED SIGNAL LEVEL VS. RADIOMETRIC TEMPERATURE

and separation distance. The results (see Figure 4.2-2) confirm the results quoted in Section 3.2. All the Bell measurements were made with radiometers calibrated at 16 GHz.

Because operating times of the ATS-6 beacons was limited by the requirement of the satellite to support other experiments, radiometer data (available 24 hrs per day) contributed significantly to the ATS-6 data bases for cumulative statistics and site diversity. At OSU radiometers were coaligned with the beacon receivers at the site diversity measurement sites, while at COMSAT Laboratories they were mounted on the same antennas as the 20 and 30 GHz receivers. At COMSAT (Ref 4.2-2) their 20 and 30 GHz sky temperature measurements were correlated, when possible, with the beacon signal strengths Typical results are shown in Figure 4.2-3 at 30 GHz This data includes about 25 to 30 hours of data from August 1974 to August 1975 taken at Clarksburg, MD. The results are bracketed reasonably well with the empirical relation for T_m = 290 and 250^{o}K, however a better numerical fit was obtained with the relation $T_{30} = 57.17\ A_{30}^{0.569}$ (shown dashed in Figure 4.2-3).

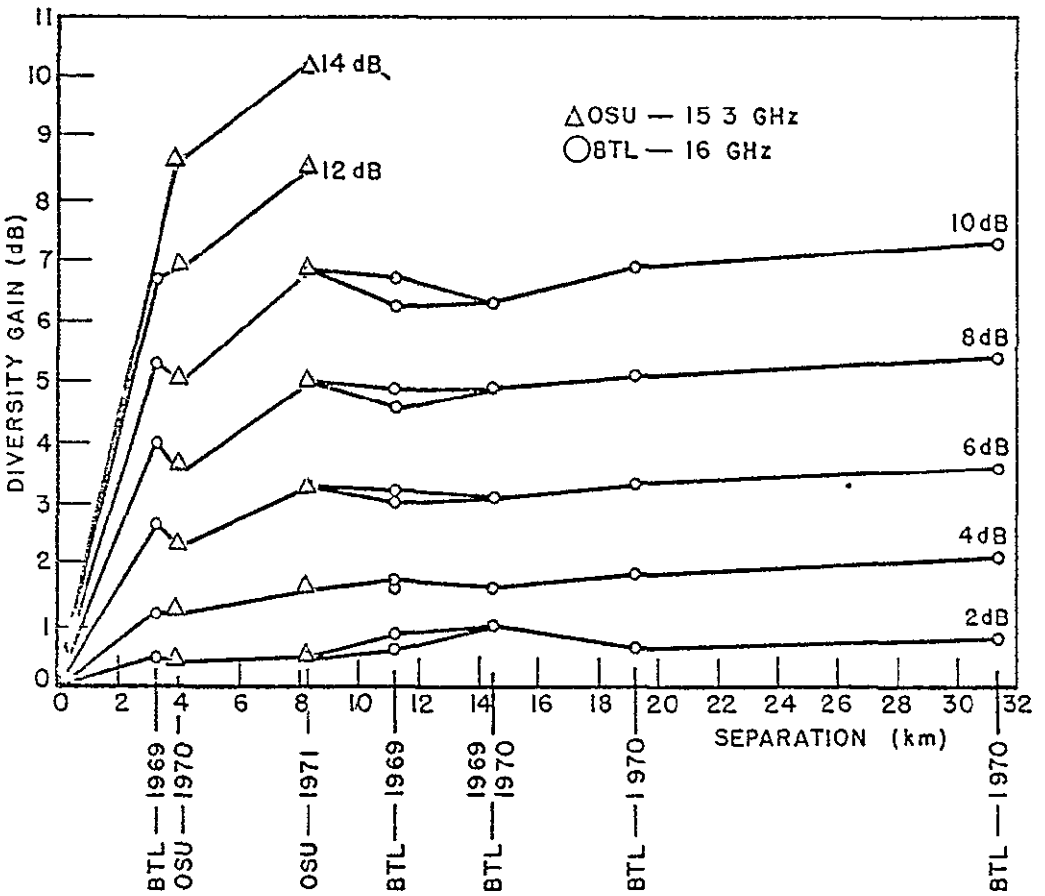

FIGURE 4.2-2. DIVERSITY GAIN VS. SITE SEPARATION DISTANCE

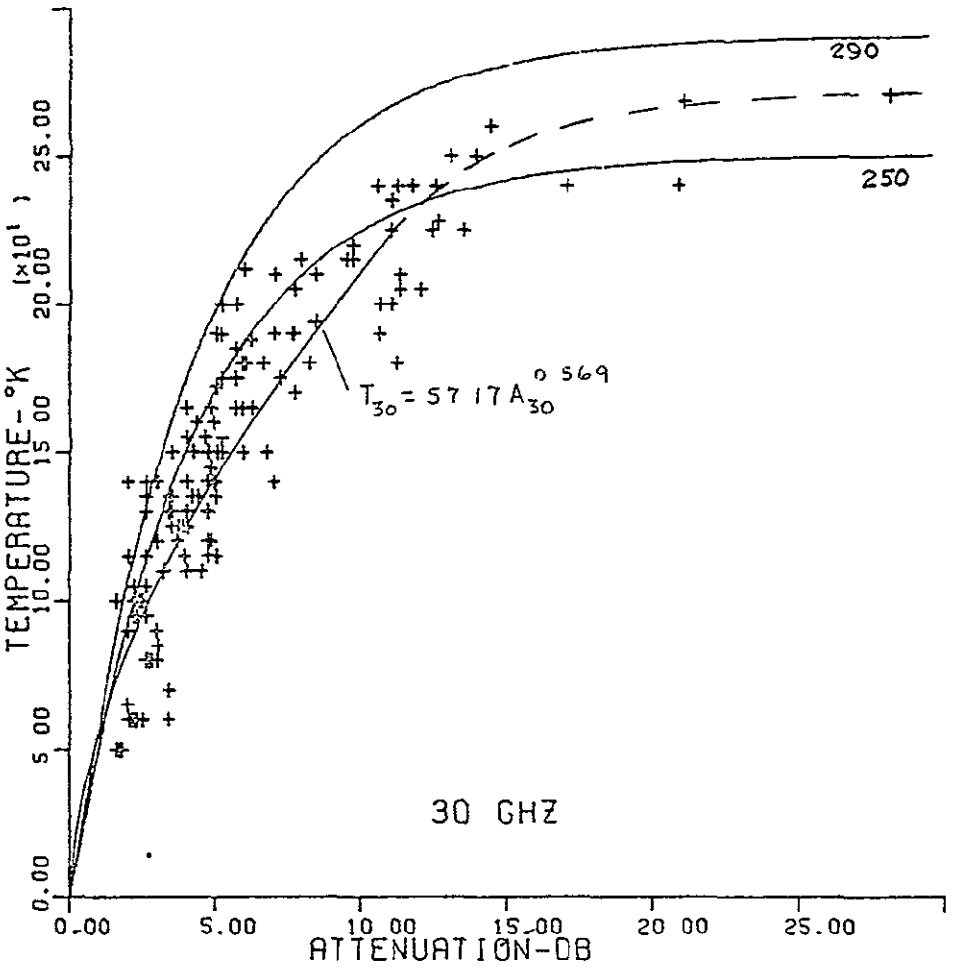

FIGURE 4.2-3. COMPOSITE SCATTERGRAM OF ALL THE SIMULTANEOUS RECORDS OF RADIOMETRIC SKY TEMPERATURES VS. SATELLITE BEACON SIGNALS AT 30 GHz (THE BEST NUMERICAL FIT CURVE IS $T_{30} = 57.17\ A_{30}^{0.569}$)

REFERENCES

4.2-1 Wulfsberg, K. N., "Apparent Sky Temperatures at Millimeter-Wave Frequencies," Phys. Science Res. Paper No. 38, Air Force Cambridge Res. Lab - 64-590, July 1964.

4.2-2 Fang, D. T. and J. M. Harris, "Precipitation-Attenuation Studies Based on Measurements of ATS-6 20/30 GHz Beacon Signals at Clarksburg, Maryland," COMSAT Lab. Final Report, NASA Contract NAS5-20740, August, 1976.

4.2-3 Bergmann, H. J. and E. E. Muller, "Radiometer Experiment at Band 18 GHz to Study Satellite System Site Diversity," 1976 Int'l Comm. Conf., Philadelphia, PA, June 14-16, 1976, pg 12-1 to 12-6.

4.3 RADAR

Radar systems have been utilized and are continuing to be applied to the correlation of the attenuation along a ground station - satellite path with ground base measurements and to study the rain cell morphologies in order to determine where the cell attenuations are most significant. In addition, the radars have been utilized in a bistatic mode to identify how much energy is scattered out of the media into other ground station receiver systems thus causing interference. In summary, radar systems are being applied to a wide variety of applications in support of propagation research

4.3.1 Rain Scatter and Absorption Effects

For correlation with ground based measurements, it is essential that the radar return signal be accurately calibrated to the rain rate. A standard empirical relation for the radar reflectivity and the rain rate R has frequently been utilized. Namely, $Z = 200R^{1.6}$, where Z is in mm^6/m^3 and R is in mm/hr (Ref 4.3-1). This standard relation has certain disadvantages (Ref 4.3-2)

1) The variance between the predicted R and measured R is large, a result due not only to averages taken over different systems and locations but also due to the inherent variability in the quantity Z being measured.
2) Z is a function of the back-scattering cross-section which is a function of frequency, i.e., the Z-R relation changes with frequency.
3) Z is obscured by the signal attenuation along the path.

By accounting for these effects and observing with radars at 3 GHz (non-attenuating) and 8.75 GHz (attenuating) and comparing the results, it was observed that the two radar measurements could be made to agree quite closely as shown in Figure 4.3-1. By utilizing the rain rates measured by rain gauges in the first 300m from the radar, the attenuation along the path was computed and the measurements altered. For rain rates above 10 mm/hr the improvement was significant enough to justify the increase in the necessary computational time (Ref 4.3-2).

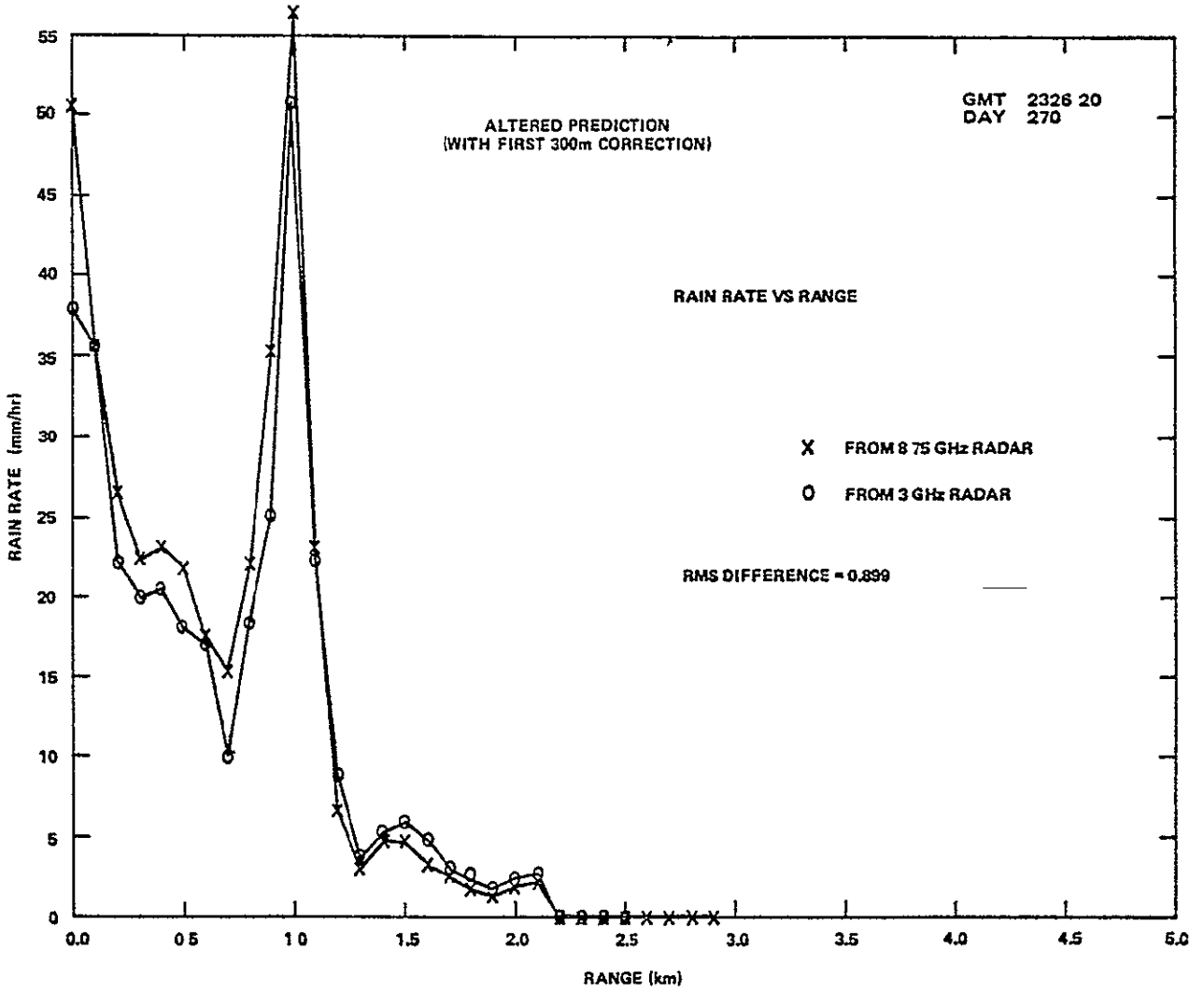

End Date
Filmed
Oct. 10, 1978

FIGURE 4.3-1. RAIN RATES FOR AN ATTENUATING AND NONATTENUATING RADAR

Investigators at Ohio State University (Ref 4.3-3) are continuing to investigate techniques for calibrating radar systems. They correlate their radar reflectivities with radiometry data, thus providing an independent measurement of the medium throughout the same region "seen" by the radar. The accuracy of this calibration technique has not been reported to date.

The above measurement techniques are currently being utilized with ATS-6 and CTS. Earlier, several of these constraints on the use of radar for measurement of rain properties were identified (but not resolved) in the late 1960's and early 70's by NASA as part of their Radio Frequency Interference and Propagation Program (RIPP). To remedy the deficiencies for estimation of terrestrial coordination distance and interference probability between ground stations, especially that arising from rain scatter interference, NASA was requested by the Office of Telecommunications Policy to study the problem, with the support of the Federal Communications Commission. The results were available for the 1971 World Administrative Radio Conference for Space Telecommunications.

The rain coordination procedure devised as part of RIPP is based upon statistical estimates of the surface rainfall rate, produced by the Institute of Telecommunication Sciences and upon an approximate description of the rain scatter process. The rain scatter process predictions utilized the bistatic radar equation and the Rayleigh scatter and incoherent scattering theories. Below 5 GHz polarization and attenuation effects were ignored, but above 5 GHz the effect of attenuation along the path and in the common scattering volume (Ref 4.3-4) were included to agree with the monostatic and bistatic (4.5 GHz) radar experimental results. These two radar systems observed the same scattering volume (rain) and demonstrated that on the average the bistatic-Rayleigh scattering is accurate, but that individual scattering events showed more fluctuations than expected. These fluctuations appeared to arise because of differences in the cell-by-cell structure and because some measurements were made for heights above the freezing level. A comparison of the measured and the calculated transmission loss between two ground stations (Ref 4.3-5) is given in Figure 4.3-2. The data presented are for conditions where clear lines of sight existed between the antennas, the scattering volume ranged in height from 3 to 11 km and scattering angles between 15^0 and 165^0 during a two-week period in July 1970 in New England.

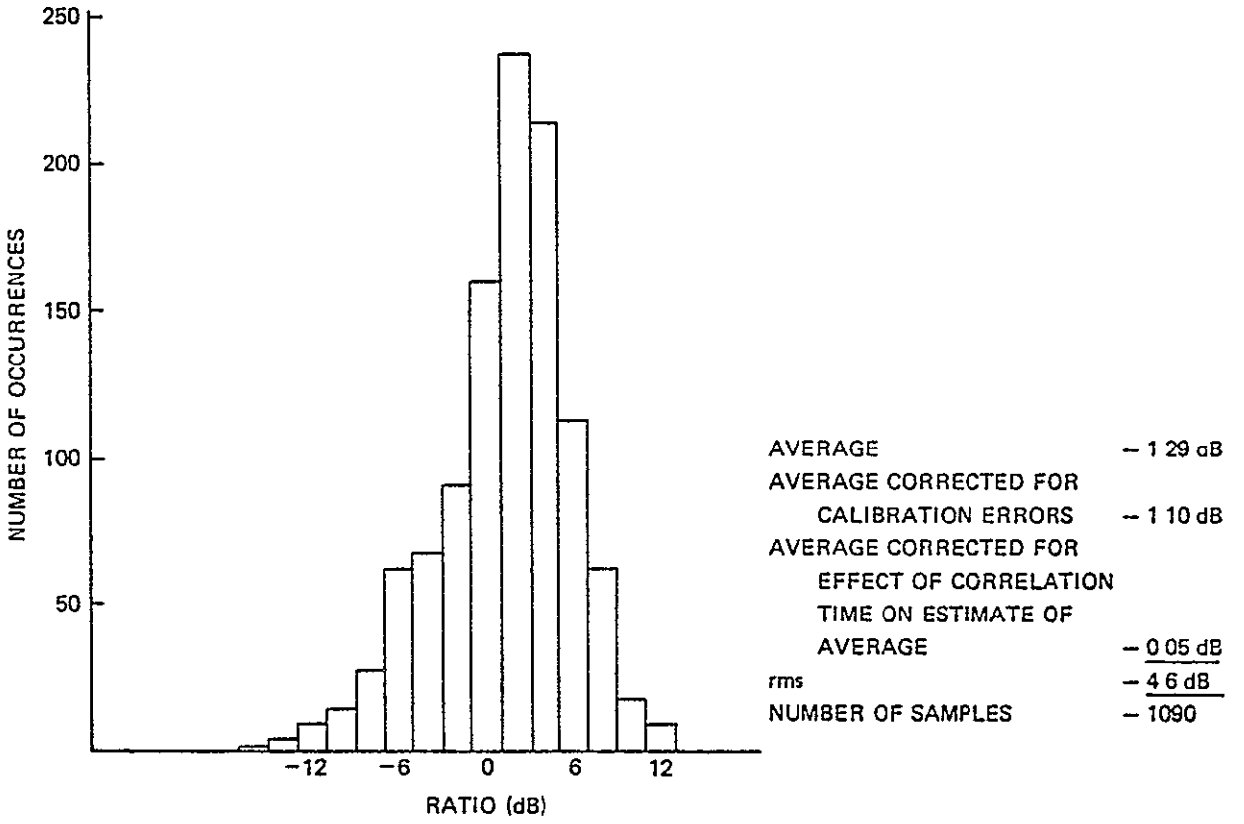

FIGURE 4.3-2. RATIO OF MEASURED TO CALCULATED TRANSMISSION LOSS BETWEEN GROUND STATIONS FROM BISTATIC RADARS

4.3.2 Radar Predictions of Rain Attenuation

The calibration of radar reflectivity and rain attenuation has been developed to sufficient accuracy that the radar results may be utilized to obtain cumulative attenuation statistics and site diversity information. This correlation has been demonstrated by the Applied Physics Laboratory (APL) experiments using the COMSAT ATS-6 (Ref 4.3-6). APL's experimental configuration, shown in Figure 4.3-3, employed a S-band, 2.84 GHz, radar at the Wallops Island, VA SPANDAR Facility. The radar's calibration has a standard deviation of 2 dB and was supplemented by 13 and 18 GHz transmitters (uplink), disdrometers for measurement of the drop size distributions and rain gauges APL investigators found that attenuation above the melting layer ("bright band") should be neglected even through the radar reflectivity is high. However, melting layers were most frequently observed when the rains were widespread, the rain rates were small (less than 10 mm/hr) and the measured fades at 18 GHz were less than several dB.

A summary of the APL results (Ref 4.3-6) with ATS-6 is given in Table 4.3-1 and an example of the 18 GHz data is shown in Figure 4.3-4. In the table the rms difference for three drop size distributions is shown. The APL distribution is that measured by the disdrometers, MP is the Marshall-Palmer distribution (Ref 4.3-7) and Joss is the thunderstorm activity distribution measured in Locarno, Switzerland (Ref 4.3-8). It is interesting to note that the MP rms difference is quite close to the measured APL data. This experiment and others have shown that radar is capable of permitting the prediction of rain attenuation. Utilizing the proper modeling procedures, attenuation and space diversity statistics may be compiled for variable elevation angles, frequencies and site diversity spacings.

APL has employed earlier radar results at Wallops Island to calculate the attenuation and site diversity characteristics at 13 and 18 GHz (Ref 4.3-9). Their diversity gain versus site separation distance results were within 1 dB of the Ohio State University measurements for fades up to 6 dB and within 2 dB at a fade depth of 10 dB. Thus using radar reflectivity data, which covers a much wider area than the line from ground station to satellite, APL found that a 15 km separation distance resulted in a near optimum diversity gain and that the diversity gain is minimally influenced by frequency.

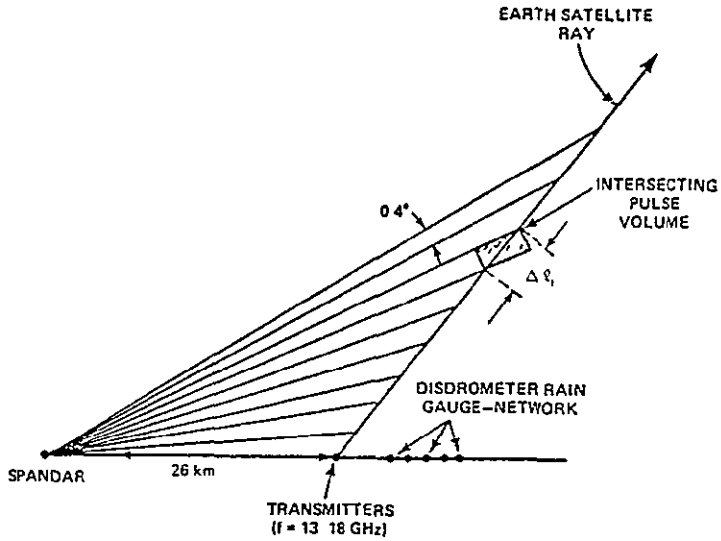

FIGURE 4.3-3. EXPERIMENTAL CONFIGURATION SHOWING 13 AND 18 GHz TRANSMITTERS 26 km FROM THE RADAR. BEAMS ARE DIRECTED IN AN UPLINK MODE TOWARD THE ATS-6 SATELLITE (NOMINAL ELEVATION = 42.3°)

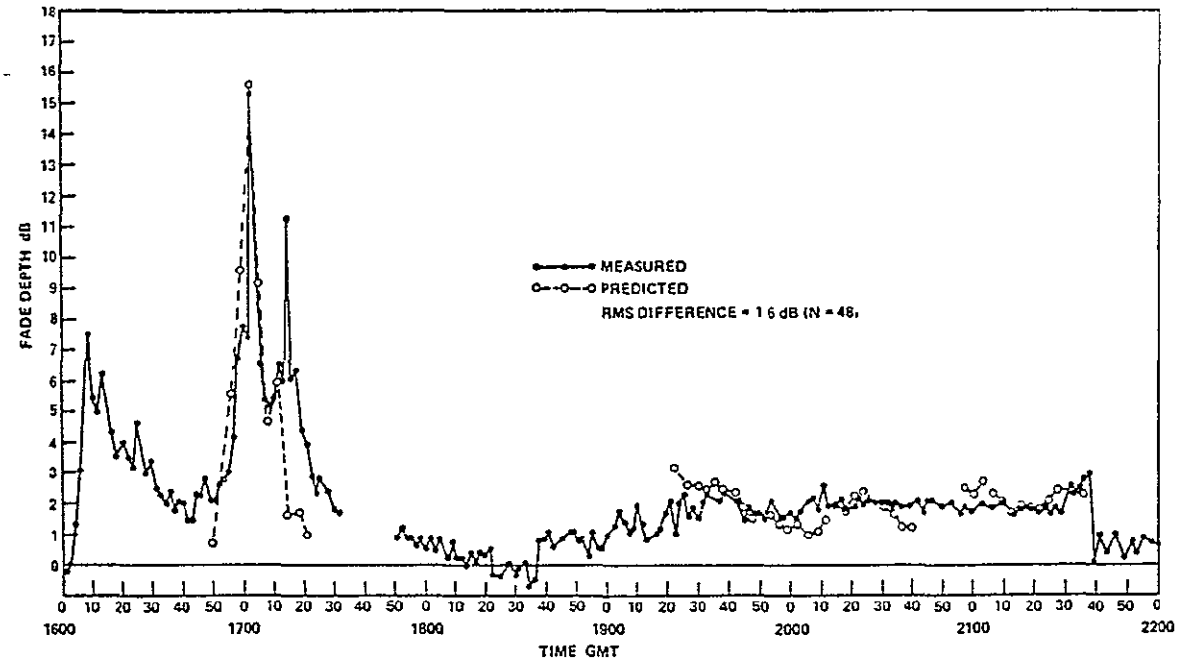

FIGURE 4.3-4 COMPARISON OF MEASURED AND PREDICTED FADE DEPTHS AT 18 GHz (DAY 235, 8/23/74)

TABLE 4.3-1. COMPARISON OF THE MEASURED AND PREDICTED FADE LEVELS

Day	N of Events Sampled > 1 dB	Peak Instantaneous Measured Fade (dB)	rms difference (dB)		
			APL	MP	Joss
f = 18 GHz					
(8/2/74) 241	16	3 0	1 3	0 4	0 8
(8/4/74) 216	10	3 3	0 4	1 2	1 8
(8/23/74) 235	48	15 3	1 6	2 0	2.7
(9/7/74) 250	28	5 0	1 7	2 3	2 8
(3/12/75) 71	12	3 1	0 5	1 1	1 8
(4/18/75) 108	37	2 1	0 4	0 7	1 1
Total	151		1 3	1 6	2.1
f = 13 GHz					
(9/7/74) 250	28	5 1	1 5	1 8	2.1
(3/12/75) 71	9	1 8	0 5	0 8	1 1
Total	37		1 3	1 6	1 9

APL has also observed (Ref 4.3-10) that by utilizing the measured median reflectivity factor versus height profiles as measured with radar and point rainfall rate data, they can predict slant path attenuation statistics at other locations, frequencies and elevation angles (greater than 20^{o}). They assume that the reflectivity-height profiles are the same at other locations, but this appears to be the case for convective rains for heights below 6 km in the U.S. Their results were quite close to experimental measurements in Texas, Maryland and England. For higher rain rates (greater than 30 mm/hr) they suggest use of two frequency fade distributions (Ref. 4.3-10) for extrapolation. However, because only a few sets of dual frequency fade statistics at a fixed elevation angle are available this extrapolation method has not been tested fully. Hopefully the COMSTAR 19 and 28 GHz statistics will provide data bases to test the proposed extrapolation procedure.

4.3.3 Radar-Derived Rain Cell Morphology

Radar reflectivity contours have been observed for rain cells to determine their general shape, i.e., circular or elliptical. If elliptical, in what direction is their semi-major axis oriented. This information would be useful in determining the optimum orientation for site diversity stations and to establish to what degree the satellite orbit locations influence the fading statistics. APL at Wallops Island, VA (Ref 4 3-11) investigated this question by separating path azimuths into NW-SE and NE-SW quadrants in their radar data for June, July and August 1973 convective rain storms. They found that the cell size statistics varied as shown in Figure 4.3-5. From these results one would expect that the diversity gain would be a maximum for stations oriented in the NW-SE direction. This has been observed experimentally at Ohio State University as mention in Section 3.2. The average cell size was 2 km larger for the NE-SW orientation compared to the NW-SE orientation. The cumulative probability statistics for a single site are also different depending on azimuth to the satellite as shown in Figure 4.3-6. The wind directions were measured during the rain events and found to come from the SW. This direction correlates well with the larger attenuation cell size, enhanced fade depths, and reduced diversity gain in the NE-SW sectors.

NASA Rosman also measured the morphology of the rain cells (Ref 4.3-12) as they passed through the ATS-6 20 and 30 GHz beams. The result for one rain

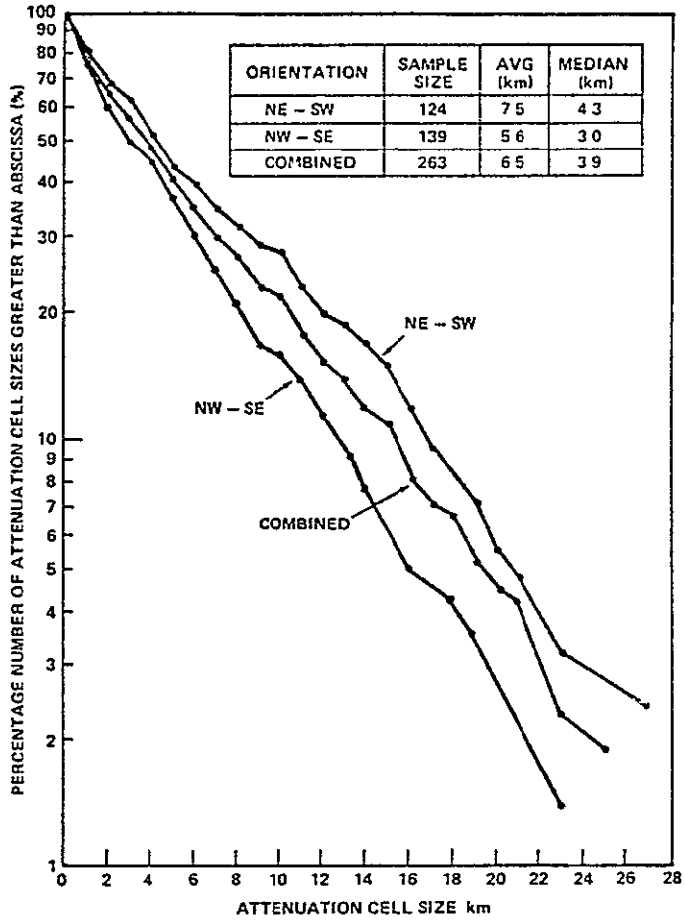

FIGURE 4.3-5. PERCENTAGE NUMBER OF ATTENUATION CELL SIZES EXCEEDING ABSCISSA AT 18 GHz FOR NE-SW, NW-SE, AND COMBINED QUADRANTS

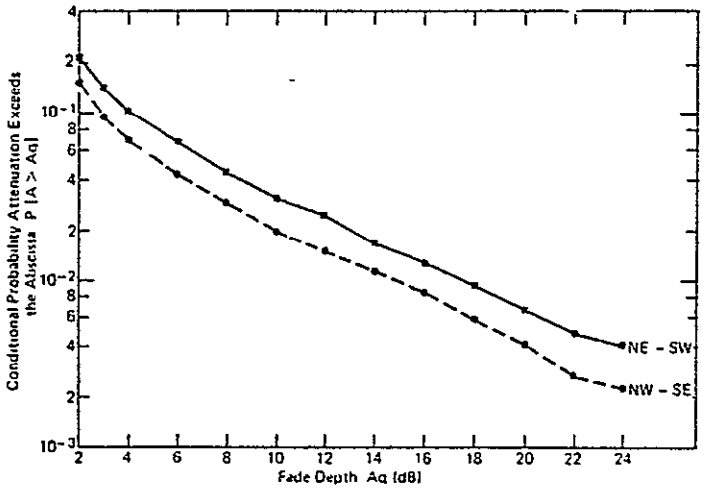

FIGURE 4.3-6. COMPARISON OF SINGLE TERMINAL PROBABILITIES FOR NE-SW AND NW-SE CASES

event at 3 and 8.75 GHz are shown in Figures 4.3-7 and -8 where the radar reflectivity (indicated by 1 to 5, see Table 4.3-2) is plotted every 20 seconds for ranges from 300 meters to 5.2 km. The accompanying 20 and 30 GHz signal attenuations are also shown at each time event when the receivers recorded data The data shows significant spatial and temporal variations. The most intense precipitation (No.'s 3,4, and 5) is measured in the close-in range bins, probably due to the high elevation angle. Also the intense rain cells are only on the order of 200 to 1000 meters thick, thus their contribution to the cumulative fade statistics is small.

TABLE 4 3-2

DEFINITION OF CONTOUR NUMBERS FOR FIGS. 4.3-7 AND -8

Contour Number	dBZ Interval	Rain Rate Interval (MM/Hr)
1	34 to 44	5-20
2	44 to 50	20-48.6
3	50 to 55	48.6-100
4	55 to 60	100-205
5	60 or greater	>205

4.3.4 Multi-Frequency Radar Measurements of Drop Size Distributions

Multi-frequency radar systems have been analyzed and operated primarily to determine the raindrop size distributions along a satellite path. The Applied Physics Laboratory (APL) analyzed various combinations of multiple wavelength radars for this purpose (Ref. 4.3-13). Their analysis was directed toward.

1) establishing the uncertainties in the estimated spectra due to a given system error,
2) range - averaging constraints, and
3) requirements of measuring a sufficient number of independent samples.

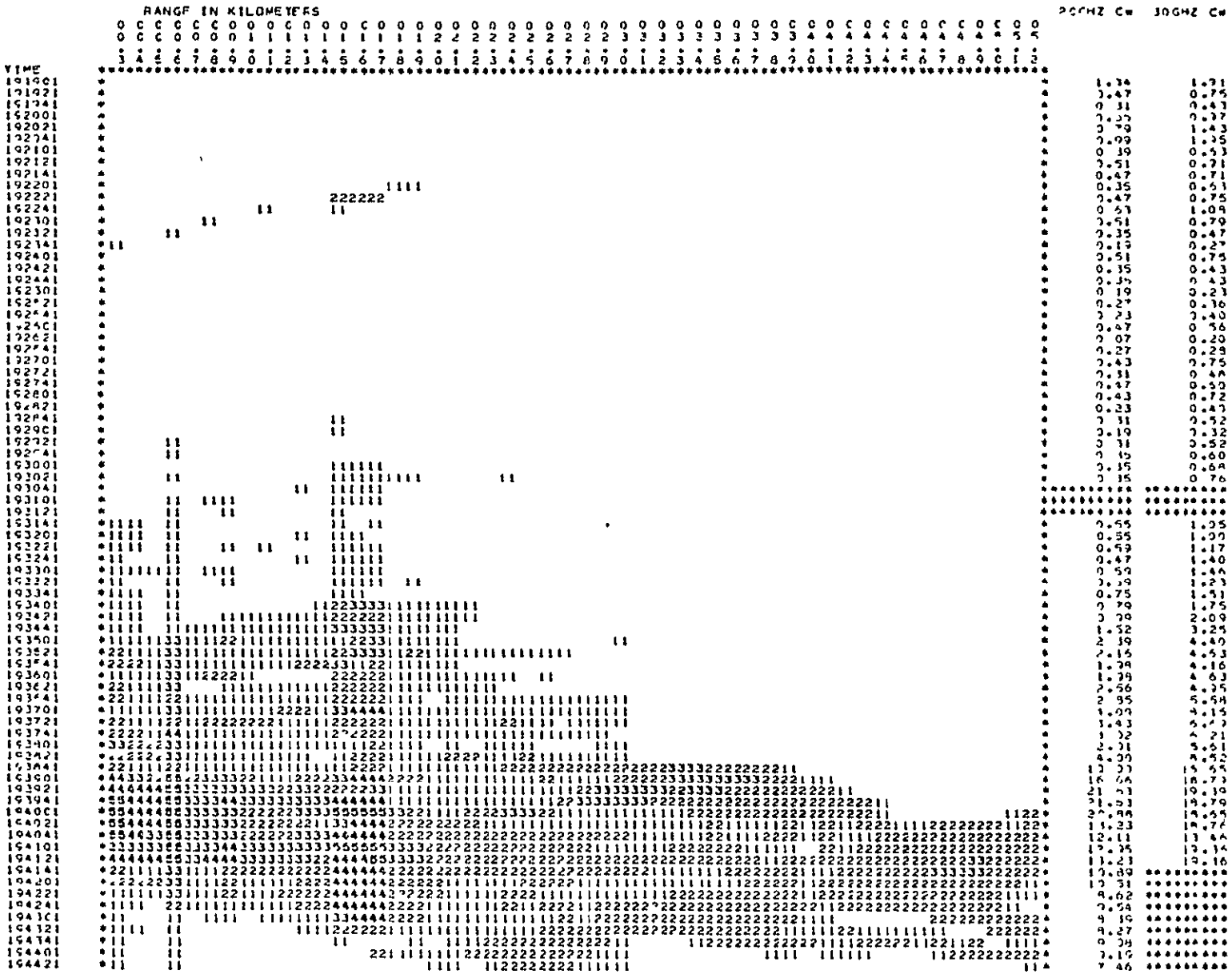

FIGURE 4.3-7. DAY 66 (1919Z to 2011Z) 3 GHz DBZ CONTOUR

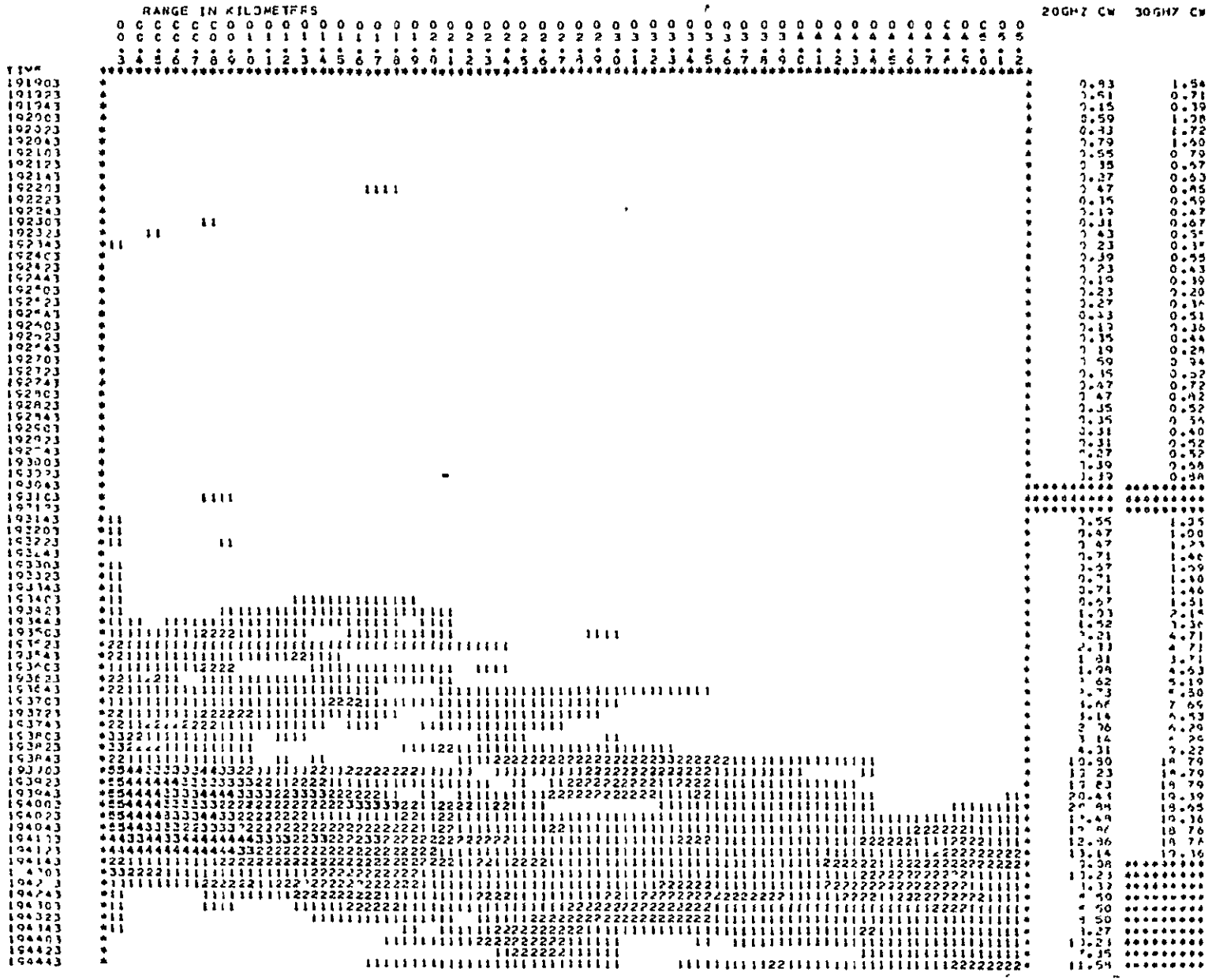

FIGURE 4.3-8. DAY 66 (1919Z TO 2011Z) 8.75 GHz DBZ CONTOUR

They analyzed 1, 3 and 10 cm wavelength radars and assumed the Marshall-Palmer (Ref 4.3-7) distribution function for the drop sizes. APL found that to determine the drop size distribution function

1) the combined system errors for both radars must be less than than 1 dB,
2) the range interval for averaging must be about 1 km (a condition not often observed for intense rains), and
3) of the order of 10^4 independent measurement samples are required to obtain average powers resulting in high confidence levels.

APL also concluded that the 10 and 1 cm combination of two radars was least sensitive to system errors, but that the 1 cm system has short range through rain.

To demonstrate the flexibility of dual-frequency radar systems and to experimentally verify the above analytic predictions, NASA at Rosman, NC installed a 3 GHz (10 cm) and 8.75 GHz (3 cm) multi-frequency radar system (Ref 4.3-12). In addition Rosman also correlated the radar reflectivity with the rain gauge measurements inorder to evaluate the Marshall-Palmer distribution parameters (Ref. 4.3-14). This method has the disadvantage that rain gauges must be located under the path and that drop velocity must be assumed to correlate the temporal effects. The Rosman results for both techniques were highly variable and did not cross-correlate between measurement methods. It appeared that determining an accurate calibration for the 8.75 GHz radar over a uniform rain rate range was a limiting factor. A technique for taking the rain rate non-uniformities into account was developed by Goddard Space Flight Center (Ref 4.3-15) but this was not applied to the Rosman results until later. However, considering the present state-of-the-art of radar systems, their constraints preclude the use of multi-wavelength and single wavelength-rain gauge systems to determine drop size distributions along the ground station-satellite path.

REFERENCES

4 3-1 Battan, L.J., "Radar Meteorology," Univ. of Chicago Press, Chicago, 1959.

4.3-2 Meneghini, R., "Review of Data Analysis Procedures for the ATS-6 Millimeter Wave Experiment," NASA/GSFC Doc. X-951-75-235, August 1975.

4.3-3 Hodge, D.B., "Meteorological Radar Calibration by Means of Radiometry," abstract of a paper to be presented at the National Radio Science Meeting, Boulder, CO., January 9-13, 1978.

4.3-4 Crane, R.K., "Microwave Scattering Parameters for New England Rain," Tech. Report 426, Lincoln Lab., October 1966.

4.3-5 "Interference Due to Rain," NASA/GSFC Doc. No. X-750-71-211, May 1971.

4.3-6 Goldhirsh, J., "Attenuation of Propagation Through Rain for an Earth-Satellite Path Correlated with Predicted Values Using Radar," IEEE Trans. Ant. Prop., Vol. AP-24, pp 800-806 (November 1976).

4.3-7 Marshall, J.S., and W. McK. Palmer, "The Distribution of Raindrops with Size," J. Meteorology, vol. 5, pp 165-166 (August 1948).

4.3-8 Joss, J., J. C. Thams and A. Waldvogel, "The Variation of Rain Drop Size Distribution in Locarno," in Proc. Int. Conf. on Cloud Physics, Toronto, Canada, August 26-30, 1968.

4.3-9 Goldhirsh, J, and F. L Robison, "Attenuation and Space Diversity Statistics Calculated from Radar Reflectivity Data of Rain," IEEE Trans. Ant. Prop., Vol. AP-23, pp 221-227 (March 1975).

4.3-10 Goldhirsh, J, "Extrapolation of Rain Attenuation Statistics to Other Locations," Proc. URSI Meeting, La Baule, France, 28 April - 6 May 1977, pp 305-310.

4.3-11 Goldhirsh, J., "Path Attenuation Statistics Influenced by Orientation of Rain Cells," IEEE Trans. Ant. Prop., Vol. AP-24, pp 792-799 (November 1976).

4.3-12 "ATS-6 Millimeter Wave Propagation Experiment, Final Data Analysis Report," prepared by Westinghouse Electric Corp., Baltimore, MD., Contract No. NAS5-20904, September 1975.

4.3-13 Goldhirsh, J, and I. Katz, "Estimation of Raindrop Size Distribution Using Multiple Wavelength Radar Systems," Radio Science, Vol. 9, pp 439-446, April 1974

4.3-14 Katz, I, and J. Goldhirsh, "Estimation of the Rain Drop Distribution Using an S-Band Radar and a Rain Gauge," Applied Physics Lab. Memo. MPD73U-063, 10 August 1973.

4.3-15 Meneghini, R., "Spatially Averaged Estimates of Attenuation Using Dual Frequency Radar Techniques," NASA/GSFC Doc. X-953-77-71, February 1977.

4.4 RAIN GAUGE MEASUREMENTS

Rain gauges provide a simple, continuous monitor of surface rain rates which have been accumulated by the National Weather Service over a period of years at many locations. Consequently, efforts have been made to extrapolate these results to cumulative fade distributions statistics. Initially, NASA-sponsored work was done for the Radio Frequency Interference and Propagation Program (RIPP) by the Department of Meteorology of the Massachusetts Institute of Technology (Reference 4.4-1). These investigators found that intensity distributions of the rainfall rates for 30 second periods varied significantly compared with the one minute to one hour resolution average rates for thunderstorms and non-thunderstorms. They concluded that hourly or daily precipitation amounts do not add information on very short-period rainfall rates beyond that contained in the annual amounts of thunderstorm and non-thunderstorm rain. It was not resolved if the half-minute rainfall rates, corresponding to spatial lengths of 0.5 to 1.0 km, provide enough detail for assessing the communication problems of link attenuation and scatter.

Later work by COMSAT with the ATS-6 millimeter wave experiment (Ref. 4.4-2) showed that the inconsistency between rain gauge measurements and link attenuation could be greatly reduced if the falling speed of the rain drops, i.e., two to nine m/sec for drop sizes of 0.05 to 0.7 cm, is taken into account. With these adjustments in time and drop size spectrum a network of six rain gauges extending 7.4 km below the 20 GHz ATS-6 beacon showed the correlation of measured to predicted attenuation shown in Figure 4.4-1. It is expected that if wind effects, evaporation, condensation, etc., were also included an improved correlation would be realized.

In addition, it is necessary to consider the positions of the rain gauges with reference to the height of the rain cloud and the characteristic size of the rain cells; both are dependent upon the rain type and other meteorological conditions. As a general rule, in order to avoid the discrepancy between the precipitation rate determined by attenuation and the precipitation rate derived from the rain gauge fields, the rain gauges should be placed so that the evaluation of the rain rate, is at a height lower than the boundary of the rain cloud and so that the distance between rain gauges is smaller than the characteristic size of the rain cells (Ref. 4.4-2).

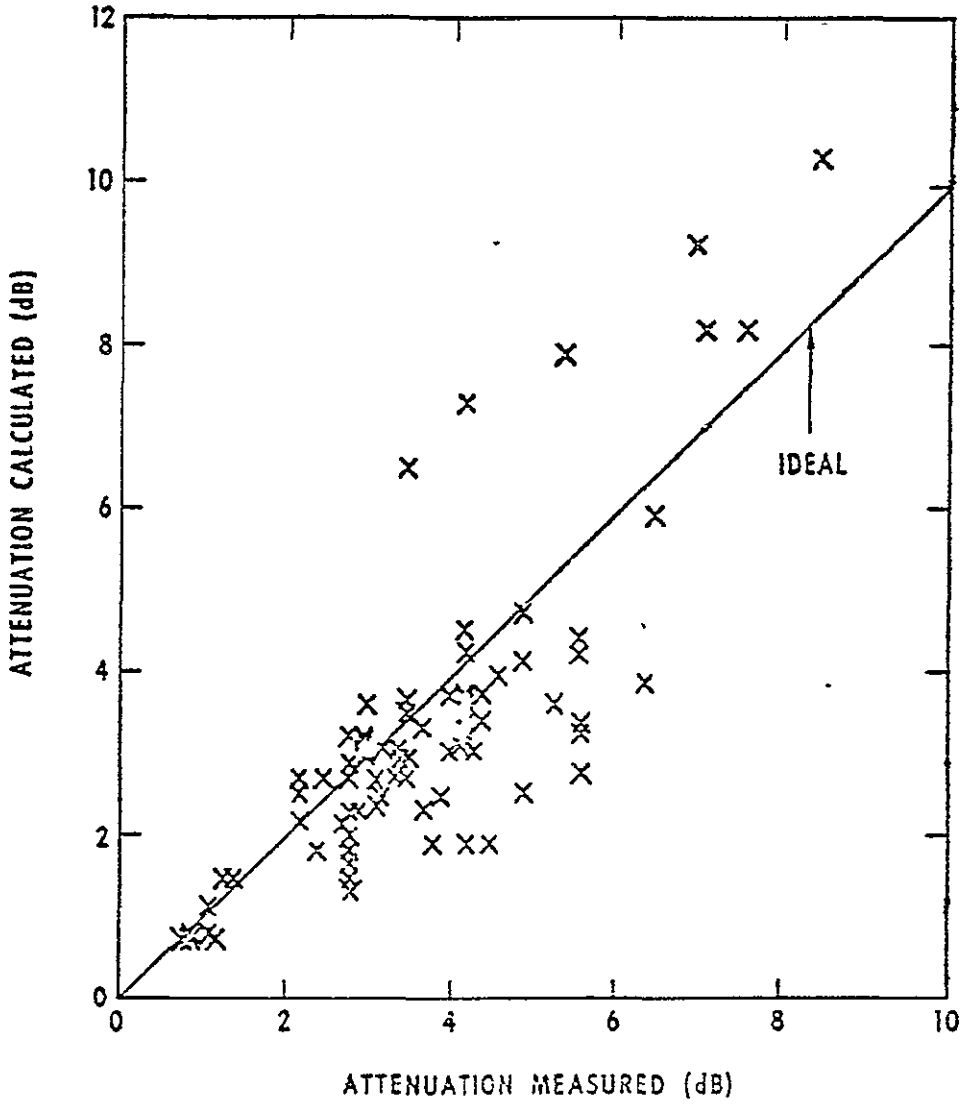

FIGURE 4.4-1. SCATTERGRAM OF 20-GHz ATTENUATION CALCULATED VS MEASURED FOR 2-HOUR PERIOD ON MARCH 19, 1975

Ohio State University has analyzed the ability of rain gagues at two or three closely space sites to determine the effective rain cell dimensions and orientation (Ref. 4.4-3) Two rain cell models were considered: the circular cell and the elliptical cell. In both models it is assumed that the rain rate is constant throughout the cell, that all cell locations are equally likely, and that the cell dimensions depend on the rain rate. By spacing the gauges about ½ km apart, the model allows one to deduce the effective cell dimensions and orientation of the semi-major axis for elliptical cells. The analysis has not been reduced to practice, but it is simple and relatively inexpensive to do so in order to test the analysis.

All of the above factors are extremely complicated because of their dependence on meteorological conditions. Therefore, efforts to incorporate surface rain measurements into precipitation attenuation studies have only been moderately successful. Additional work is still required, not only within localized areas, but extrapolation techniques to other regions of the globe remain highly unreliable.

REFERENCES

4.4-1 Austin, P.M., "Some Statistics of the Small-Scale Distribution of Precipitation," Final Report, Dept. of Meteorology, Mass. Inst. Tech., Contract NASA/ERC 0420 reprinted as NASA/GSFC Doc. X-751-72-149, July 1971.

4.4-2 Fang, D.J., and J. M. Harris, "A New Method of Estimating Microwave Attenuation over a Slant Propagation Path Based on Rain Gauge Data," IEEE Trans. Ant. Prop., Vol. AP-24, pp 381-4 (May 1976).

4.4-3 Hodge, D.B., "A Simple Method for the Determination of Effective Rain Cell Dimensions and Orientation," ElectroScience Lab., Ohio State Univ., Tech. Report 2374-15, September 1973.

V. CONCLUSIONS AND ONGOING ACTIVITIES

The understanding of millimeter wave Earth-space propagation effects has made tremendous progress in the last decade. Studies and experiments sponsored by NASA, in the frequency range above 10 GHz have yielded significant data bases for the design of advanced communications systems, such as the Tracking and Data Relay Satellite System, Intelsat V, and Satellite Business Systems, and ongoing programs with the CTS and COMSTAR satellites are developing even more extensive data bases in those areas not yet resolved.

It appears that the following propagation topics in the frequency range from 10 to 30 GHz, are now understood to such a level that they can be utilized by system design engineers:

- cumulative fade statistics for the eastern and mid-west US
- site diversity gain and station separation
- bandwidth coherence limitations
- calibration of radiometers versus path attenuations up to 10 dB
- frequency scaling or rain attenuation
- radar backscatter for a wide variety of rain cell structures

In contrast, the following areas are of interest to system designers and remain unresolved to sufficient depth to yield system designs. These include

- low angle scintillation and fading
- depolarization from both rain and ice

- angle-of-arrival variations in the signal
- use of low frequency radars for the prediction of attenuation at other frequencies.
- correlation of instantaneous rain gauge measurements with link attenuation
- theoretical modeling in support of all the above topics

NASA is continuing to support research programs in the above areas and expects that significant results for minimum additional investment will be obtained. Examples of several of these ongoing programs and some of their anticipated near-term results are now summarized.

At the University of Texas at Austin continuous measurements of the attenuation and cross-polarization isolation of the 11.7 GHz CTS beacon are being made. In excess of 11,000 hours of statistics will be acquired by the end of 1977. The data obtained so far indicates that the cross-polarization isolation (CPI) can be related to the attenuation (A) during rainstorms by a relation

$$CPI(dB) \simeq 37.5 - 16.5 \log_{10} A(dB)$$

and that ice crystals reduce the CPI below 30 dB about 17% of the time in Austin, Texas.

The Virginia Polytechnic Institute and State University group are conducting attenuation and depolarization measurements at 11.7, 19 and 28 GHz using both CTS and COMSTAR. They have developed software systems to provide over 50 different plot types for each rain event to assist in cross-correlation of data.

Ohio State's experimenters are continuing to study the angle-of-arrival and attenuation data from the CTS beacon. Their angle-of-arrival results are yielding a model for the prediction of the average antenna gain degradation as a function of frequency, antenna aperture and elevation angle. The high resolution radar and radiometer facility at Ohio is determining the statistics of rain cell dimensions based on radar calibration technique combining radiometers and radars developed at Ohio State.

The Applied Physics Laboratory of Johns Hopkins University is continuing to refine their previous work on predicting satellite link attenuations with S-band radar backscatter measurements. They are also continuing to check their method of predicting absolute rain fade distributions at other worldwide geographic locations. Eight comparisons at frequencies up to 37 GHz have been completed and the results are very promising. Rain drop size distribution effects are also being studied using independent instrumentation.

At NASA's GSFC and Rosman stations measurements of the degradation of video channels during rain events are continuing. Preliminary color bar test results indicate that significant fades (10 dB) are possible on the CTS 12-and 14-GHz links with minimal color video signal degradation. Additional statistics are now being acquired during fade periods.

NASA is currently planning additional propagation experiments with the Space Shuttle and the Public Services Communication Satellite (PSCS). The Shuttle Millimeter Wave Communications Experiment will operate in low Shuttle orbits with orbital periods of approximately 90 minutes and spend a significant percentage of time at low elevation angles from an individual ground station. Measurements (two-way) of the propagation effects on frequency re-use, wideband analog and digital techniques and multibeam communications are planned during passes over the ground stations. Aboard the PSCS, a "multi-beacon experiment" is being proposed having frequencies near 11.7, 20, 30, 43, 85 and 101 GHz. These frequencies would yield propagation data for the fixed satellite, broadcast satellite, aeronautical and maritime satellite services. In addition, an "adaptive polarization experiment," to evaluate electronically adaptive antenna techniques which could re-orient the received signal polarizations to maintain maximum isolation during a depolarization event, is being proposed for PSCS.

Thus, it appears that the next several years will yield a significant improvement in our understanding of the propagation data being measured. Three satellites are available to users and radars and radiometers are being used far more extensively. Persons requiring answers to unresolved propagation problems are encouraged to review the papers being presented at the URSI meetings. NASA is encouraging its personnel and contractors to make their results available at these meetings. Questions may also be addressed to the Communications and Navigation Division, Code 950, NASA Goddard Space Flight Center, Greenbelt, MD 20771.